Tampere University

Satyam Kapil

EFFECTIVE DESIGN OF STATCOM CONSIDERING FUNDAMENTAL FREQUENCY CURRENT, ACTIVE HARMONIC FILTERING AND ZERO SEQUENCE CURRENT

Faculty of Information Technology
and Communication Science
Master of Science Thesis
November 2019

ABSTRACT

SATYAM KAPIL: Effective Design of STATCOM Considering Fundamental Frequency Current, Active Harmonic Filtering and Zero Sequence Current
Master of Science Thesis, 90 pages
Tampere University
Master's Degree Programme in Electrical Engineering
November 2019

The main objective of this thesis was to investigate the effect of parallel reactive power compensation (RPC) and active harmonic filtering (AHF) operation on a STATCOM design, in terms of needed number of submodules (SMs), DC link voltage capacity, MV busbar voltage, zero sequence current demand, transformer and coupling inductor reactance. To achieve this objective, two design scenarios were carried out. In the first scenario, fundamental reactive current of studied STATCOM was prioritized over its current for active harmonic voltage filtering. In the second scenario, studied STATCOM was required to produce the nominal fundamental reactive power and perform active harmonic voltage filtering simultaneously.

The problem was studied in PSCAD based simulation environment. In all simulations, q-component current was supplied manually to enable the RPC operation of studied STATCOM. To enable AHF operation, harmonic current control mode was used, and the reference value of the desired harmonic filtering current was supplied accordingly. However, before proceeding with any simulation, first, the system limitations based on the studied STATCOM technology were studied and adequate majors were placed inside the simulation mode accordingly. Thereafter, simulations providing information on the basic STATCOM design operating in RPC mode only (and without AHF functionality) were carried out so that it can be compared later with the aforementioned scenarios of parallel RPC and AHF operations.

In the first design scenario, it was found out that additional AHF operation affects the STATCOM design in three ways. First was the magnitude of AHF current where an increment in the needed number of SMs w.r.t basic design was noticed with increasing magnitude of AHF current. The second was the phase angle references of AHF current where if phase angle references of AHF current are chosen such that peaks of produced voltage source converter's (VSC's) fundamental and harmonic voltages are aligned then the amount of needed SMs to produce the same VSC voltage was increased. But, if phase angle references of AHF current are such that the peaks of VSC voltages are opposite to each other, then fewer SMs are required to produce the same VSC voltage. The third effect on STATCOM design was based on the harmonic order of AHF current produced. It was noticed that when harmonic order of AHF current was high, then the amount of needed SMs to produce the same magnitude of AHF current was increased.

In the second design scenario, it was found that maximum fundamental reactive current and maximum filtering current cannot be achieved at the same time with a geometrical summation principle of these currents, but possible with an arithmetical summation principle with a trade-off between optimum utilisation of current capacity and extra hardware cost. Hence, an optimum design to achieve the maximum of RPC and AHF current simultaneously exists between economical (based on the geometrical summation principle) and conservative (based on the arithmetical summation principle) design, but rather close to the economical one. In last, it was also noticed that the maximum demand of zero sequence current occurred when STATCOM was producing fundamental reactive current and negative sequence AHF current simultaneously in the maximum capacitive operation point, with an unbalanced network. And, peaks of positive and negative sequence network voltage and peaks of produced VSC voltages (fundamental and harmonic) were aligned.

Keywords: STATCOM, MMC, reactive power compensation, active harmonic filtering

PREFACE

This Master of Science Thesis was written for GE Grid Solutions Oy, from the tenure of May'2019 to Oct'2019, as to comply with one of the requirements to complete MSc. degree in Smart Grid (Electrical Engineering) from the Tampere University.

First of all, I would like to express my gratitude to my thesis supervisor at GE, MSc. Jani Honkanen, to provide me with a comprehensive road map required to complete this thesis work within the stipulated time. His comments on the early stage of my work and help in developing the simulation environment have considerably paved the way.

A sincere thanks to Prof. Sami Repo and Prof. Pertti Järventausta for examining my thesis. Also, I would like to thank MSc. Vesa Oinonen for providing me this opportunity of thesis worker at GE and facilitating the entire thesis process. Additionally, I would like to thank my colleagues at GE and fellow students at Tampere University for an erudite discussion related to my thesis topic.

Finally, I am indebted to my family and girlfriend for their support and love throughout this beautiful journey of master studies and thesis project.

Tampere, 4th November 2019

Satyam Kapil

CONTENTS

LIST OF SYMBOLS AND ABBREVIATIONS

AC	Alternating Current
DC	Direct Current
AHF	Active Harmonic Filter
APLC	Active Power Line Conditioners
BJT	Bipolar Junction Transistor
CSC	Current Source Converters
CSI	Current Sourced Inverter
DC	Direct Current
DPF	Displacement Factor
DSBC	Double-star Bridge Cells
DSCC	Double-Star Chopper Cells
FACTS	Flexible AC Transmission System
FFS	Fundamental Frequency Switching
GTO	Gate Turn-off Thyristor
HPF	High Pass Filter
IGBT	Insulated Gate Bipolar Transistor
IGCT	Integrated Gate Commutated Thyristor
MCOP	Maximum Capacitive Operating Point
MIOP	Maximum Inductive Operating Point
MMC	Modular Multilevel Converter
MOSFET	Metal Oxide Semiconductor Field Effect Transistor
MPC	Model Predictive Control
MSC	Mechanically Switched Capacitor
NLC	Nearest Level Control
NS	Negative Sequence
p.u	Per Unit
PCC	Point of Common Coupling
PF	Power Factor
PHF	Passive Harmonic Filter
PI	Proportional Integral
PLL	Phase Locked Loop
PR	Proportional Resonant
PS	Positive Sequence
PWM	Pulse Width Modulation
RMS	Root-Mean-Square
RPC	Reactive Power Compensation
SAF	Shunt Active Filter
SDBC	Single-Delta Bridge Cells
SMs	Submodules
SRF	Synchronous Reference Frame
SSBC	Single-Star Bridge Cells
STATCOM	Static Synchronous Compensator
SVC	Static Var Compensator
SVM	Space Vector Modulation
TCR	Thyristor Controlled Reactor
TDD	Total Demand Distortion
THD	Total Harmonic Distortion
TSC	Thyristor Switched Capacitor
UPQC	Unified Power Quality Conditioner
VSC	Voltage Source Converter
VSI	Voltage Sourced Inverter

B_{TCR}	Susceptance of TCR
f_{harmonic}	Frequency of harmonics
$f_{\mathrm{fundamental}}$	Frequency of fundamental component
h	Integer multiple
$i(t)$	Non-sinusoidal current function
I_0	Current DC component
I_{h}	RMS value of harmonic current
I_{Q}	RMS value of reactive current
I_{R}	RMS value of active current
I_{TCR}	TCR current
I_1	RMS value of fundamental current
I_{STATCOM}	RMS value of STATCOM current
i_q	Current q-component
$i_{\mathrm{q,ref}}$	Reference of current q-component
$i_{\mathrm{d,ref}}$	Reference of current d-component
$i_{0,\mathrm{ref}}$	Reference of current zero-component
$I_{\mathrm{MMC,ref}}$	Reference of MMC current
$I_{\mathrm{MMC,meas}}$	Measured MMC current
I_{VSC} *or* $I_{\mathrm{VSC\_rms}}$	RMS value of VSC current (excluding zero current)
$I_{\mathrm{VSC(1)}}$	RMS value of VSC's fundamental current component
$I_{\mathrm{VSC(h)}}$	RMS value of VSC harmonic filtering current
$I_{\mathrm{VSC(active)}}$	RMS value of active current component of VSC
$I_{\mathrm{VSC(reactive)}}$	RMS value of reactive current component of VSC
$I_{\mathrm{zero,rms}}$	RMS value of zero sequence current of VSC
$I_{\mathrm{VSC(overall)}}$	RMS value of overall VSC current (including zero sequence)
$I_{\mathrm{VSC\_peak}}$	Peak value of VSC current
$I_{\mathrm{h,ref}}$	Magnitude reference of harmonic filtering current
j	Imaginary operator
P_{STATCOM}	Active power of the STATCOM
Q_{STATCOM}	Reactive power of the STATCOM
Q_{cap}	Reactive power of capacitor
S_{STATCOM}	Apparent power of the STATCOM
S_{L}	Apparent power of the load
t	time in second
V	RMS value of the voltage
$V_{\mathrm{a}}, V_{\mathrm{b}}, V_{\mathrm{c}}$	Instantaneous value of a, b and c-phase voltages
V_{α}	Voltage α- component
V_{β}	Voltage β- component
V_{d}	Voltage d-component
V_{q}	Voltage q-component
V_{m}	Magnitude of supply voltage
$V_{\mathrm{pcc,LN,meas}}$	Measured line to neutral PCC voltage
$V_{\mathrm{sec,LL,meas}}$	Measured line to line secondary side voltage
$V_{\mathrm{d,meas}}$	Measured voltage d-component
$V_{\mathrm{pcc,magn,ref}}$	Magnitude reference of PCC voltage
$V_{\mathrm{MMC,ref}}$	Reference of MMC voltage
V_{dc}	Difference between two voltage levels (DC-link voltage)
v^*	Voltage reference
V_{ref}	Reference of PCC voltage
$V_{\mathrm{VSCref\_peak}}$	Peak value of VSC reference voltage

$V_{\mathrm{DC\_max}}$	Maximum value of DC link voltage
$V_{\mathrm{DC\_min}}$	Minimum value of DC link voltage
$V_{\mathrm{VSC\_valve}}$	RMS value of VSC valve voltage
V_{S}	RMS value of source voltage
V_{L}	RMS value of load voltage
V_{1}	RMS value of fundamental voltage
ω	Fundamental angular frequency
X_{cap}	Reactance of capacitor
Z_{L}	Load impedance
$\varphi_{\mathrm{ih,ref}}$	Phase angle reference of harmonic filtering current
φ_{h}	Phase angle of harmonic current

1. INTRODUCTION

Power quality refers to the set of electrical boundaries which allow an equipment to operate with its optimum performance. However, substantial increase in non-linear loads and other devices utilising power electronic based circuits are causing serious problems to the power system in term of degraded power quality. These non-linear loads, when connected to a supplying network, can inject significant amount of harmonic currents or voltages which further results into increased power losses and performance issues of system components (e.g. transformer) [1]. Therefore, various standards have been introduced to limit the severity of harmonic emissions at the different voltage levels of an electricity supplying network [2].

Harmonic mitigation methods can be classified mainly into two categories; passive harmonic filtering and active harmonic filtering. Passive harmonic filters (PHFs) are made of arranging passive components such as, inductors, capacitors and resistors in a tuned circuit (e.g. single tuned, double tuned) which provides a low impedance path to the grid harmonic currents and thus absorbs them. Though, PHFs are cost effective, they have certain shortcomings, such as forming series and/or parallel resonance with the grid impedance and tendency to get detuned under varying network conditions. On the other hand, active harmonic filters (AHFs) utilise the voltage (or current) source converter-based topology and thus produce the necessary current to cancel out the grid harmonics. AHFs come with higher cost and complex design in comparison to PHFs but their application with multiple functions (e.g. harmonic mitigation, reactive power control, load balancing) make them more effective solutions for improving power quality. [2]

Apart from power quality issues, need of reactive power compensation is another major concern for the power transmission system. Loads like electric motors require inductive power from the grid to operate effectively and therefore, capacitive power is needed to compensate this requirement. Power lines, wind farms and solar farms might also need additional reactive power compensation for their effective operation. Flow of this reactive power not only reserves some part of transmission capacity from the active power but also causes significant energy losses. Hence, compensating reactive power at certain parts of a supplying network helps increasing the net transmittable power which may further contribute to improve steady state characteristic and thus the stability of the sys-

tem. Modern Flexible AC Transmission System (FACTS) devices like Static Var Compensator (SVC) and Static Synchronous Compensator (STATCOM) are proven to be more effective than passive compensation techniques due to their dynamic performance, in such operations. [3]

Speaking of active harmonic filtering and reactive power compensation, a single solution as STATCOM can be used to serve both purposes. STATCOM is a shunt connected device; based on either voltage source or current source converter topology. It can be used in a variety of power conditioning applications such as, harmonic filtering, harmonic damping, voltage flicker reduction, load balancing, reactive power control for voltage regulation and power factor correction, power system oscillation damping (angle stability) and any of their combinations. [2]

1.1 Objectives of the thesis

The main goal of this thesis is to investigate how to effectively design a STATCOM for the combined modes of operation of reactive power compensation (RPC) and active harmonic filtering (AHF). This combined operation should be investigated with two scenarios. The first is to design when fundamental reactive current of STATCOM is prioritized over its current for active harmonic voltage filtering. The second is to design when STATCOM is required to produce the nominal fundamental reactive power and perform active harmonic voltage filtering simultaneously.

In first scenario, the system should be investigated when initially full current capacity is used for RPC operation only to work out a basic design. After that, AHF functionality should be added such that RPC operation (in terms of overall current capacity) is prioritised first, and the remaining current capacity is given to AHF operation. Here, operation should be investigated in capacitive operation with maximum continuous PCC voltage. And, the effect of harmonic filtering current on DC link voltage, voltage source converter (VSC) voltage, VSC current and needed number of submodules (SMs) should be investigated. Further, it is of interest to know how harmonic filtering current of different magnitude, frequency, phasor rotation, and phase angle affects the overall design of studied STATCOM. Also the effect of reactance of coupling inductor and transformer on overall system design should be investigated.

In second scenario, the system should be investigated when STATCOM is producing the maximum required reactive power and performing harmonic filtering at the same time (e.g., produce 100 MVAr reactive power and decrease 5th and 7th harmonic voltages at the point of common coupling (PCC) from 2 % to 1 % simultaneously). Here, first, how

network impedance affects the filtering current, required to mitigate certain voltage distortion at the PCC, should be investigated. After that, considering the parallel operation of RPC and AHF, how different frequency current components should be summed together for rating purposes, to avoid significant over dimensioning, should be carried out. Once dimensioning is done, then the effect of AHF current (when RPC and AHF are operating at the same time) on VSC voltage, DC link voltage, and needed number of SMs should be investigated. In last, it is also of interest to know how parallel AHF filtering operation affects the needed zero-sequence current under unbalanced supply condition (considering the usual maximum continuous 2% network unbalance condition).

1.2 Scope of the thesis

Keeping the focus of the thesis into consideration, passive reactive power compensation methods have not been discussed in greater details, hence just briefly outlined. Series reactive power compensation methods are not part of this thesis. Therefore, the literature review has been carried out only for the shunt connected Passive and FACTS based compensation methods.

This thesis concentrates on STATCOM system design, therefore discussing mathematical modeling and designing of the system control doesn't fall under the scope of this thesis. However, to provide a holistic understanding of the entire STATCOM operation, its control system and modulation technique have been described concisely. While analyzing the effect of active harmonic filtering at the system design level, if findings suggest improving the overall result with possible re-tuning of STATCOM (e.g., changing system parameters), then such kind of work is certainly within the scope of this thesis. However, if findings suggest designing a new controller to improve the overall results, then such a designing process has been exempted from the scope of this thesis.

PSCAD based simulation environment has been used to implement the studied STATCOM model. Here, grid side harmonics source and other background harmonics have been disabled, since the objective of this thesis is not to evaluate the harmonic performance of studied STATCOM but to investigate how generating harmonic filtering current affect its overall design. Also, other harmonic filtering devices have not been included in the simulation model. Network impedance in simulation has been modeled as short-circuited, in order to mimic the minimum network impedance condition to generate maximum harmonic filtering current possible, a phenomenon explained in chapter 4.4.

Since the STATCOM model used in the simulation is comprised of VSCs placed in delta winding, therefore, an AHF current, which is zero sequence in terms of phasor rotation,

can not be produced with this model. Hence, all simulations have been carried out with either positive or negative sequence type AHF currents, irrespective of their frequencies (e.g., 150 Hz, 200 Hz, 250 Hz, etc.).

1.3 Structure of the thesis

Chapter 2 discusses the harmonics; origin, effects on the power system operation, standards to limit, and methods to mitigate them. Chapter 3 introduces the reactive power compensation methods. Here, more emphasis has been on the shunt connected compensation methods and especially the STATCOM technology in terms of its operation, control design, and modulation technique. Chapter 4 focuses on analysing the effect of parallel operation in AHF and RPC modes (e.g., prioritised or simultaneously), at system design and component level. Chapter 5 put forth the future work to improve the combined operation of STATCOM in AHF and RPC modes. Lastly, chapter 6 concludes the thesis content.

2. HARMONICS

Ideal AC electricity network is meant to supply perfectly sinusoidal current/voltage signals. But due to the number of reasons, it's hard to maintain such desirable conditions. Presence of harmonic content in the current/voltage signal results into the deviation from its fundamental frequency. Harmonic in the power system can be defined as a periodic sinusoidal component whose frequency is an integral multiple of the fundamental frequency component. [4]

$$f_{\text{harmonic}} = h \times f_{\text{fundamental}} \tag{1.1}$$

In equation 1.1, $f_{\text{fundamental}}$ is the frequency of fundamental component, h is the ineger multiple representing the number of harmonic (e.g. h = 2 means 2nd harmonic) and f_{harmonic} is the frequency of respective harmonic.

Considering the frequency of fundamental component ($f_{\text{fundamental}}$) as 50 Hz, frequencies of harmonics, such as 3rd, 5th and 7th harmonic can be computed as 3*50 Hz = 150 Hz, 5*50 Hz = 250 Hz and 7*50 Hz = 350 Hz respectively.

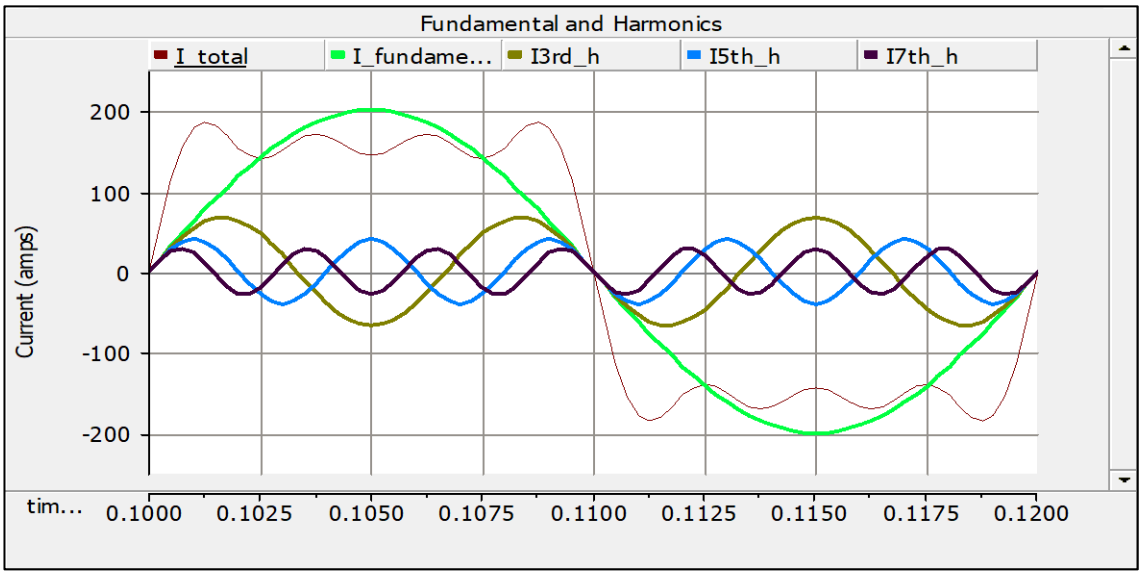

Figure 1. *50Hz sinusoidal current waveform with its harmonics.*

Figure 1. depicts a distorted current signal which comprises of fundamental, 3rd, 5th, and 7th harmonic components. To deduce and analyze such a non-sinusoidal periodic waveform, we use the theory of Fourier Series. Pronounce mathematical Joseph Fourier suggested that a set of trigonometric series elements can represent a periodic function. These elements further comprise of DC and other components whose frequencies are integer multiple of the fundamental frequency. [4]

Let $i(t)$ be a periodic non-sinusoidal function (current). Then its trigonometric series will be as follows:

$$i(t) = \frac{a_0}{2} + \sum_{h=1}^{\infty}[a_h \cos(2\pi f_1 ht) + b_h \sin(2\pi f_1 ht)] \quad (1.2)$$

Which further can be simplified as

$$\boldsymbol{i(t) = I_0 + \sum_{h=1}^{\infty} I_h \sin(2\pi f_1 ht + \varphi_h)]} \quad (1.3)$$

With

$$I_0 = \frac{a_0}{2},\ I_h = \sqrt{a_h^2 + b_h^2}\ and, \varphi_h = \tan^{-1}\left(\frac{a_h}{b_h}\right)$$

Equation 1.3 attributes to Fourier series wherein t stands for the time, a_0, a_h and b_h are the fourier cofficients, f_1 is the fundamental frequency (e.g. 50 Hz), h is the number of harmonic (e.g., 3rd, 4th, etc.), I_0 is a DC component, I_h and φ_h are magnitude (RMS) and phase angle of *h*th harmonic current component [4].

From equation 1.3, it can be concluded that the shape of resulted waveform doesn't only depend on the amplitude and number of harmonic components but also their phase relationship with the fundamental frequency component.

Even and odd components of the above-mentioned Fourier series expansion correspond to even (e.g., 2,4,6..) and odd (e.g., 3,5,7..) harmonics of a non-sinusoidal periodic waveform (current or voltage). For most of the loads, current positive and negative half waves are symmetrical (even after distortion) in nature and therefore there are usually only considerable odd harmonics present in the network. But there are also cases of imperfect gating of switching devices and half wave rectifier which may cause the even harmonics as well. [5]

Another interesting behavior of harmonics is their nature of the sequence. Harmonic sequence denotes the phaser rotation of a current/voltage harmonic component with respect to its fundamental frequency. Positive sequence harmonics rotate in the same direction with respect to fundamental frequency wherein negative sequence harmonics rotate in the opposite direction. On the other hand, zero sequence harmonics, being displaced by zero degree, also known as triplen harmonics (multiple of 3). [4] A detailed discussion summarising the effect of each harmonic sequence components has been put forth in the section 2.2.

Table 1. *Harmonic component sequencing in a balanced system [4].*

Particulars	1st	2nd	3rd	4th	5th	6th	7th	8th	9th
Frequency (Hz)	50	100	150	200	250	300	350	400	450
Sequence type	+	-	0	+	-	0	+	-	0

Table 1. represents the sequencing of each harmonic components. Starting with fundamental frequency of 50 Hz being the positive sequency component, 2nd harmonic (100 Hz) as negative sequence component and 3rd harmonic (150 Hz) as zero sequence component. Thus, pattern of sequencing repeats itself after each three harmonics, for instance, next sequence of positive, negative and zero sequenc is for the 4th,5th and 6th harmonics. Therefore, it would be pertinent to mention that in an unbalance system, harmonics can be of any abovementioned sequence.

2.1 Origin of harmonics

Voltage and current waveforms of linear loads follow each other and thus comply with the Ohm's law which states that current flowing through a resistor is directly proportional to the applied voltage (assuming resistance to be constant). Due to such linearity, current or voltage waveforms in an electric circuit appears to be perfectly sinusoidal in shape. Some of the linear loads are incandescent lighting, induction motors, power factor correction capacitor banks, damping reactors, electric heaters, etc. [4]

On the other hand, in non-linear loads, current doesn't show the linear characteristic with respect to the applied voltage. In case of non-linear resistor its resistance changes as a function of the applied voltage. Due to this varying resistance, resistor current doesn't look identical to the applied voltage and seems distorted. Therefore, it can be implied that non linear resistor produces the current harmonics which casues the distortion in its output current. Power converters, cycloconverters, etc. are the power electronic based devices attributing to non-linear loads. [4]

As Grady et al. [6] suggested, harmonic sources in the power system can be categorised to saturable devices and power electronic devices. In saturable devices, harmonics are produced due to iron saturation, as in the case of transformers. Power electronics based loads tend to operate with different switching conditions. For instance, giving the firing pulse to an IGBT for only half cycle of the source voltage will cause output current to follow the voltage for half cycle only. [6]

For holistic overview Table 2. summarises the type of harmonics in the power system along with their sources. DC type harmonics are caused by the devices like half-wave rectifiers, arc furnaces and etc. Since the frequency of such harmonics are of zero in value, therefore, they are given the name of 'DC'. Further, odd and harmonics are those components who frequencies are the multiple of odd and even numbers. The main sources of these harmonics are non linear loads and half-wave rectifiers respectively. The odd multiples of third harmonics are called triplen harmonics. These harmonics are

usually caused by the unbalanced three phase load and may result into overloading of neutral conductor, if not compensated. In balanced supply network every harmonic has a certain phasor sequence, as shown in Table 1, and based on their frequency they can be categorised as positive, negative and zero sequence harmonics. Harmonic whose frequency is lower than the fundamental frequency known as subharmonic. In last, if frequency of a harmonic is not the integer multiple of fundamental frequency then it is known as inter-harmonic and usually caused by the cyclo-converters. [5]

Table 2. *Type of harmonics and their sources [5].*

Harmonic Type	Frequency	Source of harmonic
DC	0	Electronic switching devices, half-wave rectifiers, arc furnaces (with random arcs)
Odd harmonics	h*f1 (h = odd)	Nonlinear loads and devices
Even harmonics	h*f1 (h = even)	Half-wave rectifiers, geomagnetic induced currents (GICs)
Triplen harmonics	3h*f1 (h = 1, 2, 3, 4, . . .)	Unbalanced three-phase load, electronic switching devices
Positive-sequence harmonics	h*f1 (h = 1, 4, 7, 10, . . .)	Operation of power system with nonlinear loads
Negative-sequence harmonics	h*f1 (h = 2, 5, 8, 11, . . .)	Operation of power system with nonlinear loads
Zero-sequence harmonics	(same as triplen harmonics)	Unbalanced three-phase load, electronic switching devices
Interharmonic	h*f1 (h = not an integer multiple of f1)	Static frequency converters, cycloconverters, induction machines, arcing devices, computers
Subharmonic	h*f1 (h < 1 and not an integer multiple of f1, e.g., h = 15 Hz, 30 Hz)	Fast control of power supplies, subsynchronous resonances, large capacitor banks in highly inductive systems, induction machines

2.2 Harmonic effects

Effects of harmonics in the power system can be categorised into two main categories; network level and system component level.

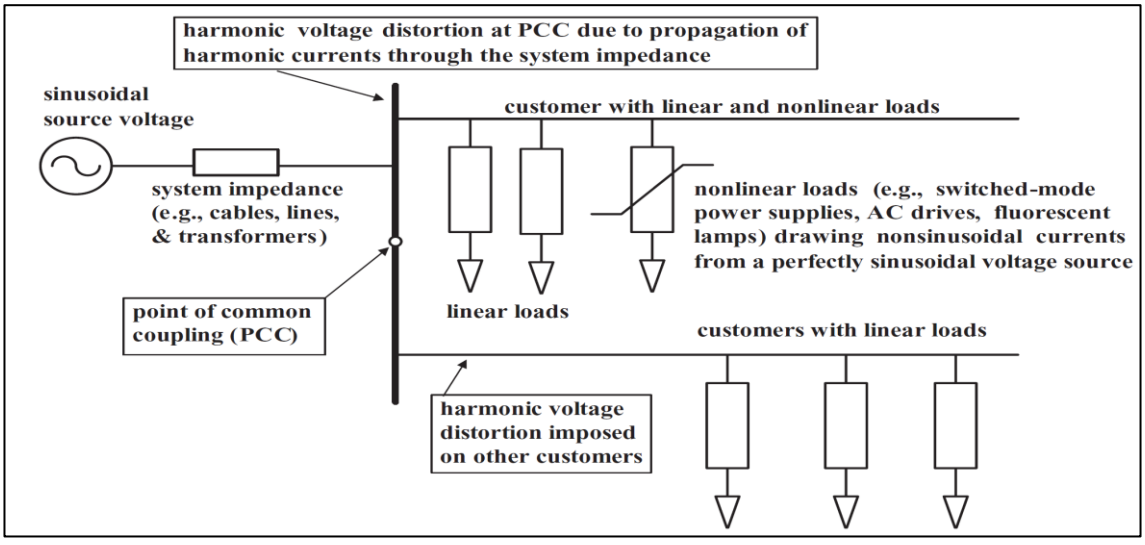

Figure 2. *Harmonic voltage propagation due to non-linear loads [5].*

Figure 2. depicts a small network comprising of linear and non-linear loads connected through the system impendence to a sinusoidal voltage source. Here, non-linear loads draw a harmonic current from the network. This current while flowing through the system impedance will cause a voltage drop (harmonic voltage drops to be precise) across the network. Hence, after subtracting this harmonic voltage drop from the source voltage it will be noticed that resultant voltage at the point of common coupling (PCC) has become distorted due to the harmonics. Thus, harmonics caused at the local level (non-linear load) have the widespread effect (network level) in power system, if no curative step is taken at the point of origin. For instance, voltage harmonics at the connection point of motor cause the harmonic fluxes to be produced inside the motor windings. These harmonic fluxes effect the rotation frequency in a way that motor starts rotating with a frequency other than the synchronous one. Hence, the additional fluxes, caused by voltage harmonics, produce high frequency currents inside the motor which further results in additional losses, heating, decreased efficiency and vibration in rotor. [5]

Harmonics have negative impacts on various system components. Speaking of transformer, additional heat is the most vital effect caused by the harmonic content available in the network. This extra heat deteriorates the transformer's rating to operate within the defined temperature limit. Moreover, in the presence of harmonics, a transformer's inductance may cause resonance with the system's capacitance. [7] Here the concept of resonance has been explained in detail at the end of this subchapter. Moving further, Elmoudi et al. [8] suggested that current harmonics contribute to increase in eddy current and stray losses of the transformer. Distortion in current may cause the protection relays to trip in unfaulty condition and failing in tripping during a fault [7]. In the case of rotating machines, harmonics result in increasing the copper and iron losses along with pulsating torque, which is produced due to the interaction of harmonic and fundamental component of the magnetic field [9].

As mentioned earlier, in term of phasor rotation with respect to fundamental frequency, harmonics can be categorised as positive, negative, and zero sequence component. Each of these harmonic sequences affect the power system differently. Due to same phaser rotation with the fundamental component, positive sequence harmonics add up with the fundamental component and result in a composite waveform. Peak to peak value of this composite waveform might be higher than the peak to peak value of fundamental waveform alone. Thus, this higher peak to peak value or increased magnitude in general may contribute in causing the overloading of conductors, transformers and power lines. [5]

On the contrary, due to the opposite rotation with the fundamental component, negative sequence harmonics give birth to pulsating mechanical torque inside an induction motor. Being the worst ones, zero sequence harmonics (also known as triplens when system is balanced) circulate between the phases and neutral (or ground) wire of a three-phase system. Amount of zero sequence harmonic current in neutral wire is three times higher than its value in phase wire, since all phase currents coincide in the neutral. Consequently, the main effects due to the zero sequence harmonics are overloading of neutral conductor and telephone interference. Type of transformer winding connection plays a big role in preventing the propagation of zero sequence harmonics. For instance, in “grounded wye-delta” type of transformer zero sequence harmonics enter from the wye side and due to their nature of zero displacement, they sum up in the neutral conductor. However, on the other side of the transformer where windings arrangement is in delta form, these harmonics can enter and flow inside the delta due to its ampere-turn balance property. But these harmonics remain trapped there and do not appear in the delta side-line current of the transformer. [5]

Capacitor banks used for the purpose of power factor correction and voltage support may sometimes contribute to causing harmonic resonance. [10] Capacitor may appear also from cables, which have high capacitance. Basically, every circuit comprised of capacitance and inductance may have one or more natural frequency of resonance and when this frequency matches with the frequency of harmonic current produced by a non-linear load then amplification of that harmonic current often occurs. Such a phenomenon of harmonic current amplification due to the system resonance is known as harmonic resonance. [11] This amplified harmonic current flowing in the network may result in breaker tripping, blown fuses, audible noises in the capacitor, and disrupting the operation of neighboring equipment [10].

Harmonic resonance can be further divided into two main types as series and parallel resonance. Parallel resonance occurs when the system inductance and power factor correction (PFC) capacitor are in parallel to the harmonic producing source. On the contrary, when system inductance and PFC’s capacitance are in series with respect to harmonic sources, then series resonance occurs. [6] As Eghtedarpour et al. [10] discussed, in the case of parallel resonance, the net impedance at resonant frequency, seen from the harmonic source side become very large. Further, multiplying this impedance with the harmonic current (even small) flowing through the network will cause significant distortion in voltage. High distortion in voltage will be at the remote point in case of series resonance and harmonic source (e.g., non-linear load) side in case of parallel resonance [6]. Traditional solutions to prevent harmonic resonance is to use reactor in series with

the PFC capacitor, which further act as a tuned filter circuit [12]. However, the main problem with such combination of the filter circuit is that it gets de-tuned due to ever changing dynamics of the system network; change in system impedance caused by network switching, change in load, etc [12].

2.3 Harmonics emission indices and standards

The very essence of harmonic emission calculation is to unfold the mystery of a distorted waveform in the form of its harmonic and fundamental frequency components. Accordingly, the following formulas have been discussed to provide the reader with enough mathematical understanding behind harmonic emission measurement before discussing the standards of limiting harmonics.

Total harmonic distortion (THD) is widely known distortion index for power quality related issues. It is the ratio of RMS values of all harmonic components available in a signal to the RMS value of its fundamental component: expressed in percentage. Hence, In terms of current and voltage, THD can be defined as follows. [4]

$$THD_{\text{voltage}}(\%) = \frac{\sqrt{\sum_{\text{h}=2}^{\infty} V_{\text{h}}^2}}{V_1} * 100 \tag{1.4}$$

$$THD_{\text{current}}(\%) = \frac{\sqrt{\sum_{\text{h}=2}^{\infty} I_{\text{h}}^2}}{I_1} * 100 \tag{1.5}$$

Here, V_{h} andI_{h} are the RMS value of hth harmonic voltage and current component wherein V_1 and I_1 refer to the RMS value of fundamental voltage and current component respectively.

Though THD provides a quicker measurement of distortion as one figure, detailed information of signal spectrum is lost. Moreover, it doesn't incorporate the amplitude information of a signal which sometime doesn't provide the actual insights about how sever the harmonic emission is. For instance, fundamental current changes depending on the operating points and therefore, current THD can be very high when the fundamental current is small. [5]

Considering above mentioned drawback of THD, standards like IEEE-519, further suggested replacing the fundamental component in THD calculation with the RMS value of rated or load current. Doing so has included the information of varying amplitude too. Fundamental voltage component doesn't change much in different network loading con-

ditions (e.g. weak network with large load or stiff network with small load) but fundamental current component varies a lot. Hence, Total Demand Distortion (TDD) is the ratio of RMS values of all harmonic current components (I_{h}) to the RMS value of the rated current (I_{rated}) signal. [4]

$$TDD(\%) = \frac{\sqrt{\sum_{h=2}^{\infty} I_{\mathrm{h}}^2}}{I_{\mathrm{rated}}} * 100 \tag{1.6}$$

The relationship between power factor, displacement factor, and THD is one the important aspect in dealing with harmonic filtering related problems because knowing their values help in designing various harmonic filter components. Displacement factor (DPF) is the cosine of angle between current and voltage at the fundamental frequency. It is the same as the power factor when the waveform is perfectly sinusoidal. [4]

$$DPF = \cos\varphi_1 \tag{1.7}$$

Here, φ_1 is the phase difference between voltage and current at fundamental frequency.

Consequently, power factor (PF) can be defined as follows. [4]

$$PF = \frac{I_{\mathrm{rms-1}}}{I_{\mathrm{rms}}} * \cos\varphi_1 = \frac{DPF}{\sqrt{1+THD^2}} \tag{1.8}$$

Here, THD is in % and equals to the value of $\frac{\sqrt{I_{\mathrm{rms}}^2 - I_{\mathrm{rms-1}}^2}}{I_{\mathrm{rms-1}}} * 100$ where I_{rms-1} is the fundamental RMS current and I_{rms} is the total RMS current.

The most widespread and acknowledged power quality standards are from the Institute of Electrical and Electronics Engineers (IEEE) and International Electrotechnical Commission (IEC). Among these power quality standards, some of them aim to recommend the practices and guidelines for harmonic control, such as IEEE 519 and IEC 61000 series (e.g., IEC 61000-3-6). [4]

Both IEEE and IEC standards have the recommendation of harmonic limits for the wide range of voltage levels in a network (e.g., 35kV, 69 kV and 161kV, etc). However, considering the scope of this thesis, only recommendations for medium voltage (MV), high voltage (HV) and extra high voltage (EHV) levels, as per their related standards, have been discussed accordingly.

IEEE 519 -2014, it provides the recommendations of current and voltage distortion limits along with the indication of how to control the harmonic emission [13]. As part of shared responsibility, it explains that based on inherent stake of all users, they should limit the harmonic emission to a reasonable value on their individual level [14]. Moreover, system

operators/owners are responsible for restricting the current/voltage distortion while adjusting the impedance characteristics of their supplying networks [14].

Table 3. *IEEE 519-2014 voltage distortion limits [15].*

Bus voltage V at PCC	Individual harmonic (%)	Total harmonic distortion THD (%)
V≤ 1.0 kV	5.0	8.0
1 kV < V≤ 69 kV	3.0	5.0
69 kV < V≤ 161 kV	1.5	2.5
V> 161 kV	1.0	1.5

Table 4. *IEEE 519-2014 current distortion limits (69-161 kV) [15].*

Maximum harmonic current distortion in percent of I_L (harmonic order: odd)						
I_{sc}/I_L	3 ≤ h< 11	11 ≤ h< 17	17 ≤ h< 23	23 ≤ h< 35	35 ≤ h≤ 50	TDD
<20	2.0	1.0	0.75	0.3	0.15	2.5
20 - 50	3.5	1.75	1.25	0.5	0.25	4.0
50 - 100	5.0	2.25	2.0	0.75	0.35	6.0
100 - 1000	6.0	2.75	2.5	1.0	0.5	7.5
>1000	7.5	3.5	3.0	1.25	0.7	10.0

Table 5. *IEEE 519-2014 current distortion limits (above 161 kV) [15].*

Maximum harmonic current distortion in percent of I_L (harmonic order: odd)						
I_{sc}/I_L	3 ≤ h< 11	11 ≤ h< 17	17 ≤ h< 23	23 ≤ h< 35	35 ≤ h≤ 50	TDD
<25	1.0	0.5	0.38	0.15	0.1	1.5
25 < 50	2.0	1.0	0.75	0.3	0.15	2.5
≥ 50	3.0	1.5	1.15	0.45	0.22	3.75

Prior to discussing the above shown tables, definition/clarification for some of the terminologies is required. Starting with point of common coupling (PCC), it is the nearest electrical point on a supplying network where customer loads are connected or could be connected. Thereafter, short circuit ratio (I_{sc}/I_L) is the ratio of short circuit current (amperes) to the load current (amperes), at a particular location. In last, harmonic measurements can be divided into short time meansurement and very short time measurements. In case of very short time, harmonic measurements are performed with aggregation of 15 cycle over the interval of 3 seconds wherein short time harmonic measurements are carried out over the interval of 10 minutes while aggregating 200 very short time values of a certain frequency. [15]

Table 3 represents the voltage harmonic limits at the PCC in percent of the line to neutral voltage rated at power frequency. Here IEEE 519-2014 further suggests that weekly 95th percentile of short time harmonic measurement values should be less than the limits

shown in Table 3. and daily 99th percentile of very short harmonic measurement values should be 1.5 times lesser than the values shown in the Table 3. [15]

Table 4 and Table 5 depict the current distortion limits where a user, connected at voltage level of 69-161 kV and above 161 kV, should restrict the amount of harmonic emission as: (1) 99th percentile daily very short time measurement values of harmonic current should be lower than twice the values specified in Table 4 and Table 5, (2) 99th percentile weekly short time measurement values of harmonic current should be lower than 1.5 times the values mentioned in Table 4 and Table 5, (3) 95th percentile daily short time values of harmonic current should be smaller than the values specified in Table 4 and Table 5 for 69-161 kV and above 161 kV connected consumer respectively. [15]

S. M. Halpin [14], further clarifies that as IEEE 519-2014 standard is based on the shared responsibility concept. Hence, Table 3. shows the voltage distortion limits maintaining which is the part of system operators' responsibility. On the other hand, Table 4 and Table 5 represent the current distortion limits of which to maintain is the part of user/consumer's responsibility. Interestingly, current distortion limits in Table 4 and Table 5 can also be referred to individual voltage distortion limits of Table 3. through a system impedance; derived through the short circuit ratio and assuming the value of load current as 1.0 pu. [14]

The IEC standards have a comprehensive approach in defining harmonic limit criteria for the utility-customer interface as well as the customer equipment. Speaking of assessment for emission limits in MV, HV, and EHV network systems, IEC/TR 61000-3-6 standard is widely known. And, since the application of studied STATCOM technology is at the MV/HV voltage level, therefore this standard has been discussed further in more detail. However, other IEC standards defining the limits of harmonic current emission for customer equipment connected to LV and/or public network with different current ratings (e.g. ≤16, > 16 A and ≤ 75 A) are IEC 61000-3-2, IEC/TS 61000-3-4 and IEC 61000-3-12. [4]

McGranaghan et al. [16] asserted that unlike other standards, IEC/TR 61000-3-6 provides guidelines to assess harmonic emission in a network, rather than providing limits to be met. The main goal of this standard is to guide through the system operators for carrying out the best engineering practices for ensuring the quality of supply to all connected consumers. [16]

IEC/TR 61000-3-6 standard for voltage distortion is based on the idea of planning and compatibility levels. Compatibility levels serve the reference values to coordinate with the immunity and emission of equipment connected at the LV/MV voltage level. However,

planning levels can be used to define the limit of harmonic emission in a supplying network, taking into the account presence of all possible harmonic sources. The system operators define these planning levels for all voltages of the supplying network. Hence, it can be treated as their internal objectives to deliver the quality of power supply. [17]

Table 6. *IEC/TR 61000-3-6 indicative planning levels for voltage distortion [17].*

Odd harmonics non-multiple of 3			Odd harmonics multiple of 3			Even harmonics		
Harmonic order h	Harmonic voltage %		Harmonic order h	Harmonic voltage %		Harmonic order h	Harmonic voltage %	
	MV	HV-EHV		MV	HV-EHV		MV	HV-EHV
5	5	2	3	4	2	2	1.8	1.4
7	4	2	9	1.2	1	4	1	0.8
11	3	1.5	15	0.3	0.3	6	0.5	0.4
13	2.5	1.5	21	0.2	0.2	8	0.5	0.4
$17 \le h \le 49$	$1{,}9\frac{17}{h} - 0{,}2$	$1{,}2\frac{17}{h}$	$21 < h \le 45$	0.2	0.2	$10 \le h \le 50$	$0{,}25\frac{10}{h} + 0{,}22$	$0{,}19\frac{10}{h} + 0{,}16$

Compatibility levels are equal or greater than the planning levels. But planning levels are defined in a way that they allow the coordination between different voltage levels and their respective harmonic voltage limits. Having said that, and since different network structures and operating conditions affect the planning levels, only indicative values should be assigned. Thus, Table 6 represents the indicative values of planning levels for voltage distortion at different voltage levels; MV (1 kV < $V_{nominal}$ ≤ 35 kV), HV (35 kV < $V_{nominal}$ ≤ 230 kV) and EHV (230 kV < $V_{nominal}$) respectively. Here, harmonic voltage (distortion) has been shown in the percent of fundamental voltage component for different harmonic frequencies. [17]

2.4 Mitigation methods

As mentioned earlier, in the last few decades, the number of non-linear loads connected to the electricity supplying network has been increased drastically and thus caused the problem of harmonics. Before discussing mitigation methods, one should first understand how harmonics are affected by the different network conditions. In general, with semiconductor loads, if grid's strength is strong then it gives high amplitude on the current harmonics and lower on the voltage harmonics [18]. Moreover, the amplitude of harmonic current, for some of the non-linear loads, depends on the effective impedance of the system (e.g., source impedance + any added line impendence) [19].

Problems caused by harmonics can be eradicated by increasing the level of immunity for system components, restricting the amount of emission produced by equipment (e.g.,

non-linear loads) and lastly with the help of harmonic mitigation techniques. New harmonic mitigation technologies along with reformulated and improved classical ones are available today. Some of the mitigation techniques are based on passive harmonic filters, active harmonic filters, hybrid harmonic filters, phase shifting transformers and K-factor transformers, etc. However, considering the scope of this thesis, only passive and active harmonic filtering method will be discussed further. [20]

2.4.1 Passive harmonic filter (PHF)

Passive harmonic filters are circuits comprised of passive elements (e.g., resistors, inductors, capacitors) which can be arranged in many different orders to serve various functions (e.g., damping, harmonic filtering, and reactive power compensation, etc). The main goal of passive filters is to reduce the harmonic level in a network and in some cases to produce reactive power at the fundamental frequency as well. Based on the type of connection, PHFs can be categorised as shunt, series and hybrid type with further subcategory based on the topology of tuned, damped or tuned-damped circuits. Figure 3, represents the family of passive harmonic filters based on their type of connection and topology. Here, at second level of subcategory, only shunt type PHF is expanded further due to its wide application and popularity among other harmonic mitigation techniques. [21]

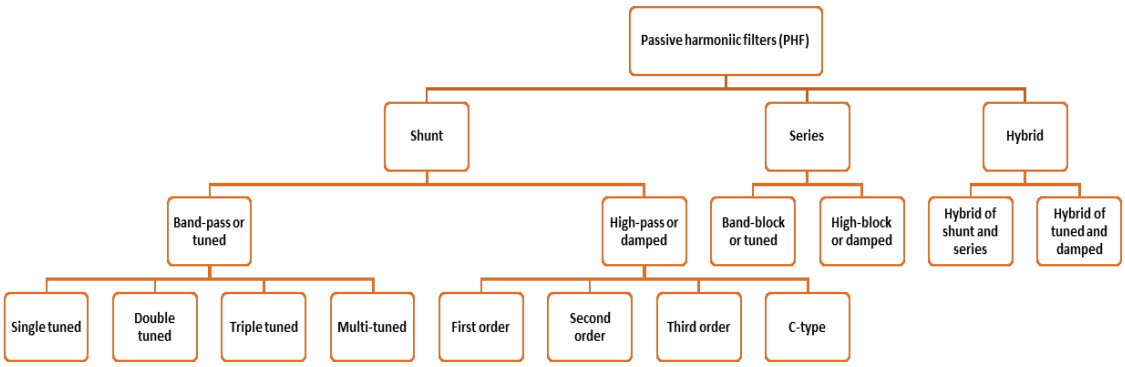

Figure 3. *Passive filters classification based on topology [21].*

Shunt harmonic filtering is based on the concept of providing low impedance path to a harmonic current so that it can be prevented from entering further into the network and forced to confine through a circuit made of passive elements (e.g., L, C). Among these passive elements, the capacitor may have negligible internal losses, but this is not the case with the inductor. Therefore, the inductor is presented with a resistor in series, as to address its internal power losses. Figure 4 depicts the various type of shunt passive filters wherein Figure 4(a) represents the single tuned or notch filter, tuned at a particular frequency of filtering (e.g., 150 Hz). It is a simple RLC series circuit where capacitor and

inductor values are driven through the amount of reactive power needed and value of tuned frequency, respectively. Moreover, value of resistance R defines the sharpness of filter and limit the amount of harmonic current flowing through the filter. Double or multi tuned circuits can be made while combining two or more single tuned filters in a circuit, as shown in Figure 4(b). [21]

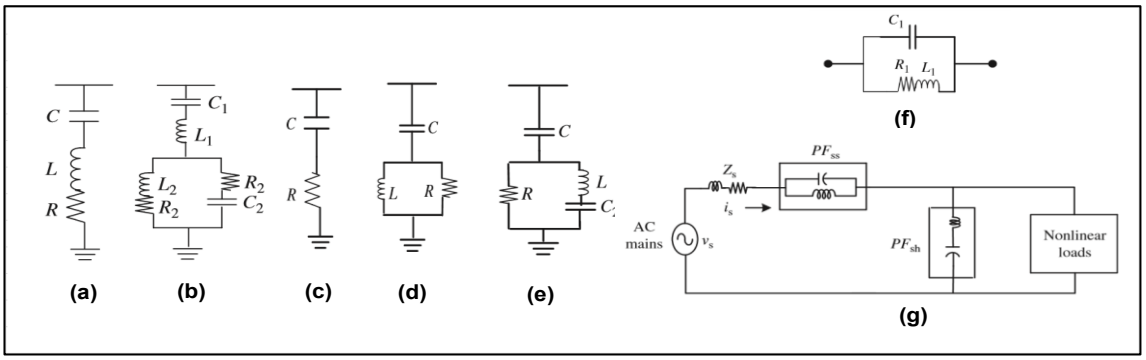

Figure 4. Shunt passive: *(a) single tuned, (b) double tuned, (c) first order, (d) second order, (e) C-type.* ***Series passive:*** *(f) single tuned. Hybrid passive: (g) combination of passive series filter ($\boldsymbol{PF_{ss}}$) and passive shunt filters ($\boldsymbol{PF_{sh}}$) [21].*

High-pass filters (HPF) are used to prevent the flow of high order harmonics (at least 2-4 different order harmonics) in the system. Due to the presence of resistor, these filters can provide the damping and thus they are also known as damped filters. However, presence of resistor not only restrict the filtering limit of the filter but also increases its losses. As shown in Figure 4(c), first-order high pass filters are simple RC circuit which can be used to regulate the voltage at PCC even in the presence of high order harmonics. Second-order high pass filters, depicted in Figure 4(d), are often used in the system since they come with better harmonic filtering and damping characteristics. HPF components are less affected by the temperature and frequency variation and therefore tend not to get detuned easily. Structure of the C-type filter is similar to second-order HPFs except for the added second capacitor C2 in series with inductor L, as shown in Figure Figure 4(e). Here, the series combination of second capacitor and inductor form resonance at the fundamental frequency, hence, preventing the flow of fundamental current through the resistor and therefore minimising losses. However, if resonance circuit of L and C2 is tuned to higher frequency, losses might increase. [21]

As shown in Figure 4(f), unlike shunt, series passive filters are the parallel arrangements of passive components (e.g., inductor, capacitor, etc.) connected in series with a supplying network or a harmonic producing load requiring harmonic filtering. A series passive filter offers low impedance to the current component at the fundamental frequency, hence allowing it to flow through the circuit with negligible voltage drop. But it offers high

impedance to the harmonic components and thus blocking their flow through the circuit. Series passive filters are used to filter a particular harmonic current, such as third harmonic. Due to the series connection, these filters need to carry full rated load current, which may restrict their application to single-phase low power rating equipment/networks only. Moreover, they consume reactive power (lagging) at a fundamental frequency which causes a voltage drop in the network and proven to be a downside of series harmonic filters. [21]

Considering drawbacks of both series and shunt passive filters, one possible way is to put them together in the certain configurations which offers the best performance. Such a combined configuration, as presented in Figure 4(g), is referred to a hybrid passive filter. Single-tuned series passive filter's drawback of absorbing reactive power, when implemented in hybrid filter, can be utilised in consuming the excess reactive power generated by a shunt passive filter under the light loading conditions. Moreover, series passive filter can also help in blocking the resonance occurring between the supplying system and a shunt passive filter. [21]

J. C. Das [22] argued that though PHFs have potential of being maintenance-free, scalable in size (large MVars and power), cost-effective and possibly faster response of one cycle or less when implemented with SVC, they also come with significant limitations. PHFs are rigidly placed, and therefore, their tuning frequency and filter's size can not be changed. Given this situation, PHFs are not a good option for changing system conditions. These changing conditions may even result in detuning of the filters. Apart from sporadic system conditions, detuning can happen due to increase in designed tolerance limit; further caused by the aging, temperature, and deterioration. Effective design of passive filters is largely affected by the system impedance and may even cause a problem in the stiff network. Stepless control of filter for reactive power control in changing load conditions is not possible; either it can be switched on or off. [22] Resistive component of the filter may cause losses in large size application. In last, a parallel resonance between the filter's capacitance and line inductance may cause the harmonic amplification in the system [21].

2.4.2 Active harmonic filter (AHF)

To overcome the drawbacks of passive filters for being fixed in size and compensation, problems of resonance, detuning, etc., there was a need to look for other harmonic mitigation techniques. Thanks to the growing field of power electronics, it was possible to develop dynamic and adjustable harmonic filtering solutions. These solutions are known as active harmonic filters (AHFs) if only used for harmonic compensation. But if they

serve multiple purposes, such as harmonic compensation, reactive power compensation, load balancing, voltage flicker mitigation, etc., then they are well known as active power line conditioners (APLCs). [23]

Based on topology AHFs can be classified as series, shunt and hybrid filters wherein connection with the power supply may vary from case to case or depending upon the filter's application (e.g., Single phase-2 wire, Three phase- 3 or 4 wire, etc.). AHFs have gone through tremendous development based on the breakthrough in power electronic switches technology, system and control techniques, microelectronics, and converter design. The essential components of an AHF are passive elements (e.g., inductor, capacitor), power electronic switches and its control system. Speaking of power electronic technology, AHFs are made of different switches such as bipolar junction transistor (BJT), metal oxide semiconductor field effect transistor (MOSFET), gate turn-off thyristor (GTO), insulated-gate bipolar transistor (IGBT), integrated gate-commutated thyristor (IGCT), etc. Some of the control strategies are instantaneous reactive power theory, synchronous frame theory, hysteria control, etc. [23] Part of controller devices for AHFs started with discrete signal and later got shifted to digital signal processor based technologies [24], [25]. To incorporate the dynamic and steady performance of AHFs for sporadically changing system conditions, complex algorithms for real-time control are developed and further supported by the improvement in control platforms of proportional integral, fuzzy logic, variable structure and neural network-based controls [26]–[28].

Considering converter design, AHFs can be categorised as a current sourced inverter (CSI) or voltage sourced inverter (VSI), for each of the topology (e.g., shunt, series) and type of connection (e.g., two-wire, three-wire) with the power supply [2]. As shown in Figure 5(a) CSI based AHF topology is comprised of self-commutating device (e.g., IGBT) in series with a diode and self-supporting dc current source or energy storage (usually inductor). Figure 5(b) depicts a VSI based AHF topology comprised of self-commutating device in parallel to a diode along with self-supporting dc voltage source or energy storage (usually capacitor). Though, CSI based topology is fairly reliable, it comes with higher losses and requirement of high value parallel capacitors. VSI based topology is slightly cheaper, lighter and scalable and therefore, most popular in AHF application. Majority of literatures have used the terminology 'voltage source converter (VSC)' instead of 'voltage source inverter (VSI)' since it serves both function of AC and DC conversion. [23]

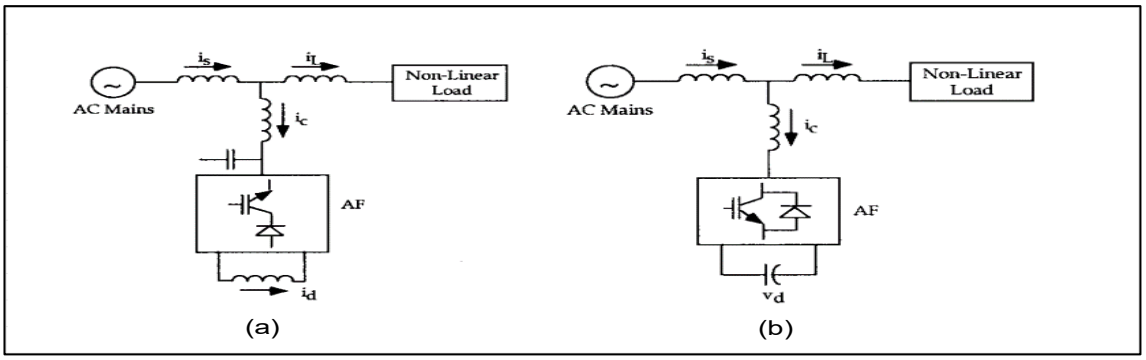

Figure 5. *Active Filter: (a) CSI based- current fed, (b) VSI based- voltage fed [23].*

Figure 6(a) depicts the shunt arrangement of an active harmonic filter, simply known as shunt active filter (SAF). In Figure 6(a), a SAF is comprised of VSC and stepdown transformer. This VSC is connected to a capacitor (or energy storage in some cases) on its DC side, and AC side is connected to the power supply in shunt mode. The main objective of a SAF is to generate compensating current, which is equal in magnitude but opposite in phase to the load harmonic current [23]. VSCs of SAF can be either half bridge or full bridge converter circuits in three phase delta, star or double star arrangement for HV/MV applications [21]. A static synchronous compensator (STATCOM) can be referred to a SAF if implemented to serve not only reactive power compensation but also the other functions of current quality related problems such as, harmonic filtering, unbalance current compensation etc [29].

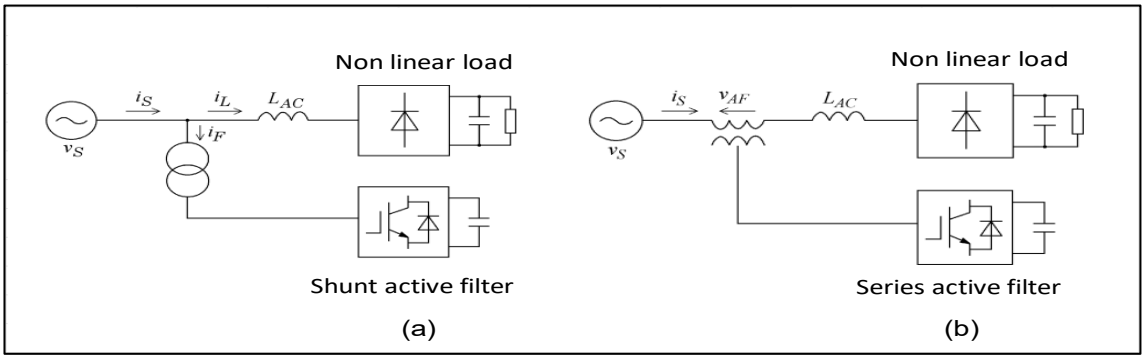

Figure 6*. (a) Shunt active filter (b) Series active filter [2].*

Shunt active filters operate based on the feedforward concept; the controller of SAF measures the value of load current (i_L) and detects the amount of harmonic component (i_{Lh}) in it. Thereafter, it produces the compensating current (i_F=$-i_{Lh}$) to cancel out the current harmonics [2].

The main application of series active filters is to mitigate voltage harmonics. It can also be used to eliminate other voltage quality related problems such as voltage flicker, volt-

age sag, voltage unbalance, etc. Series active filters, as shown in Figure 6(b), are connected in series with the supplying network and/or before the load through a transformer and they produced the required amount of voltage component to cancel out the network harmonic voltages. Like shunt active filters, they can also be categorised based on converter circuits (e.g. CSI or VSI) and type of connection (e.g., 2-wire, 3-wire, 4-wire, etc.) with power supply. [30]

Unlike shunt active filters, control strategy of series active filters is based on the concept of feedback; controller measures the instantaneous value of supplying current (i_S) and separates the harmonic component (i_{Sh}) value from the net supplying current. Using this harmonic current component(i_{Sh}) and adequate feedback gain(K) value, series active filter calculates the needed amount of compensating voltage $(v_{AF} = -K * i_{Sh})$. Thereafter, applying this compensating voltage at the primary side of connecting transformer results into decreasing the current harmonics and consequently a reduction in net voltage harmonics as well. [2]

Hybrid filters can be categorised into three segments; passive-passive filters, active-active filters and active-passive filters. As the name suggests this kind of filters are a combination of two or more different filters (e.g., active and passive) depending upon the type of application. Passive-passive hybrid filters have already been discussed in section 2.4.1, therefore active-active and active-passive hybrid filters are part of this section. As shown in Figure 7(a), this kind of filter is the combination of series and shunt active filters which sometimes is also known as unified power quality conditioner (UPQC) or universal active filter due to its versatile functions. Its series-shunt combination helps in eliminating current and voltage harmonics, negative sequence voltage, and regulating the PCC voltage. However, due to a large number of switches and other components involved, it has disadvantages of higher cost and complex control design. [23]

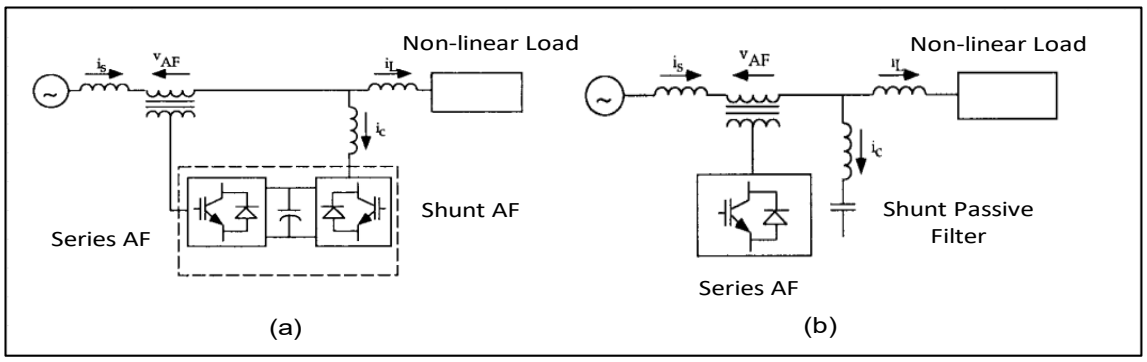

Figure 7. Hybrid Filter: *(a) combination of active-active filters (or UPQC) (b) combination of active-passive filters [23].*

In case of active-passive filter based hybrid topologies, different arrangements can be made using (1) Series AHF and Shunt PHF, (2) Shunt AHF and Shunt PHF, (3) Series AHF in series with Shunt PHF, etc. [31]-[33]. The most popular arrangement is series AHF and shunt PHF based hybrid filter, as shown in Figure 7(b). It comes with reduced cost, in comparison to purely active filter-based solutions because majority of harmonic compensation part of the unit is taken care by the passive filters (usually for low order harmonics). [23] Here active filter plays the role of a harmonic isolator between the load and source side, hence, forcing harmonics to shunt passive filter and letting them confine through it [2].

In conclusion, it is hard to argue whether pure active filters (e.g., active-active) or hybrid active filters (e.g., active-passive) are the best solutions for harmonic filtering because choosing one is based on the trade-off between cost and performance. Pure active filters come with higher cost and a rather versatile functions of power conditioning (e.g., reactive power control, load balancing, harmonic mitigation, etc.) but hybrid active filters are more effective if used for harmonic filtering only. [2]

3. REACTIVE POWER COMPENSATION (RPC)

Like harmonics, reactive power also poses severe threats to the power system. Majority of power quality issues are influenced by the presence of unwanted reactive power and can be resolved if adequate compensation techniques put into the place. Capacitor and reactor store the reactive power generated by an AC source in the quarter of the fundamental cycle and transfer it back to the source in the next quarter of the fundamental cycle. Hence, the oscillation of reactive power occurs between the AC source and capacitor or reactor (or other devices which utilise reactive power for producing magnetic field; motors) at twice the frequency of fundamental cycle in an AC system (e.g. 100 Hz for 50 Hz rated system). [31]

Categorically reactive power compensation may serve two main objectives; load balancing and voltage support. Load balancing attributes to improve system power factor, amount of real power drawn, and mitigating harmonics produced by the non linear load. In case of voltage support, reactive power is used to alleviate the voltage fluctuation at a certain network point (e.g. PCC) and thus maintaining a flat voltage profile. [31] Moreover, efficient reactive power compensation enables the economical dispatch of real power [32]. Some of the reactive power compensation techniques, based on the mature technology, can be dived into the three main segments as (1) Passive Var compensation (e.g. series and shunt capacitor/reactor), (2) Rotating synchronous Var compensator (e.g. synchronous condenser) (3) FACTS based solutions (e.g. SVC, STATCOM, UPQC, etc.) [31]. However, keeping the objectives of this thesis into consideration, only shunt based passive and FACTS Var solutions have been outlined in the following subchapters, with more emphasis on the STATCOM technology.

3.1 Passive Var compensation

Passive Var compensators are made of reactive elements such as reactor and capacitors, connected in series or shunt configuration with the power supply. The main objective of series compensation is to alter the network's parameters (e.g. voltage, current) wherein shunt compensation is used for changing the load side impedance. But using both scenarios, effective control of reactive power flow can be carried out. [31]

Classification of passive Var compensators based on the topology can be summarised as shunt, series, and hybrid compensators. Further, they can be divided based on the number of phases such as two-wire, three-wire, or four-wire compensators. The series

topology of passive Var compensators has a limited implementation in electricity network due to their impact on the performance characteristic of load and tendency to create series resonance. Their main application is in transmission network to shorten its length (with decreased voltage drop) and thus to provide improved power transfer capability. On the other hand, shunt topology doesn't affect the operation of load much and therefore proven to be more effective passive Var solution when compensation is needed at the load side. But they are also widely used in the power distribution network for voltage regulation. [21]

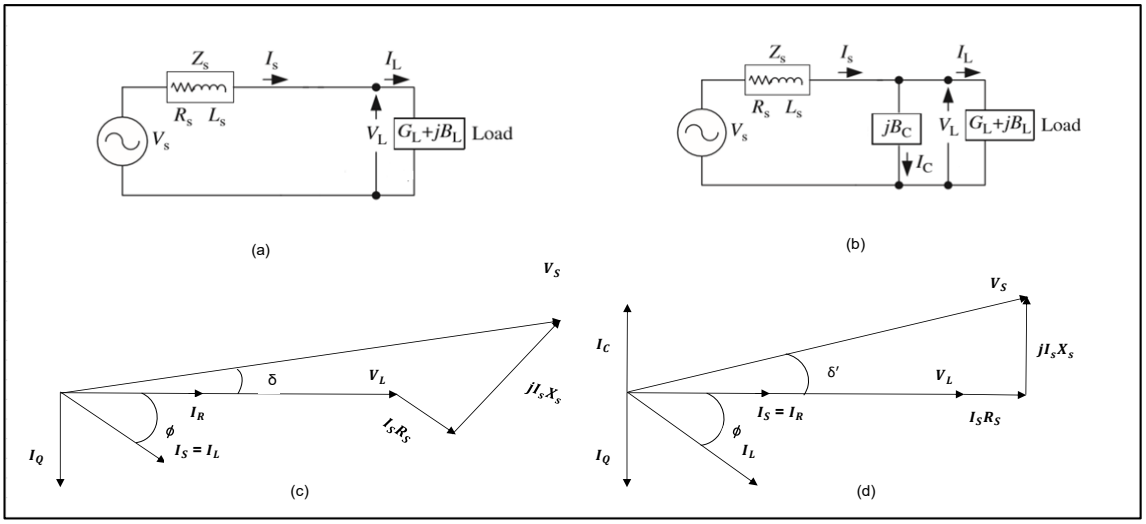

Figure 8. *(a) Network without compensation, (b) Network with shunt Var compensation, (c) phasor of network without compensation, (d) phasor of network with compensation [21].*

Figure 8 demonstrates the fundamental principal behind shunt compensation technique. In Figure 8(a), an inductive load (Z_{L}) is feeding through a power source (V_{S}). Since load is inductive, hence it's drawing reactive (I_Q) and active current (I_R) from the source for its effective operation. Due to this reactive current, amount of resulted current has increased, and when flowing through the system impedance, it will cause more losses in the form of voltage drop. However, flow of this reactive current can be prevented if it can be supplied locally (e.g., near to load) with the following designing strategy [21].

Figure 8(a) and Figure 8(c) shows the case of single-phase inductive load without Var compensation. Therefore, supply/load current can be computed as:

$$I_{\mathrm{s}} = I_{\mathrm{L}} = \frac{V_{\mathrm{L}}}{Z_{\mathrm{L}}} = V_{\mathrm{L}}(G_{\mathrm{L}} + jB_{\mathrm{L}}) = I_{\mathrm{R}} + jI_{\mathrm{Q}} \tag{3.1}$$

Here, I_{R} is active component of source current and in phase with the load voltage V_{L} wherein I_{Q} is the reactive component of source current and in quadrature with the load voltage.

Apparent power of the load:

$$S_{\mathrm{L}} = P_{\mathrm{L}} + jQ_{\mathrm{L}} = V_{\mathrm{L}} * V_{\mathrm{L}}(G_{\mathrm{L}} - jB_{\mathrm{L}}) = V_{\mathrm{L}}^2(G_{\mathrm{L}} - jB_{\mathrm{L}}) \quad (3.2)$$

From equation 3.1 and 3.2 it can be concluded that if we connect a compensator having admittance value of $-jB_{\mathrm{L}}$(capacitive), it will produce a current of $I_{\mathrm{C}} = -jV_{\mathrm{L}}B_{\mathrm{L}}$ (opposite to I_{Q})

Now the supply current post compensation, using Figure 8(b), will be.

$$I_{\mathrm{s}} = I_{\mathrm{L}} + I_{\mathrm{C}} = V_{\mathrm{L}}(G_{\mathrm{L}} + jB_{\mathrm{L}}) - jV_{\mathrm{L}}B_{\mathrm{L}} = V_{\mathrm{L}}G_{\mathrm{L}} = I_{\mathrm{R}} \quad (3.3)$$

Needed rating of compensator

$$S_{\mathrm{C}} = P_{\mathrm{C}} + jQ_{\mathrm{C}} = V_{\mathrm{L}} * I_{\mathrm{C}}^* = V_{\mathrm{L}} * (-jV_{\mathrm{L}}B_{\mathrm{L}})^* = jV_{\mathrm{L}}^2B_{\mathrm{L}} \quad (3.4)$$

Here, $\mathrm{P_C}$ will be zero, since we only need reactive power (capacitive in this case).

Hence, shunt compensator produces the equal amount of reactive current (but in opposite phase (180°) to cancel out the reactive current demand of inductive load from the main supply. Doing so results into making the net supplying current purely resistive ($I_{\mathrm{s}} = I_{\mathrm{R}}$). This current when flowing through the system impedance causes less losses and thus improved voltage profile at the load side, as depicted in Figure 8(d). [21]

Reactive power compensation in shunt mode can be carried out in three possible way: (a) current-source, (b) voltage-source or (c) capacitor/inductor, Var generators. Voltage or current source-based shunt compensation methods (e.g., STATCOM) have been discussed in the latter part of this thesis. Reactive power generated by current or voltage sourced Var generators is independent of the voltage at the point of connection, if same is operating within the defined Var limit. However, this is not the case with capacitor (or inductor) based compensators because of the following reason. [31]

$$Q_{\mathrm{cap}} = V * I_{\mathrm{cap}} \ or \ \frac{V^2}{X_{\mathrm{cap}}} \quad (3.5)$$

Here, Q_{cap} is the amount of reactive power generated, I_{cap} is the reactive (capacitive) current, V is the voltage at the point of connection and X_{cap} is the value of reactance for capacitor. For inductive load, reactive power generated by the shunt compensator will be capacitive and inductive in case of capacitive load. However, it can be inferred from equation 3.5 that the amount of reactive power generated/absorbed by a shunt compensator is proportional to the square of connection point voltage. So, changing in system

voltage will result in significant variation of generated/absorbed reactive power by the compensator, and thus, the load either will be under-compensated or over-compensated.

Fixed shunt passive compensators are not the best solutions under changing system conditions. But controllability over Var generation/absorption can be achieved if used capacitors/inductors are equipped with the electromechanical switches. With the help of relay and circuit breakers, the number of capacitors/inductors inside the compensation circuit can be switched in or out depending on the requirement of total Var. The probable consequences of using mechanically switched passive compensators will be the slow and erratic control, the possibility of high inrush current and need of frequent maintenances. In last, considering total cost, they are rather cheaper in comparison to modern FACTS based solutions. [33]

3.2 SVC

Static Var Compensator (SVC) is a shunt linked thyristor-controlled Var (i.e., leading or lagging) generator. Due to the presence of thyristors, it has been given the name “Static.” The main application of SVC is to maintain its coupling end network (HV/MV) voltage to a predefined reference value. Apart from voltage control, other functions of SVC are reactive power control, power oscillation damping, and load balancing. SVC is one of the members of FACTS family; preliminary used for increasing the system’s transferability and controllability in term of power flow and thus improving its stability. [34]

Though the design of SVCs may vary from case to case, its main components are Thyristor Controlled Reactors (TCR), Thyristor Switched Capacitor (TSC), harmonic filters, stepdown transformer and sometimes mechanically switched reactors or capacitors too. A typical arrangement of these components for HV/MV SVC application can be represented through the configuration shown in Figure 9. [35]

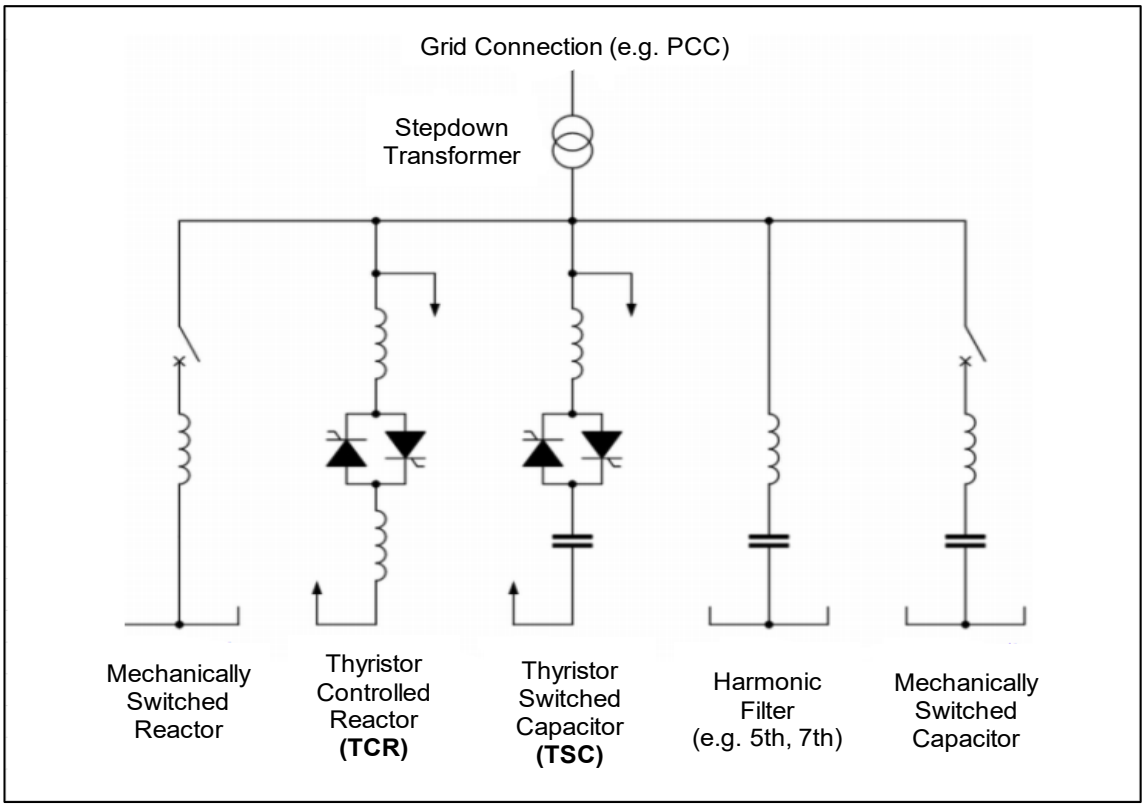

Figure 9. *A general SVC configuration [35].*

TCR is the combination of anti-parallel thyristors connected in series with a linear air-core reactor. These thyristors act like a switch while one of them conducting in the positive half cycle and another in the second half cycle of the mains supply. The conducting mechanism of the thyristor is controlled by its firing angle; measured through zero crossing value of the voltage across the thyristor's terminals. This firing angle varies from 90° to 180° wherein 90° contribute to full conduction of thyristor and 180° being the angle of no conduction at all. Varying the fire angle values in between 90° and 180° enables TCR current to flow in the form of discontinuous pulses, symmetrically placed in both positive and negative half cycle of AC power supply. However, to better understand such behavior of TCR current, the following equation has been worked out. [36]

$$I_{\mathrm{TCR}} = V_{\mathrm{s}} * B_{\mathrm{TCR}} \tag{3.6}$$

From equation 3.6, it can be implied that since the applied voltage is constant, the amount of fundamental current (reactive current) for a TCR is directly proportional to its susceptance. But this susceptance further depends on the firing angle of thyristors, which means varying the firing angle will result in the variation of susceptance and consequently adequate variation in the reactive current of TCR. [36]

Thyristor Switched Capacitor (TSC) also comprises of antiparallel thyristors valve in series with a capacitor and an inductor. But in TSC, thyristor's conduction control is not based on the variation of firing angle, so, either they are switched ON with full conduction or remains switched OFF. It means the output current of TSC is purely sinusoidal in steady-state condition. [31]

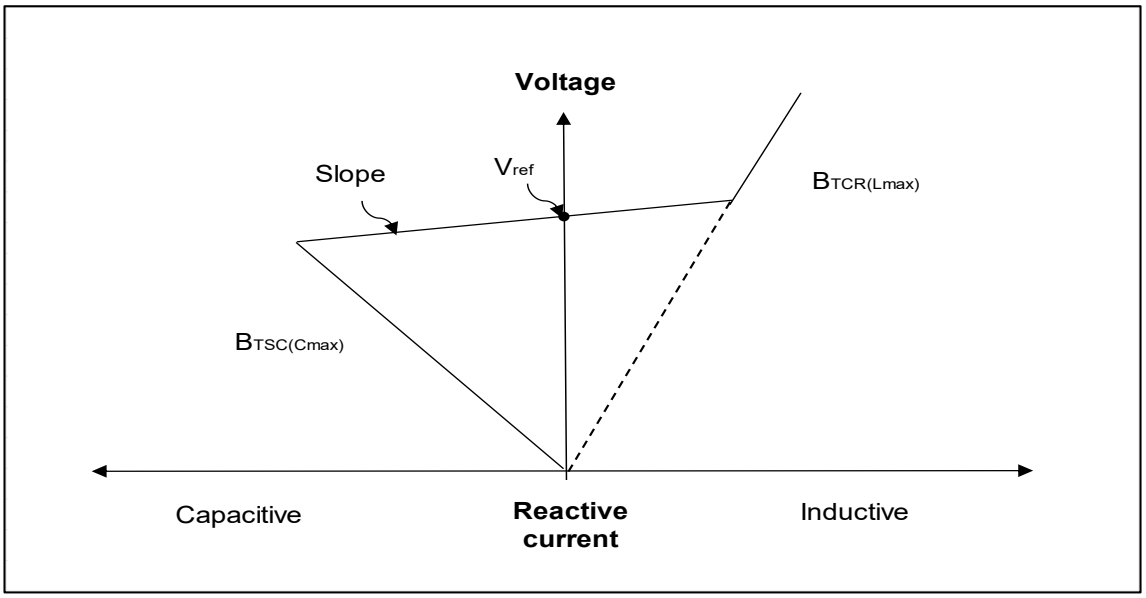

Figure 10. *SVC's V-I characteristics*

In voltage regulation, SVC's susceptance is varied to achieve the desired voltage level at PCC. As represented in Figure 10 of V-I characteristics, a SVC can maintain the constant voltage at a given reference value ($\mathrm{V_{ref}}$) while varying the output current (driven from variation in susceptance) over its range of controllability ($B_{\mathrm{TSC(Cmax)}} < B_{\mathrm{SVC}} < B_{\mathrm{TCR(Lmax)}}$) [37]. Outside its controllable range, SVC behaves like a capacitor during undervoltage condition and like an inductor during overvoltage conditions [38]. Hence, the amount of reactive power generated or absorbed in such conditions follows equation 3.5, as mentioned earlier.

Incorporating slope in SVC characteristic comes with the advantages of a significant reduction in its power rating, enabling parallel operation with other compensators to achieve cost-effective controlling objective and finally, slope helps in preventing SVC to reach its maximum operating limits quite frequently. [38]

Grigsby et al. [38] have suggested that SVC is more effective in voltage control operation when short circuit impedance of the system is quite high (e.g., weak grid) but its controller's response becomes sluggish in strong grid conditions. Mathur et al. [39] have rightly argued that there is no single configuration (e.g., FC-TCR, MSC-TCR, TSC-TCR, etc.) of SVC, which offers the best reactive power compensation solution. But considering,

operational frequency, response time, losses, capital cost, and other factors, “TSC-TCR” based SVC configuration is the most viable option [36].

3.3 STATCOM

The other important member of FACTS family is the static synchronous compensator (STATCOM). The primary aim of STATCOM is to provide the dynamic and fast reactive power compensation support to a network at the point of its coupling. [31] However, since it is a power conditioning device, hence, it can be implemented to solve other power quality related issues as well, such as harmonic filtering, load balancing, power oscillation damping, voltage regulation, etc. [2].

Like SVC, STATCOM is also a shunt connected compensation device, but its structure and operational principle differ from the SVC. Speaking of structure, STATCOM is a converter-based circuit, connected in parallel to the network through its coupling reactor and acting like a controllable voltage source. It is analogous to a synchronous machine in term of generating sinusoidal voltage with the fundamental frequency and freedom to control amplitude and phase-angle at its output. [31]

Since STATCOM is a self-commutated converter-based device and its generated reactive power is proportional to the PCC voltage, therefore it can generate one p.u. of reactive power even in significantly undervoltage conditions. On the other hand, thyristor-based devices like SVCs are not capable of doing the same because their shunt connected capacitor or reactor’s current capability is proportional to PCC voltage squared. Moreover, STATCOMs are smaller in size comparing to SVCs due to almost no requirement of passive elements and therefore have small footprints. Further, self-commutated converters offer a quick response which enables a STATCOM to control the reactive power faster and more precisely. Due to the modern power electronic switches (e.g., IGBT, IGCT), different converter topologies (e.g., modular multilevel converter), adequate control and modulation techniques, STATCOMs have been able to offer plenty of benefits. For example, lower harmonics emission, short term transient overloading capability, parallel power conditioning operations (e.g. harmonic filtering) and no inrush current generation etc. But some of the shortcomings of STATCOM, such as high capital cost and intricate control design, put it behind the SVCs, in term of world-wide implementation or popularity. [34]

3.3.1 Operation principle

Figure 11(a) depicts the single line diagram of a STATCOM. The main components of a STATCOM can be summarised as the DC capacitors, voltage source converters (VSC), coupling reactors, and a stepdown transformer. DC capacitor sometimes can be replaced with a DC energy source, if active power support from the STATCOM is also needed (e.g., application in wind farm). The main function of a capacitor is to provide constant DC voltage to the VSC, which is further connected in shunt mode with the mains supply through a coupling reactor and a stepdown transformer. A STATCOM can be viewed as a synchronous machine acting like a controllable voltage source behind the coupling reactance. [38]

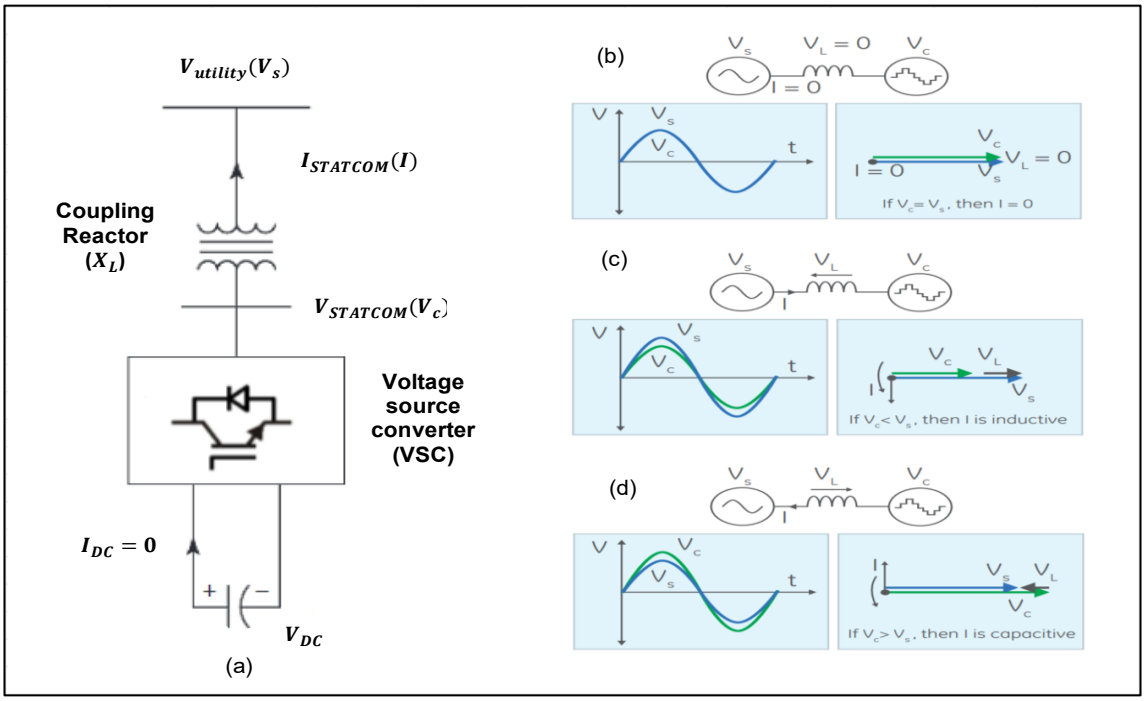

Figure 11. *STATCOM: (a) Single line diagram, (b) Standby mode, (c) Inductive mode, (d) Capacitive mode [38], [39].*

Reactive power compensation using a STATCOM is based on the concept of voltage amplitude difference. According to which, if STATCOM voltage (V_c) is higher than the connection point voltage (V_s) then a current ($I_{STATCOM}$) flows from the STATCOM to the connection point (e.g., PCC) and thus causes the generation of capacitive reactive power, shown in Figure 11(d). On the contrary, if V_c is lower than V_s then current flows from the connection point to STATCOM and causes the absorption of inductive reactive power, shown in Figure 11(c). However, if V_c and V_s both are equal in amplitude, then there will be no flow of current from either side. Thus, STATCOM will remain in standby mode as shown in Figure 11(b). [38]

To better understand the above stated fact, let's take the example of a STATCOM (V_c) connected to the utility supply point (V_s) through a coupling reactor X_L as depicted in Figure 11(a).

STATCOM current:

$$I_{\mathrm{STATCOM}} = (V_\mathrm{s} - V_\mathrm{c})/jX_\mathrm{L} = (V_\mathrm{s} - V_\mathrm{c}\angle -\theta)/jX_\mathrm{L} = (V_\mathrm{c}\, sin\,\theta - j(V_\mathrm{s} - V_\mathrm{c}\, cos\,\theta))/X_L \quad (3.7)$$

Here, I_{STATCOM} is the STATCOM current and θ is the phase angle of STATCOM voltage w.r.t to supply voltage.

Apparent, active and reactive power of the STATCOM:

$$S_{\mathrm{STATCOM}} = V_\mathrm{s} * I^*_{\mathrm{STATCOM}} = V_\mathrm{s} * ((V_\mathrm{c}\, sin\,\theta - j(V_\mathrm{s} - V_\mathrm{c}\, cos\,\theta))/X_\mathrm{L})^* \quad (3.8)$$

$$S_{\mathrm{STATCOM}} = P_{\mathrm{STATCOM}} + jQ_{\mathrm{STATCOM}} = (V_\mathrm{s}V_\mathrm{c}\, sin\,\theta + j(V_\mathrm{s}^2 - V_\mathrm{s}V_\mathrm{c}\, cos\,\theta))/X_\mathrm{L} \quad (3.9)$$

$$P_{\mathrm{STATCOM}} = (V_\mathrm{s}V_\mathrm{c}\, sin\,\theta)/X_\mathrm{L} \quad (3.10)$$

$$Q_{\mathrm{STATCOM}} = (V_\mathrm{s}^2 - V_\mathrm{s}V_\mathrm{c}\, cos\,\theta)/X_\mathrm{L} \quad (3.11)$$

From equation 3.10, it can be noticed that while varying the phase angle between STATCOM and connection point voltage, active power exchange can be controlled. However, considering STATCOM application for only reactive power compensation-based operations, we can assume that its active power exchange with the system is zero (if neglecting the losses); which is only possible when STATCOM and connection point voltage both are in phase (mean $\theta = 0$).

Therefore,

$$P_{\mathrm{STATCOM}} = (V_\mathrm{s}V_\mathrm{c}\sin 0°)/X_L = 0 \quad (3.12)$$

$$Q_{\mathrm{STATCOM}} = (V_\mathrm{s}^2 - V_\mathrm{s}V_\mathrm{c}\cos 0°))/X_\mathrm{L} = (V_\mathrm{s}^2 - V_\mathrm{s}V_\mathrm{c})/X_\mathrm{L} \quad (3.13)$$

Now, equation 3.13 concludes that if the magnitude of generated STATCOM voltage (V_c) is higher than the connection point voltage (V_s) then reactive power flows from the STATCOM to connection point (negative sign of Q_{STATCOM}; capacitive power). On the contrary, if V_c is lower than (V_s) then reactive power flows from connection point to STATCOM (positive sign of Q_{STATCOM}; inductive power).

Reactive power exchange of the STATCOM is enabled by the mechanism of input and output power of its converter (e.g., VSC). The converter is comprised of power electronic switches which directly connect the DC side of a STATCOM to its AC side output. Hence, if we neglect the losses, then the amount of instantaneous power should be equal at both of its AC and DC terminals. Active power provided by the DC source, as an input to the converter, will be zero if we assume that the converter is only responsible for reactive

power exchange. Also, DC source doesn't directly contribute to reactive power generation at the converter's output terminal. But it is the combined operation of DC source and switches with adequate control technique which connects the VSC's output terminal in a way that reactive currents circulate among the terminal phases and establish the reactive power exchange with the system. [38]

To establish reactive power exchange, DC capacitor voltage should remain fairly constant throughout the STATCOM operation. But losses within the converter cause the capacitor voltage to drop. These losses arouse mainly due to the switching of power electronic devices. Therefore, to maintain the required constant DC voltage, these losses should be feed from the AC mains. Additionally, some STATCOM applications are to provide both real and reactive power support. In such applications, DC source used at the converter side is a battery or energy storage (with a significant amount of active energy) which enables the real power support operation of a STATCOM during various network contingencies (e.g., faults, loss of mains, etc.). The exchange of real power between STATCOM and AC mains can be enabled while varying the phase angle between STATCOM voltage and connection point voltage. If STATCOM voltage is made to lead from the connection voltage, then the flow of real power will be from STATCOM to the AC mains. But if STATCOM voltage is made to lag by the connection point voltage, then real power will flow from AC mains to the STATCOM. [40], [41]

As depicted in Figure 12 of V-I characteristics, while participating in the reactive power compensation, a STATCOM can control its output current over the rated maximum capacitive and inductive range, irrespective to the system voltage. Because, it has the same current rating in both capacitive and inductive region which means certain MVA of a VSC provides the double dynamic range of MVAr to STATCOM. Further, it signifies that a STATCOM can produce continuous maximum capacitive current even with as low voltage as 0.15 pu. A STATCOM can be an effective solution when voltage support is required during the fault or post fault conditions, especially when low voltage or sudden voltage collapse create the bottleneck for other compensation devices (e.g., PHFs, SVCs). The dotted region in Figure 12 represents the increased transient limit of a STATCOM in both capacitive and inductive region, but operation here requires a pay-back time otherwise DC link voltage of STATCOM may vary. In the capacitive region, transient overcurrent is limited by the maximum turn-off capability of VSC's switches (e.g., IGBT) and in inductive range, it is limited by the maximum junction temperature of the switches. [36]

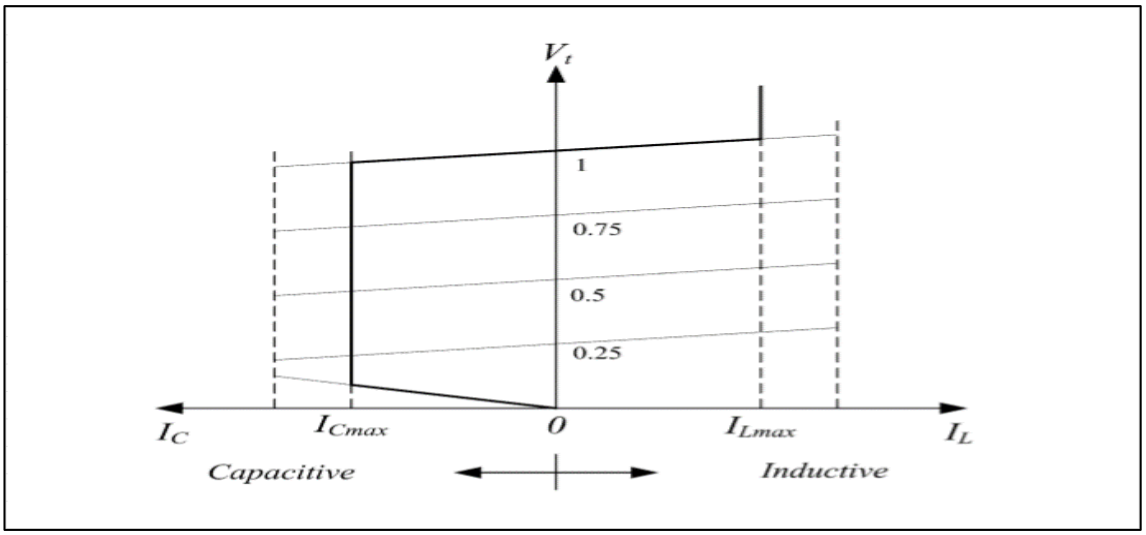

Figure 12. *STATCOM's V-I characteristics [42].*

The most vital part of a STATCOM is its converter. There are mainly two types of converters distinguished based on the DC source used; voltage source or current source converter. Voltage source converters (VSCs) usually have the capacitor as its DC source, and current source converters (CSCs) have inductor for the same purpose. Advantages of low THD, no need of bulky inductor and modularity make the VSCs a popular choice for the industrial application of STATCOMs. Further, STATCOM topologies depend on the type of converter and switching devices used. Speaking of switching devices, self-commutated controllable switches like gate turn-off thyristor (GTO), insulated gate bipolar transistor (IGBT) and integrated gate commutated thyristor (IGCT) have captured the majority of share in commercial applications. GTOs based VSCs are used in higher power rating applications wherein IGBT and IGCT based VSCs are used for the low to medium power applications. However, high power with IGBT and IGCT based VSCs can also be reached using MMC based topology. [43]

STATCOM topologies based on VSCs can be classified into two categories as multipulse and multilevel. And, STATCOM operation can be carried out based on two methods, namely fundamental frequency switching (FFS) and pulse width modulation (PWM). Since FFS based operations utilise low switching, hence they are stable in nature but may produce more harmonics if adequate converter topology (e.g., multilevel) is not used. On the other hand, PWM based operations are executed with the higher switching frequency, which contributes to higher switching losses. [44]

Multipulse converters are usually two-level converters with different pulse arrangements, such as two level- 6 pulse, 12 pulse, 24 pulse, etc. Higher pulse arrangements reduce the harmonic content in converter's output, but requirements of total switches and cou-

pling magnetics for such arrangements increase the total capital cost. Multilevel converters are mainly divided into three types as (a) diode clamped, (b) flying capacitor, and (c) cascaded multilevel converter. More level can be achieved in multilevel converters without using ample of power electronic switches. The presence of less switches in a converter facilitates its easy controlling operation as well as less losses and voltage stress on its switches. Besides these benefits, modularity feature of cascade type multilevel converters brings more edge to the STATCOM technology in term of flexibility to expand the solution according to its application (e.g., MV or HV), cheaper and faster manufacturing process, etc. Therefore, modular multilevel cascade converter (MMCC) or simply "Modular Multilevel Converter (MMC)" has certainly been able to attract the attention of engineers and FACT industries for its further R&D and application in HV/MV rated STATCOM solutions. [44]

3.3.2 MMC based STATCOM technology

H. Akagi [49], adequately argued that term 'modular' and 'multilevel' in Modular Multilevel Converter (MMC) technology doesn't provide any information to power electronics beginners about what its circuit configuration is really comprised of. Therefore, the right word would be modular multilevel cascade converters (MMCC) which now provides us the information that it's an arrangement of modular converters in cascade order. However, to keep up with industry practices, MMCC has been referred to MMC throughout this thesis work. MMC family has four members named as single-star bridge-cells (SSBC), single-delta bridge-cells (SDBC), double-star chopper-cells (DSCC) and double-star bridge-cells (DSBC), wherein cell means a "voltage source converter". Here, the very first difference is based on the cell configuration wherein bridge-cell refers to full-bridge converter (4 switches) and chopper-cell refers to half-bridge converter (2 switches). Second difference is based on the arm (cascade connection of bridge/chopper cell) arrangement either in delta or star configuration along with the center-tapped inductor used. However, speaking of reactive power compensation, only SSBC and SDBC based MMC configurations are widely used in STATCOM application. [45]

MMC based SSBC, or SDBC topology of a STATCOM is the cascade arrangement of full-bridge VSCs. A single full bridge VSC is called submodule (SM), shown in Figure 13(b), and connecting these submodules in series gives the one leg (phase) of MMC. Further, these legs either can be connected in delta (as shown in Figure 13(a)) or star configuration to form a three phase STATCOM solution. Here, one submodule is comprised of four solid state switching devices and a dedicated capacitor. Speaking of switching device, it may be GTO, IGBT or other self-commutated switches. In the case

of IGBT, an anti-parallel diode is connected to enable the flow of current in both directions. As depicted in Figure 13(c), if Vdc is the submodule capacitor voltage then every submodule can produce three voltage level as +Vdc, -Vdc and 0, while turning SM switches “ON” or “OFF” in different combination and instance. Having said that, the net voltage of a module/phase is the summation of each submodule’s voltage output. So, if there is ‘n’ number of submodules in a phase (module) then it will contain ‘2n+1’ voltage levels at its output terminal. For instance, a MMC comprised of 8 submodules (in each phase) produces the 17 level staircase like voltage at its respective output terminal, resembling very close to a sinusoidal waveform, as depicted in Figure 13(d). [42]

Peng et al. [46] suggested the first MMC based STATCOM technology in 1996 while outlining its benefits against the multilevel diode clamp and flying capacitor-based converters in high voltage applications. They argued that clamping diodes increase the total solution cost, come with the problems of packaging and parasitic inductance, which further limit their implementation up to maximum seven levels in practical use. Moreover, flying capacitor-based converters were expected to solve the voltage balancing problem in the multilevel application. But couldn’t achieve much success, since they require a large number of capacitors and high switching frequency based controlling techniques for capacitor voltage balancing. Alternatively, MMC technology came to rescue from these problems while eliminating the need for clamping diode and flying capacitor. Each full-bridge converter (SM) of MMC is feed through a separate DC source, potentially capacitor. Each SM is switched once in a line cycle and combining voltage of all SMs contribute to a multistep staircase voltage with significantly less harmonic content. Desired voltage level for a STATCOM application can be achieved while combining identical MMC submodules in series. Due to lower component involvement and simplicity of submodule structure, packaging of MMC modules is easy. Adding redundant submodules in each phase of the MMC structure increases its fault tolerance limit, and faulty submodule can be bypassed to provide uninterrupted system operation. [46]

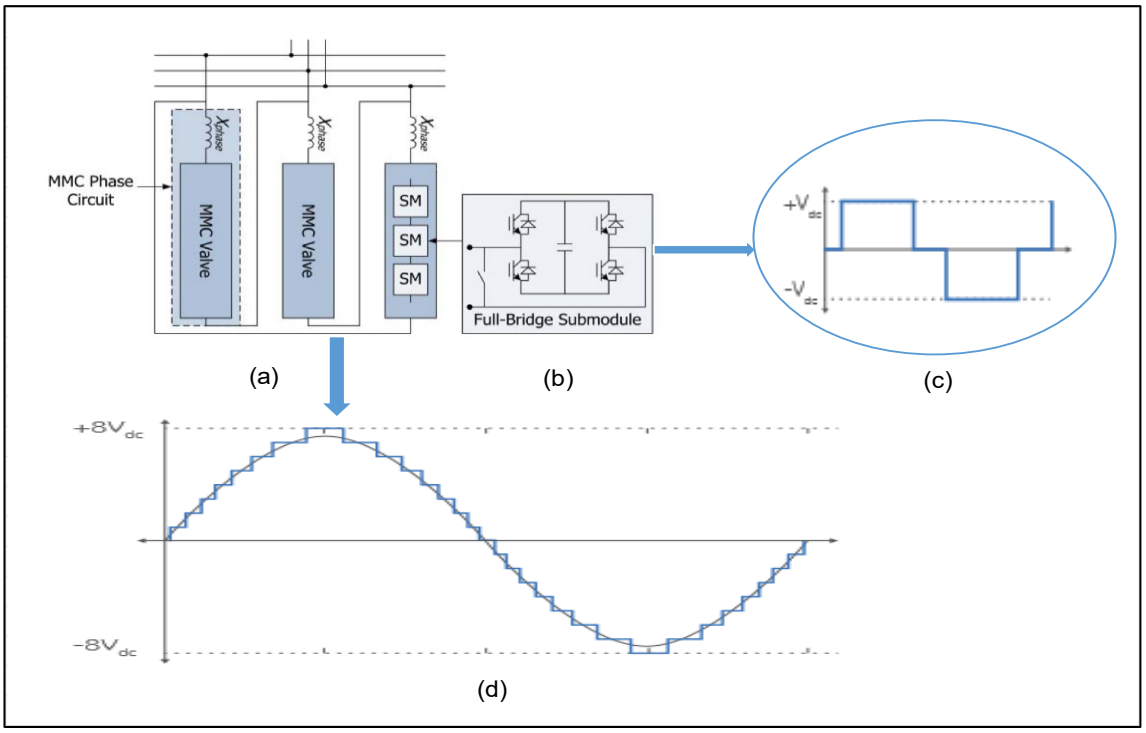

Figure 13. *(a) Single line diagram of SDBC-MMC based STATCOM, (b) Valve submodule of MMC, (c) one submodule's voltage output, (d) One phase voltage output of STATCOM [39], [47].*

3.3.3 STATCOM control

In this subchapter, control design of SDBC-MMC based STATCOM (or in short MMC based STATCOM) technology has been discussed. The overall STATCOM control has been discussed in the three main sections. First, control objectives have been briefly outlined, followed by the comparison of different control strategies currently used. Thereafter, theories facilitating system control, such as the stationary frame and synchronous reference frame, have been discussed. In last, control design of the studied STATCOM has been shortly explained.

MMC based STATCOM configuration comes with the advantages of modularity, zero sequence current based internal DC link arm balancing, high voltage, and high power capability with low rated components, etc. Nonetheless, these features of the said STATCOM entail complex control strategies. Moreover, it would be pertinent to mention that the choice of converter defines its control design requirements. In case of MMC based STATCOM configuration, control objectives can be mainly divided into the two parts; (a) control of exchanging current and thus the power between converter and connection point, (b) balancing of DC capacitor voltage. These objectives can be achieved through the linear or non-linear controller-based approach. [48]

Proportional Integral (PI) controller is the most straightforward controller used in STATCOM application. It is implemented in the synchronous reference frame (d-q) to carry out respective controlling actions. It requires robust synchronization and transformation of three-phase AC quantities into the DC quantities of rotating d-q domain. The other way to carry out controlling actions in linear mode is through directly working with three phase AC quantities (ABC frame). For instance, proportional resonant (PR) controller can implement the linear controlling methods based on the α-β frame or three phase frames. [48] Speaking of non-linear approaches, two main control strategies for STATCOM applications are used based on hysteria control and model predictive control (MPC) [49], [50].

Defining a control strategy which provides the best results is not an easy task since it depends on the plenty of aspects, such as computational burden, steady-state & dynamic behavior of the control technique used, type of converter, power rating and level of application (e.g. industrial, utility) [48]. So, in other words, performance requirements define the implementation requirements which further define the utilized control strategy and related technology.

Control scheme used for the studied STATCOM is based on the linear controller approach, especially PI and PR controllers. Here, the controlling strategy has been implemented partly in the synchronous reference frame and remaining in three phase frames, Figure 14 outlines the same. However, before discussing the purpose of every controlling block, the theory of synchronous reference frame and operation principle of phase locked loop (PLL) should be outlined shortly.

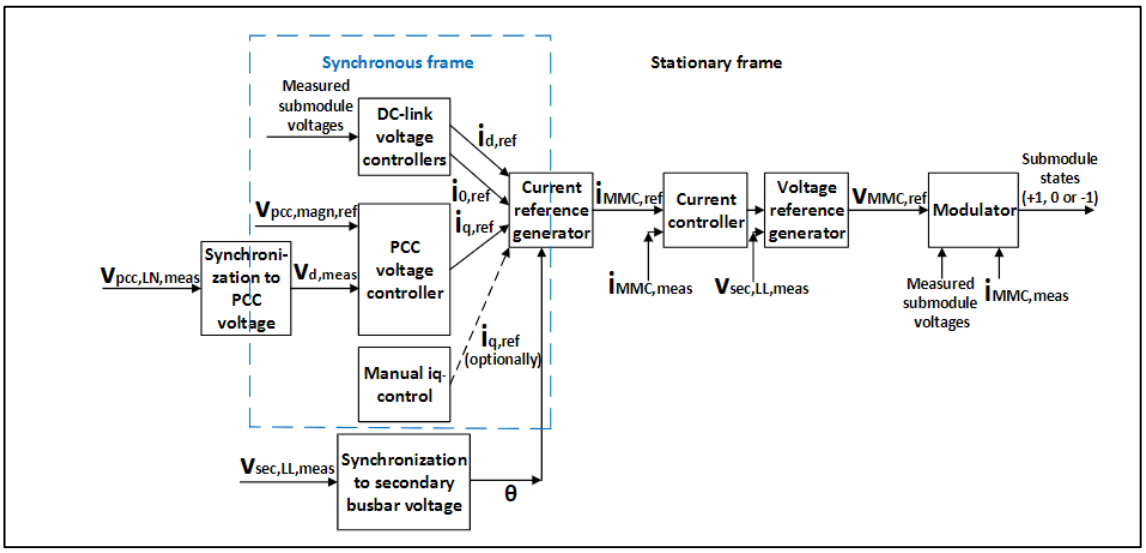

Figure 14. *Equivalent block diagram of STATCOM control [51].*

To save the computational time of controlling operation, three phase grid side or STATCOM quantities, especially current and voltage, are needed to be converted and altered in numbers and type of signal (AC to DC), without losing the essence of information. Therefore, synchronous reference frame theory employs the Clarke's and Park's transformation strategies to convert the three phase balanced AC quantities into the DC values (and/or space vectors) and thus can ease the entire controlling operation. [52]

Assume a three-phase balanced system where V_{a}, V_{b} and V_{c} are the instantaneous voltage values of phase a, b and c. Here, knowing the information of only two phases (e.g. V_{a} and V_{b}) can help to figure out the third one, because in balanced network V_{a}+V_{b}+$\mathrm{V_c}$ = 0. Hence, the notion that three phase balanced AC system can be retrieved through two phases leads to the advent of Clarke's transformation or stationary reference frame theory as shown in equation 3.15. [52]

$$\begin{bmatrix} V_{\alpha} \\ V_{\beta} \end{bmatrix} = \begin{bmatrix} 1 & -\frac{1}{2} & -\frac{1}{2} \\ 0 & \frac{\sqrt{3}}{2} & -\frac{\sqrt{3}}{2} \end{bmatrix} \begin{bmatrix} V_{\mathrm{a}} \\ V_{\mathrm{b}} \\ V_{\mathrm{c}} \end{bmatrix} \tag{3.15}$$

Here, V_{α} and V_{β} are voltage α and β- component. And, zero sequences component has been omitted due to the assumption of balanced three phase AC system where V_0 turn out to be zero.

Computing their values provides the information that they are shifted $90°$ apart from each other and therefore form a complex plane. Applying sum operator to these component values, for each instantaneous phase voltages, results into the space vector ($V_{\alpha\beta}$), rotating with fundamental angular frequency of ω, as shown in Figure 15. And, if we take the projection of stationary frame components (V_{α} and V_{β}) on a rotating reference frame (with complex plane) then these components can be reduced to DC values; due to the rotation with same angular frequency, space vectors seem standstill in synchronous frame. Thus, the process is called Park's transformation and can be represented through the following equation. [53]

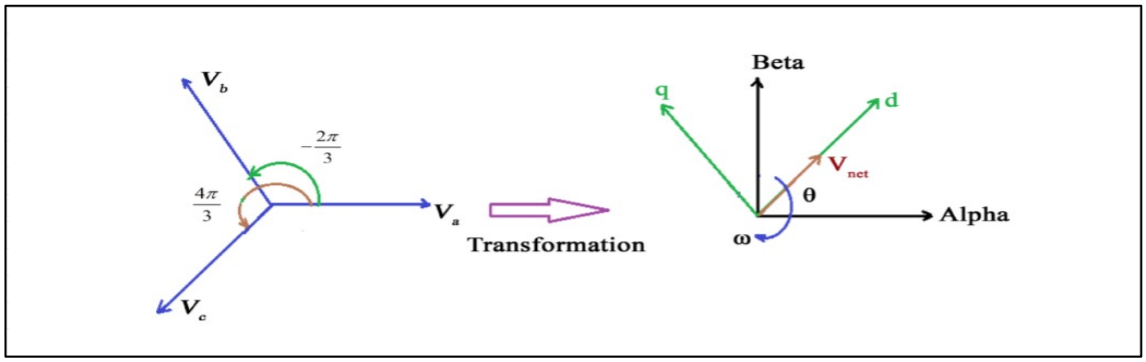

Figure 15. *Transformation to synchronous reference frame [53].*

$$\begin{bmatrix} V_{\mathrm{d}} \\ V_{\mathrm{q}} \end{bmatrix} = \begin{bmatrix} \cos\theta & \sin\theta \\ -\sin\theta & \cos\theta \end{bmatrix} \begin{bmatrix} V_{\alpha} \\ V_{\beta} \end{bmatrix} \tag{3.16}$$

Where V_d and V_q are the voltage d and q components of a three phase AC voltage in the synchronous reference frame. And, angle θ represents the transformation angle.

To solve equation 3.16, α and β component values are computed through the Clarke's transformation, and information on transformation angle using a synchronous reference frame (SRF) based PLL controller. PLL is a PI controller, based on the feedback control loop to track the phase angle of its input signal. In SRF PLL, the transformation angle (PLL-output) value is measured until V_d component comes in alignment with the grid vector voltage (PLL-input). Confirming such alignment is based on the value of q component. Because when V_d will be aligned with grid voltage then V_q component becomes zero and same can be understood with the following equation. [53]

After solving equation 3.15 and 3.16:

$$\begin{bmatrix} V_{\mathrm{d}} \\ V_{\mathrm{q}} \end{bmatrix} \approx \mathrm{V_m} \begin{bmatrix} \cos(\omega t - \theta) \\ \sin(\omega t - \theta) \end{bmatrix}, \text{ if } \theta \approx \omega t \text{ then } V_{\mathrm{d}} \approx V_{\mathrm{m}} \text{ and } V_{\mathrm{q}} \approx 0 \tag{3.17}$$

Where, V_{m} is the voltage magnitude of grid voltage, ωt is the actual voltage vector angle and θ is the PLL's tracking angle. Hence, when θ is close to the actual angle then $\sin(\omega t - \theta)$ tends to approach zero, which in turn makes the V_q component also zero. Hence, d component now equals to the magnitude of grid voltage. Further, utilising this information of voltage components, the instantaneous power in synchronous reference frame can be calculated as follows.

$$S = P + jQ = V_{\mathrm{dq}} I^{*}_{\mathrm{dq}} = \left(V_{\mathrm{d}} + jV_{\mathrm{q}}\right) * \left(I_{\mathrm{d}} - jI_{\mathrm{q}}\right) = \left(V_{\mathrm{d}} I_{\mathrm{d}} + V_{\mathrm{q}} I_{\mathrm{q}}\right) + j(V_{\mathrm{q}} I_{\mathrm{d}} - V_{\mathrm{d}} I_{\mathrm{q}}) \tag{3.18}$$

Putting $V_{\mathrm{q}} = 0$ from the equation 3.17.

$$P = V_{\mathrm{d}} I_{\mathrm{d}} \tag{3.19}$$

$$Q = -V_{\mathrm{d}} I_{\mathrm{q}} \tag{3.20}$$

Equations 3.19 & 3.20 show that when voltage d component is aligned with the grid vector voltage then instantaneous active power is associated with its direct current and instantaneous reactive power with its quadrature current component. Consequently, utilising this d-q theory, three phase quantities of STATCOM can be converted such that its reactive and active power can be controlled independently. Or in other words, nature of operating with the DC values makes the synchronous reference frame theory (d-q theory) a classical choice for the linear control of a STATCOM.

STATCOM control design is largely influenced by its type of application. Studied STATCOM has been chosen for the application of reactive power compensation and active harmonic filtering. For such an application, active and reactive current components of STATCOM are the main control variable. Therefore, a cascade control strategy has been adopted in two main sections; (1) inner current controller, (2) cluster voltage controller. The inner current controller is used for controlling the output current while generating adequate voltage references for the modulator. On the other hand, the function of cluster voltage controllers is to regulate the capacitor DC voltage while determining the reference values of direct current and zero sequence current. In the end, references for the quadrature current component can be either generated by the voltage controller or a manual reactive power controller can be implemented. [48]

Starting with synchronisation block, it is used for tracking line to neutral fundamental voltage at the point of common coupling (primary side of coupling transformer) and produces the direct voltage component (V_{d}) of PCC voltage, while controlling its quadrature component (V_{q}) to zero. The output of this synchronisation block is the magnitude value of $\mathrm{V_d}$ which is equal to the magnitude of $V_{\mathrm{pcc,LN,meas}}$ but in d-q domain. Another synchronisation block used is for tracking the secondary busbar voltage, but here output is the transformation angle post synchronising three phase $V_{\mathrm{sec,LL,meas}}$ voltage in the d-q domain. [51]

Second, dedicated voltage controllers for specific tasks have been assigned. Type of controller used here is PI (proportional integral) since controlling variables are DC values in the d-q domain. PCC voltage controller generates the reference for current q-component ($\mathrm{i_q}$), because the amount of reactive power generated or absorbed is proportional to the quadrature current i_{q}, as shown in equation 3.20. The reference for $i_{\mathrm{q,ref}}$ is generated by monitoring the magnitude difference of measured d-component PCC voltage ($V_{\mathrm{d,meas}}$) and provided reference PCC voltage ($V_{\mathrm{pcc,magn,ref}}$). DC-link voltage controllers are comprised of two PI-controllers. DC capacitor voltage may deviate from its nominal value due to general losses in VSC: conduction and switching losses in IGBTs and diodes along with some capacitor losses. Further, these losses can be compensated through active power absorption from the grid, as shown in equation 3.19, and it is proportional to the current d-component. First PI-controller helps in maintaining the average DC voltage in all three branches while producing the required reference for current d-component ($i_{\mathrm{d,ref}}$). Further, deviation in DC capacitor voltage, caused by the unbalanced supply conditions, can be compensated with circulating zero sequence current in the

delta branches of MMC. Hence, second PI-controller is used to generate the reference for zero sequence current ($i_{0,\mathrm{ref}}$). [51]

Third, there is a current reference generator which combines and converts all current references (in d-q frame) coming from the voltage controllers into a single current reference value, $I_{M\mathrm{MC,ref}}$ (in ABC frame) for each of the MMC phases. The transformation angle used here comes from the synchronisation block of secondary busbar voltage. Fourth, there is the current controllers wherein control variables are in the three phase quantities, hence PI controller can not be used any longer. Therefore, three PR (proportional resonant) controllers are used, for each of the MMC branches. Main function of the current controller is to minimise the difference between MMC current reference generated and MMC current value measured ($I_{\mathrm{MMC,meas}}$) in each of the delta branches. Thereafter, the output of current controller and measured line to line secondary busbar voltage ($V_{\mathrm{sec,LL,meas}}$) with harmonics or only fundamental is feed into the voltage reference generator which as a result generates the adequate voltage reference ($V_{\mathrm{MMC,ref}}$) for MMC modulator. [51]

3.3.4 Modulation technique

The switching function of a converter is defined by its modulation technique. A good modulation technique will ensure that the converter's generated voltage is close to the desired voltage value, the converter has low switching losses and improved harmonic performance, etc. The real problem comes in applying the traditional modulation methods to multilevel topology, due to the involvement of large cell numbers. In fundamental switching frequency (FSW) based modulation, commutation of each cell happens only once per fundamental cycle. Multicarrier pulse width modulation (PWM) is based on the comparison of carriers and reference signals. Hybrid PWM is the combination of both FSW and carrier PWM based switching. Space vector modulation (SVM) utilises the theory of space vector wherein best switching combinations and their operational time (based on the reference signal) are varied within a control cycle to generate almost sinusoidal shape output. [48]

For the studied STATCOM, voltage reference generator provides the three-phase reference values of MMC voltage (to be produced) as an input to the modulator. After processing, modulator converts this information into the state of submodule as +1, -1 or 0. Where +1 means submodule is connected and should produce +V_{DC} voltage at its output terminal, -1 means it is connected and should produce -V_{DC} voltage at the output terminal and in the end 0 means submodule should be bypassed.

However, DC capacitor voltage of submodules, when connected, may drop with respect to their nominal value or rise as well depending upon the active power flow within the converter. But it should remain unchanged when the submodule is completely bypassed. Uneven DC voltage distribution has detrimental effect on the submodule capacitors. Therefore, an algorithm is used as the part of modulator functions which ensure the balancing of DC voltage while choosing the adequate submodule to be connected or bypassed, depending upon the measured submodule voltage and direction of active power flow.

4. AHF EFFECTS ON THE STATCOM DESIGN

MMC technology is a popular choice for the application of STATCOM and active harmonic filtering simultaneously due to its quality of being modular, scalable, and involvement of fewer electronic devices, etc. Freedom of including many submodules in MMC design results in decreasing the switching frequency of semiconductor devices within the submodule, high overall switching frequency, and wider control bandwidth of the converter. Hence, aforesaid advantages of MMC technology give it an edge in comparison to other counterparts of power conditioning solutions. [54]

In this chapter, system studies for an effective design of STATCOM (SDBC based MMC technology) participating in parallel operation of reactive power compensation and active harmonic filtering (for low order harmonics) have been carried out. Hence, to achieve the main objectives of this thesis, first, the system limitations (e.g., IGBT current, DC link voltage ripple) of studied STATCOM, along with their causes, have been discussed. Thereafter, the simulation environment providing information on components used, their parameter details, assumptions made to alter system function (if any), and other operational boundaries have been explained.

Continuing further, basic scenarios for studied STATCOM, operating only in RPC mode (both capacitive and inductive), have been worked out. The basic scenarios provide the information on STATCOM design (e.g., used number of submodules, coupling reactor value, etc.) before adding AHF functionality to it. Once system limitations and information on the basic STATCOM design (with RPC mode only) have been carried out, then the next task was to simulate the different scenarios of combined RPC and AHF operation. Subsequently, system parameters (or design in general) associated with the simulation results of combined RPC and AHF scenarios (chapters 4.3. and 4.4) have been compared and analysed with the results of basic scenarios (RPC only), to assess the feasibility of an effective STATCOM design.

In last, it was of interest to clarify that there is no terminological difference between the term “STATCOM and “VSC.” The term STATCOM has been referred to an overall product which includes, VSCs, coupling reactor, and other components. However, term VSC has only been used to explicitly specify the converter part of studied STATCOM and its related operation.

4.1 System limitations

While operating in RPC mode, studied STATCOM either produces or absorbs the reactive current, depending upon the magnitude difference between its terminal voltage and voltage at the PCC. Moreover, active current flows from the grid to the converter while making STATCOM's voltage lagging by the PCC voltage with a small angle. The main application of active current is to feed the converter losses, and it is usually very small in magnitude. Hence, so far, it has been realized that overall STATCOM current (or VSC current) is comprised of two main components as active and reactive current. But there is another current component known as zero-sequence current. As mentioned in chapter 3.3.1, zero sequence current is the circulating current inside the delta winding of three-phase STATCOM branches. This current component is used for balancing the DC-link branch voltages of the STATCOM.

Additionally, if AHF functionality of studied STACOM is also enabled, then one more current, known as harmonic filtering current, got added to the list of STATCOM current components. Therefore, in combine RPC and AHF operation of studied STATCOM, its net current will be comprised of four current components such as, reactive current, active current, zero sequence current, and harmonic filtering current. Rating of this net STATCOM current depends on the various factors such as system components used (e.g., power electronic switches), level of application (e.g., MV, HV) and, etc.

Studied STATCOM has been implemented for the HV/MV application, wherein detailed information on system parameters will be provided later in chapter 4.2. Speaking of components, VSCs used inside the STATCOM have a significant influence on its current rating. MMC based STATCOM technology uses the series combination of VSCs to form a leg. Further, a VSC is comprised of four semiconductor switches (one switch comprising of IGBT and diode), and therefore maximum current carrying capability of these switches is one of the deciding factors for the overall STATCOM or VSC current (I_{VSC}) rating [61]. Characteristics of module packaging influence the VSC current rating too [55]. The RMS value of VSC current and its relationship with other current components (also in RMS) can be summarised as following [4].

$$I_{\mathrm{VSC}} = \sqrt{I_{\mathrm{VSC(1)}}^2 + I_{\mathrm{VSC(h)}}^2} \tag{4.1}$$

Here, I_{VSC} is the RMS value of VSC current, $I_{\mathrm{VSC(h)}}$ is the RMS value of VSC harmonic filtering current and $I_{\mathrm{VSC(1)}}$ is the RMS value of VSC fundamental current component.

As per the theory of harmonics, RMS value of net harmonic current squared (and in this case harmonic filtering current generated by VSC) is nothing but RMS currents of different frequencies added in squares, as mentioned below. [4]

$$I^2_{\mathrm{VSC(h)}} = I^2_{\mathrm{h2,rms}} + I^2_{\mathrm{h3,rms}} + I^2_{\mathrm{h4,rms}} + I^2_{\mathrm{h5,rms}} + \cdots = \sum_{\mathrm{k=2}}^{\infty} I^2_{\mathrm{hk,rms}} \quad (4.2)$$

Where, $\mathrm{I_{hk}}$ represents the RMS values of different harmonic (frequency) currents, such as 2nd, 3rd, 4th and 5th harmonics respectively.

Referring to the operational principle of STATCOM described in chapter 3.3.1, active component of VSC (STATCOM) current is in phase with the PCC voltage but quadrature to its reactive current component. Hence, applying the same principle to fundamental VSC current, it can be constituted as follows.

$$I^2_{\mathrm{VSC(1)}} = I^2_{\mathrm{VSC(active)}} + I^2_{\mathrm{VSC(reactive)}} \quad (4.3)$$

Where, $\mathrm{I_{VSC(active)}}$ is the active current component of VSC's fundamental current and $\mathrm{I_{VSC(reactive)}}$ is the reactive current component of the same.

Thus, using equation 4.3 and 4.2, RMS value of VSC current can be rewritten as mentioned below.

$$I_{\mathrm{VSC}} = \sqrt{I^2_{\mathrm{VSC(active)}} + I^2_{\mathrm{VSC(reactive)}} + \sum_{\mathrm{k=2}}^{\infty} I^2_{\mathrm{hk,rms}}} \quad (4.4)$$

However, equation 4.4 doesn't include the information on zero sequence current, needed to balance the DC link voltage among the VSC's branches due to network contingencies (e.g. unsymmetrical load, faults, etc.). This zero-sequence current ($I_{zero,rms}$) when added arithmetically, to consider worst case (since the phase angle of zero sequence current varies between different scenarios), with VSC's active current, reactive current and filtering current's square root values provide the overall RM rating of VSC current, as mentioned below

$$I_{\mathrm{VSC(overall)}} = \sqrt{I^2_{\mathrm{VSC(active)}} + I^2_{\mathrm{VSC(reactive)}} + \sum_{k=2}^{\infty} I^2_{\mathrm{hk,rms}}} + I_{\mathrm{zero,rms}} \quad (4.5)$$

Equation 4.5 represents the rated RMS value of the overall VSC (STATCOM) current and has limitation of 1000 A in the delta winding of the studied STATCOM, due to earlier mentioned reasons (e.g. IGBT switch, internal busbar, etc.). Moreover, peak value of instantaneous VSC current $I_{\mathrm{VSC\_peak}}$ for the studied STATCOM is restricted to 2100 A.

Speaking of voltage, studied STATCOM has two limitations. First, safety margin or remaining capacity between DC link voltage and the peak of VSC's voltages, after producing the desired VSC voltage. In RPC operation, DC link voltage of VSC oscillates at

second harmonic (twice the fundamental frequency) and affects the number submodules required to produce the desired VSC voltages and so thus the currents. Choosing a smaller number of submodules than the required values results in not having enough capacity in DC link voltage to produce the desire VSC voltage. To validate whether chosen number of submodules is enough to produce required VSC voltage, one of the possible ways is to plot DC link voltage and VSC reference voltage together in a x-y plane. Once plotted, the peak value of VSC reference voltage should be less than the DC link voltage. The margin between VSC reference voltage peak and DC link voltage ensure enough voltage capacity in DC link to produce the desired VSC valve voltage. And, in this thesis it was assumed that any value of remaining DC link capacity between 1kV to 3kV is an adequate safety margin.

Second voltage-based limitation is related to the insulation level of studied STATCOM's valve voltage. Here, the maximum phase-to-phase RMS value of secondary bus bar voltage (secondary side of STATCOM transformer) and STATCOM valve RMS voltage should stay well below 72.5 kV RMS insulation level given in the IEC 60071-1 standards. [56]

4.2 Simulation setup

To investigate the impact of combine RPC and AHF operation on system design, already available PSCAD based STATCOM simulation model is used and its parameters are changed to correspond the studied STATCOM. Here, some changes to the harmonic controls of the used simulation models are also carried out to investigate the design issues better. This model is comprised of an ideal voltage source, network impedance, a step-down transformer (Y-d), and in last, a shunt connected STATCOM. The ideal voltage source used is capable of producing positive and negative sequence voltages at 50 Hz of the fundamental frequency. A set up of three-phase voltage sources in delta arrangement has been referred as a modular multilevel converter. The three-phase voltage output of the modeled STATCOM is in alignment with the control operation, and the modulation technique explained in chapters 3.3.3 and 3.3.4, respectively. Further, the STATCOM model is also comprised of coupling reactors, parasitic resistances, and other measurements (e.g., current, voltage, harmonic, etc.) devices. Referring to Figure 16, it represents all the aforementioned system components in the form of a simplified single line diagram.

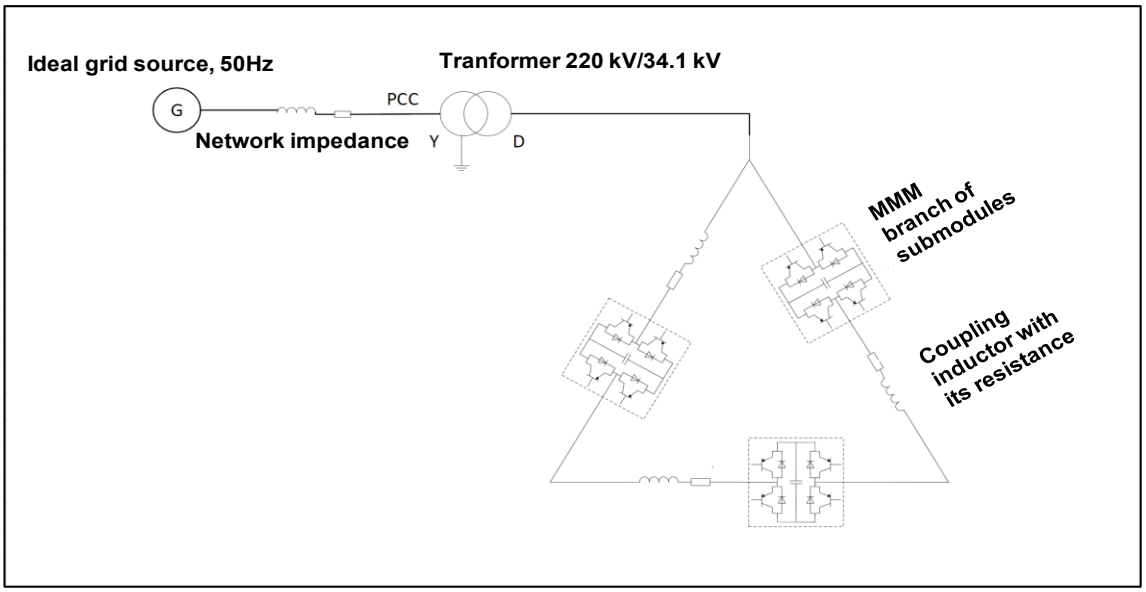

Figure 16. *Single line diagram of simulation model [51].*

An effective STATCOM design can be worked out while considering all possible worst conditions the overall system can offer. Starting with the network, one of the possible worst situations to a STATCOM operating with harmonic filtering is when network impedance is at its lowest, a phenomenon described in chapter 4.4. Here, low impedance requires a rather high harmonic filtering current to compensate for the same level of voltage distortion in comparison to other higher network impedance values. For example, for simplicity of the analysis, there are no harmonic voltages in the network which to be actively filtered. Instead network is short-circuited, and harmonic current control mode is used to mimic the harmonic voltage filtering in different network scenarios. With Thevenin equivalent network, it would be difficult to create small impedance operation points for harmonics (which exist in the real networks). Therefore, unreasonably high network harmonic voltages should be used in the simulations to get large harmonic current outputs from STATCOM which are of primary interest from design point of view. With the short-circuited network even large harmonic currents produced by STATCOM do not cause harmonic voltages to PCC. In the simulations, the need for active harmonic filtering current (harmonic current reference) is determined by the user.

Manual current q-component control is used in all simulations to enable RPC operation of studied STATCOM and reference value of current q-component ($I_{\mathrm{q,ref}}$) has been supplied accordingly to generate the desired reactive current. To enable AHF operation, the harmonic current control mode of studied STATCOM has been used and the reference value of desired current harmonics is supplied accordingly. To make sure generated harmonic current follows its reference value, resonant branches for respective harmonics,

with adequate gain value, have been added to the existing PR controller. Adding references of reactive current, harmonic current, zero sequence current and active current results into overall VSC current reference ($I_{\mathrm{VSC,ref}}$). But before adding them together, adequate limitations (according to the current priority- reactive or harmonic) to restrict overall VSC current RMS value below 1000 A (in delta winding) has been used inside the current reference generator.

The overall simulation results have been categorised into two chapters of 4.3 and 4.4 respectively, based on different priority modes of STATCOM's RPC and AHF operations. Thus, details on chosen system parameters have also been discussed at the beginning of those chapters accordingly. In last, actual simulation model may include more components, parameters, and functions but since they do not contribute much in the understanding of this work, therefore have not been explained here.

4.3 Case 1: RPC operation prioritized over AHF

In this chapter, investigation on how the combined operation of RPC and AHF of studied STATCOM affects its design has been carried out. Here reactive power compensation is prioritised over harmonic voltage filtering. For example, if 50 % capacity of a 100 MVAr rated STATCOM is needed for reactive current, then rest can be used to produce the filtering current. The sequence of prioritisation has been chosen in a way that first zero sequence current is prioritized, and second is active fundamental frequency current, then reactive fundamental frequency current and in last harmonic filtering current. Here, zero sequence current and active fundamental frequency current need to be prioritized first since without them the STATCOM DC-link voltage control would be lost and STATCOM could not operate.

In a balanced network, harmonics of different order have certain type of sequence (e.g. 3rd harmonic as zero sequence). However, in practical application electricity network is usually unbalanced. Having said that, sequence theory of harmonics is no longer applicable because same harmonic (as with balanced network) now can be of any sequences, for instance, 3rd harmonic can be of positive, negative or zero sequence in nature.

Studied STATCOM is made of three phase submodule branches placed in a delta arrangement, and therefore it can not generate a harmonic current, which is zero sequence in nature. Considering the abovementioned issues, zero sequence type of harmonic filtering current can not be produced by the studied STATCOM. Therefore, it has been decided that, initially design cases would be carried out to investigate the impact of dif-

ferent magnitudes and harmonic orders of filtering current. Here, phasor rotation of harmonic current would be chosen as positive sequence in nature. But later, same harmonic currents will be simulated as negative sequence to analyse the impact of phasor rotation on the design process as well.

In this part of the simulation, the chosen grid side line to line (L-L) RMS voltage was 220 kV (1.0 per unit) in magnitude, positive sequence in nature and perfectly sinusoidal at 50 Hz. Network impedance was short circuited; explanation given in chapter 4.2. Transformer with YNd11 connection, 220 kV primary side nominal L-L RMS voltage, 34.1 kV secondary side nominal L-L RMS voltage and leakage reactance of 0.10 per unit (p.u) was chosen. STATCOM was rated at 100 MVAr of power. Capacitance of one submodule was 7000 μF. The inductance of coupling coil was chosen to be 13 mH. Information on number of submodules used per branch was retrieved after simulating the basic scenario as mentioned in chapter 4.3.1. Moreover, detailed information on network and STATCOM parameter have been enclosed in Appendix A, Table 1.

Speaking of designing approach of case-1, first the basic scenarios have been worked out; providing information on the needed number of submodules with capacitive and inductive operating point in RPC mode only. Thereafter, simulation results showing effect of required VSC voltage waveform and VSC DC-link voltage waveform on needed number of submodules due to different combination of fundament reactive and harmonic filtering current, have been carried out. In all scenarios, current and voltage limitations mentioned in chapter 4.1 were also considered.

The main objective of case-1 simulations was to figure out the worst-case design of studied STATCOM. This design should be valid in both the capacitive and inductive operating points of the STATCOM. But harmonic filtering in overvoltage situation (e.g. 1.35 p.u of PCC voltage) has been assumed to be disabled since practical priority in such condition is to maintain the nominal reference voltage at the PCC (e.g. 0.9 to 1.10 p.u). Therefore, the entire current capacity was used to produce only fundamental inductive current. On the other hand, worst case STATCOM design with AHF in capacitive operating point has been worked out with scenarios of different combine requirements of fundamental reactive current and harmonic filtering current. Freedom with fundamental reactive was only to choose its different magnitude. But harmonic filtering current was manipulated with different magnitude, different harmonic orders and phase sequences (positive or negative only). A scenario of harmonic filtering current comprising several frequencies (harmonic order) was also considered. In last, apart from the reactive and harmonic filtering current, impact of coupling reactance and transformer reactance on effective STATCOM design have been investigated.

4.3.1 Basic design with RPC mode only

A 100 MVAr STATCOM was dimensioned based on two extremes. First, maximum continuous voltage where maximum capacitive current should be produced. Second, the short-time overvoltage situation where maximum inductive current should be produced. Chosen network voltage values were 1.10 p.u for maximum continuous voltage in extreme capacitive operating point and 1.35 p.u for overvoltage condition in extreme inductive operating point. Fundamental capacitive and inductive current in both extreme operating points were rated with +1.0 p.u and -1.0 p.u (or ±1.0 kA) respectively. As per the basic design, the required number of submodules (SMs) to produce ±1.0 p.u of fundamental reactive current in both extreme operating points was 34. To validate this submodule number, some current and voltage results with aforesaid operating point values, system parameters described at the beginning of chapter 4.3 and system limitations defined in chapter 4.1 were simulated with PSCAD model and shown in Figure 17 and Figure 18 respectively.

Figure 17 represents the current and voltage results simulated in the maximum capacitive operating point to produce fundamental reactive current. Figure 17(a) shows the waveforms of DC link voltage labelled as *"*VDC_tot_AB*"*, VSC's reference & produced valve voltage as *"*Vvsc_ref_AB and Vvsc_valve_AB*"* and MV busbar voltage as *"*VMV_AB*"* respectively. Figure 17(b) represents the waveforms of VSC's reference and produced phase current in delta winding labelled as *"*Ivsc_ref_AB and Ivsc_AB*"* respectively. To simulate these results, manual current q-component ($I_{\mathrm{q,ref}}$) control mode was chosen to produce 1.0 p.u of fundamental capacitive current.

Figure 17(a) shows that with 34 SMs, the maximum of DC link voltage ($V_{\mathrm{DC\_max}}$) is 66.78 kV and the peak of VSC reference voltage ($V_{\mathrm{VSCref\_peak}}$) is at 63.82 kV. This signifies that there is 2.96 kV of voltage capacity left in DC link. A safety margin to avoid overlapping between DC link and peak of VSC reference voltage, or to ensure enough capacity in DC link to produce required voltage, should be chosen (e.g. between 1.0 to 3.0 kV). Increasing the number of SMs (e.g. 35) from this point would result into more than required free capacity in DC link voltage and thus not an effective design. Decreasing number of SMs (e.g. 33) would result into overlapping of $V_{\mathrm{DC\_max}}$ and $V_{\mathrm{VSCref\_peak}}$ and thus violation of one of the system limitations defined in chapter 4.1.

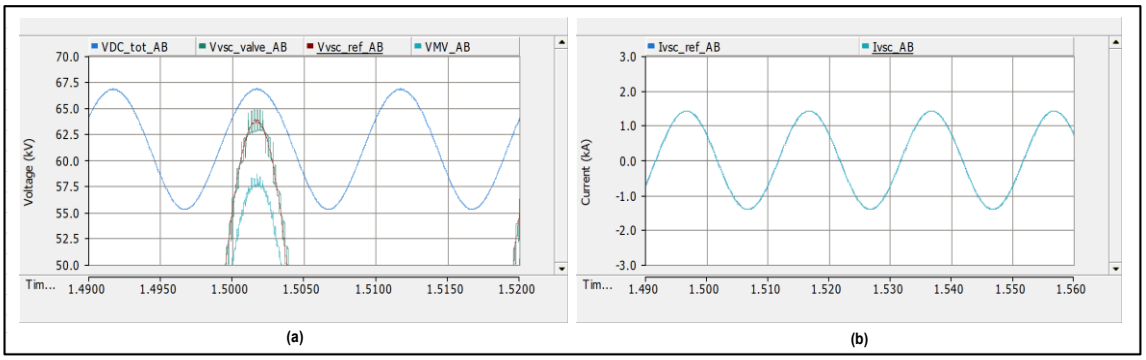

Figure 17. *Simulated (a) DC link, VSC valve and MV busbar voltages in maximum capacitive operating point (MCOP), (b) VSC phase current in delta winding*.

Here, RMS value of MV busbar voltage and VSC valve voltage also remains below 72.5 kV. Figure 17(b) shows that peak of VSC current ($I_{\text{vsc\_peak}}$) stays below 2.1 kA and its RMS value ($I_{\text{vsc\_rms}}$) is 0.9997 kA. Consequently, these results comply with all of the current and voltage limitations mentioned in chapter 4.1. Thus 34 submodules for maximum capacitive operating point is the valid number for an effective STATCOM design.

Thereafter, current and voltage results for maximum inductive operating point, to produce fundamental reactive current, were simulated and shown in Figure 18. To simulate these results chosen grid source voltage and $I_{\text{q,ref}}$ values were 1.35 p.u and -1.0 p.u (- sign for inductive current) respectively. And, number of SMs chosen was 34.

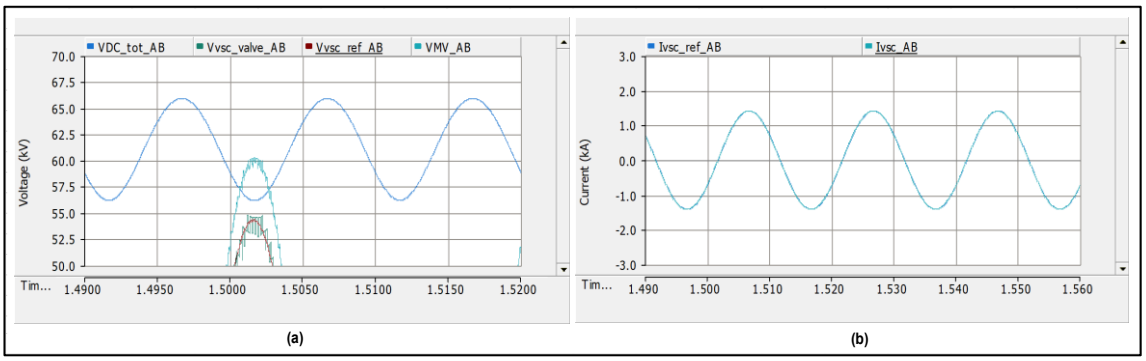

Figure 18. *Simulated (a) DC link, VSC valve and MV busbar voltages in maximum inductive operating point (MIOP), (b) VSC phase current in delta winding*.

Unlike capacitive, in extreme inductive operating point, maximum of DC link voltage and peak of VSC valve voltage are not aligned. But it is the minimum of DC link voltage ($V_{\text{DC}_{\text{min}}}$) and peak of VSC reference voltage which creates the bottleneck, if aligned. Figure 18(a) shows that with 34 submodules, value of $V_{\text{DC\_min}}$ is 56.18 kV and value of $V_{\text{VSCref\_peak}}$ is at 54.37 kV. This signifies the free capacity of 1.81 kV in DC link voltage. Changing the number of submodules further (e.g. 33 or 35) either results into no free

voltage capacity or more than required voltage capacity in DC link voltage. Moreover, RMS values of MV busbar and VSC valve voltages were also below 72.5 kV.

In Figure 18(b), value of $I_{\text{vsc\_peak}}$ stay below 2.1 kA and $I_{\text{vsc\_rms}}$ turned out to be 0.9998 kA. Hence, results shown in Figure 18 comply with all of the current and voltage limitations mentioned in chapter 4.1. Thus 34 submodules for maximum inductive operating point is the valid number for an effective STATCOM design.

So far, a basic design, in term of number of submodules, for the maximum capacitive and inductive operating point of fundamental reactive current has been carried out. Here, 34 submodules sought to be enough for producing maximum fundamental capacitive and inductive current in both operating points. Value of safety margin to ensure enough DC link voltage capacity has been assumed to be in between 1.0 to 3.0 kV.

4.3.2 AHF current's phase angle impact on design

In combine RPC and AHF operation, VSC's output current is comprised of fundamental current and harmonic components of filtering current. The magnitude reference of fundamental reactive current is computed through equation 3.7, mentioned in chapter 3.3.1. And, its phase angle references are either leading or lagging the VSC voltage by 90°, depending upon the operating point (inductive or capacitive). In case of harmonic filtering current, its magnitude and phase angle references are computed through the required filtering harmonic voltage at the PCC. But in this case 1, since RPC is prioritized, this harmonic current is limited to the capacity that is left after RPC operation.

In all simulations, references to fundamental and harmonic filtering current have been supplied manually to work out with an effective design in the worst conditions possible. Magnitude reference of reactive current was supplied manually through q-component ($I_{\text{q,ref}}$) and phase angle references while adding/subtracting 90° in detected phase angles of PCC voltage. Further, magnitude reference of harmonic filtering current was also supplied manually through $I_{\text{h,ref}}$ current component and phase angles of detected PCC secondary side fundamental voltage (MV busbar voltage) were used as its phase angle references. In last, to produce filtering current of different harmonics (e.g. 3rd, 5th or 7th), manual frequency references (e.g. 150, 200, 250 Hz) were also supplied to the harmonic controller.

Different magnitude of harmonic filtering current affects the STATCOM design differently and that has been shown in the next chapter of this thesis. However, it was of interest to know what phase angle reference values cause the worst-case design. Therefore, initially, a sample magnitude reference case was decided; fundamental reactive current in

maximum capacitive operating point was prioritized such that 10% of VSC current capacity was available to generate harmonic filtering current. Using the abovementioned magnitude references (e.g. 0.10 p,u for $I_{\mathrm{h,ref}}$) of VSC's currents, simulation results with different phase angle reference ($\varphi_{\mathrm{ih,ref}}$) of AHF current were carried out, to see their impact on overall design.

Figure 19 represents the VSC voltage results where supplied AHF current's magnitude reference was at 0.10 p.u and its phase angle references were shifted by +60° w.r.t phases of MV bus bar voltage. The frequency of generated AHF current was 150 Hz (3rd harmonic, positive sequence in nature) and the number of SMs to produce required VSC voltage was 35. Choosing such phase angle references of AHF current make the produced VSC's fundamental and 3rd harmonic voltage peaks to be aligned, as shown in Figure 19(b). Peak alignment of produced VSC's fundamental and harmonic voltage further results into the relatively higher peak of net VSC valve voltage, in comparison to other phase angle references of AHF current.

Figure 19(a) shows when produced VSC's fundamental and harmonic voltage peaks are aligned, then peak of overall VSC valve ($V_{\mathrm{VSC\_valve}}$) voltage is at 67.14 kV. This value of $V_{\mathrm{VSC\_valve}}$ is turned out to be at its highest in comparison to other peak values simulated with different phase references of AHF current. Moreover, the available DC link voltage capacity ($V_{\mathrm{DC\_max}} - V_{\mathrm{VSCref_{peak}}} = 69.18 - 66.91 = 2.27\ \mathrm{kV}$) in this situation is also at its lowest.

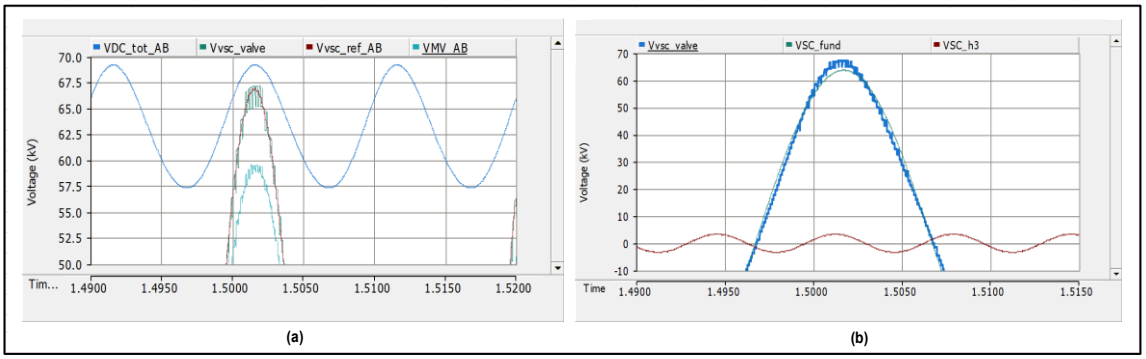

Figure 19. *Simulated (a) DC link, VSC valve and MV busbar voltages in MCOP generated with 0.90 p.u of reactive current and 0.10 p.u of AHF current magnitude reference (AHF current phase references shifted with +60°), (b) VSC overall valve, fundamental and harmonic voltage*.

Figure 20 represents the VSC voltage results where all parameters, as explained in above scenario were kept the same (e.g. AHF current magnitude reference, harmonic

type, number of SMs, etc.) except the phase angle references. Here, phase angle references of AHF current were shifted by +240° w.r.t phases of MV bus bar voltage. Choosing such phase angle references of AHF current makes the produced VSC's fundamental and 3rd harmonic voltage peaks to be opposite to each other, as shown in Figure 20(b). Since peaks of these voltages are in opposite direction, therefore, the peak of overall VSC valve voltage also got decreased significantly in comparison to its value in Figure 20(b).

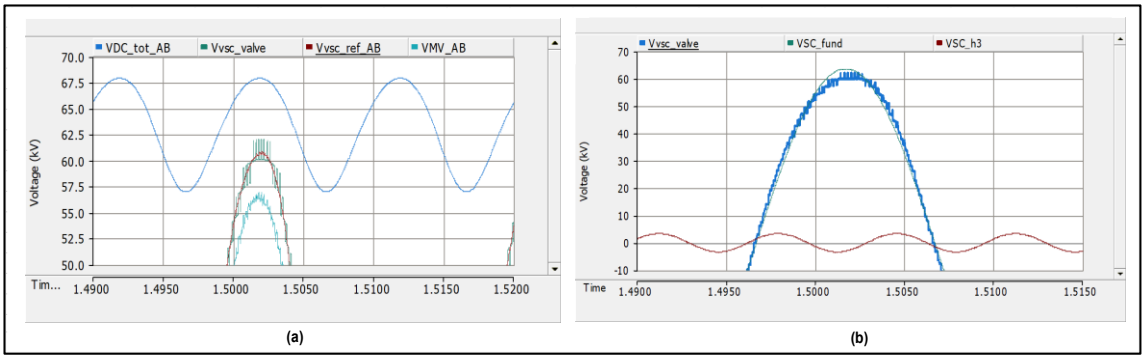

Figure 20. *Simulated (a) DC link, VSC valve and MV busbar voltages in MCOP generated with 0.90 p.u of reactive current and 0.10 p.u of AHF current magnitude reference (AHF current phase references shifted with +240°), (b) VSC overall valve, fundamental and harmonic voltage*.

Figure 20(a) shows when produced VSC's fundamental and harmonic voltage peaks are in the opposite direction, then the peak of overall VSC valve ($V_{\mathrm{VSC\_valve}}$) voltage is at 62.05 kV. Lower $V_{\mathrm{VSC\_valve}}$ peak also result into increasing the available DC link voltage capacity ($V_{\mathrm{DC\_max}} - V_{\mathrm{VSCref_{peak}}} = 67.93 - 60.88 = 7.05\ \mathrm{kV}$) which supposedly can be utilised to decrease the number of required SMs from 35 to 34.

Consequently, the phase angle of AHF current affects the effective STATCOM design in a way that if peaks of produced VSC's fundamental and harmonic voltages are aligned, then higher number of SMs is required, in comparison to the situation when peaks are not aligned. But if peaks are opposite to each other, then there is a probability at least with low order harmonic filtering current that less SMs might be needed to produce the same VSC voltage. Moreover, because needed AHF current phase varies depending on operating point and is not known in design phase, the worst-case approach needs to be taken to be able to operate in all operating points.

4.3.3 AHF current's magnitude and frequency impact on design

In this section, the impact of different magnitudes and frequencies of AHF current on STATCOM design has been investigated. The reactive current has been prioritised first, and thereafter remaining current capacity was allocated to AHF current. For instance, 80% of VSC current was utilised to generate fundamental reactive current and rest for AHF current generation. Speaking of frequencies, 3rd, 4th and 5th harmonics (150, 200 and 250 Hz) have been chosen to work out in this section. The phasor rotation of these harmonics has been assumed to be positive sequence in all simulations. Only the number of SMs, reactive current's magnitude reference, AHF current's magnitude, frequency and phase angle references were changed in the simulations, else other system parameters remained the same as defined earlier in chapter 4.3. All simulation results have been worked out in the maximum capacitive operating point (MCOP).

Initially, simulation results with AHF current of 3rd order harmonic have been carried out. The magnitude references were chosen such that after prioritising the fundamental reactive current, remaining capacity for AHF current magnitude reference were sought to be 20%, 40% and 60% of overall VSC current capacity. Thereafter, using the same set of AHF current magnitude reference, simulation results with 4th, 5th and combined (3rd+4th+5th) order of harmonics were worked out. Both worst (peak aligned) and best (peak opposite) phase angle references, as defined in chapter 4.3.2, were used with aforesaid simulation results.

Figure 21 represents the case where after prioritising fundamental reactive current, 20% of current capacity was available to produce 3rd order positive sequence AHF current. The phase angle references of 3rd order AHF current for worst peak situation, as explained in chapter 4.3.2, were sought to be shifted by +60° w.r.t phases of MV bus bar voltage. The number of SMs used in this situation is 34 analogous to the situation when full current capacity was used to generate only fundamental reactive current in MCOP region (basic case design).

Figure 21(a) shows the waveforms of VSC's voltages when simulated with aforesaid AHF current's magnitude, frequency and phase angle references. Here, it can be clearly seen that peak value of VSC reference voltage ($V_{\mathrm{VSCref_{peak}}} = 73.93\ \mathrm{kV}$) is higher than maximum of DC link voltage ($V_{\mathrm{DC\_max}} = 67.80\ \mathrm{kV}$). it signifies that available DC-link voltage is not enough to produce the desired valve voltage and thus the overall VSC current. Further this DC link voltage was produced with 34 SMs and if same is not enough then there is clearly a requirement to increase the number of SMs.

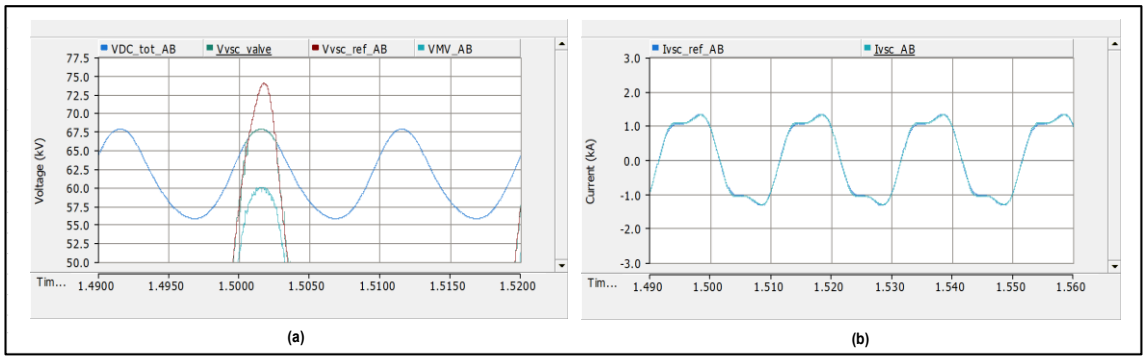

Figure 21. *Simulated (a) DC link, VSC valve and MV busbar voltages in MCOP region and 3rd order AHF current with 0.20 p.u of magnitude, worst peak phase angle (+60°) and 34 submodules, (b) VSC phase current in delta winding*.

Thereafter, simulations with the same AHF current references but with the increased number (e.g. 35, 36) of SMs were repeated until enough DC link voltage is achieved. Figure 23 shows the waveforms of VSC's voltages and current with 37 SMs. In Figure 23(a), values of $V_{\mathrm{VSCref_{peak}}}$ and $V_{\mathrm{DC\_max}}$ are 69.94 kV and 73.35 kV respectively. It shows that now there is 3.41 of remaining capacity in DC link voltage and therefore required VSC voltage can be produced without violating the safety margin. Further, the RMS value of MV bus bar voltage is 23.64 kV which is lower than the insulation voltage limit of 72.5 kV as defined in chapter 4.1.

Figure 23(b) represents the VSC's current waveform. Here it can be clearly seen that peak of VSC current stays below 2.1 kA. It's net RMS value ($I_{\mathrm{vsc\_rms}}$) in delta winding (i.e. AB phase) was 0.9960 kA wherein RMS value of fundamental current component was at 0.9758 kA and 3rd order AHF current component was at 0.1996 kA. So, considering all system limitation required number of SMs to produce such an AHF current was 37.

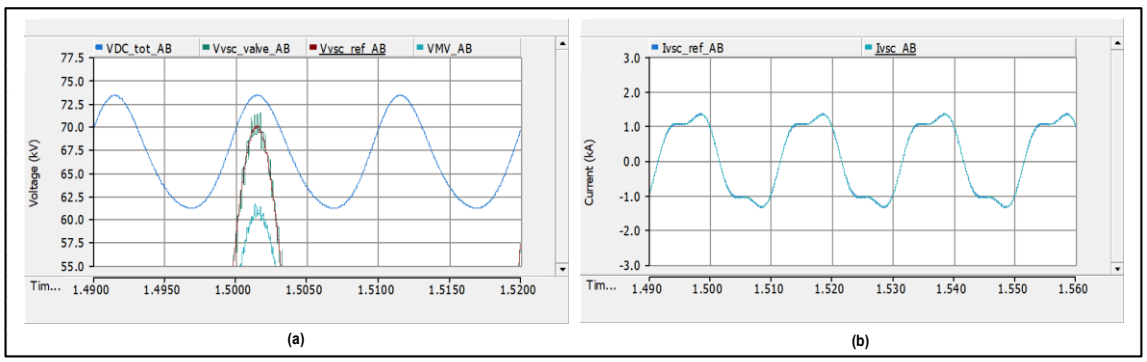

Figure 22. *Simulated (a) DC link, VSC valve and MV busbar voltages in MCOP region and 3rd order AHF current with 0.20 p.u of magnitude, worst peak phase angle (+60°) and 37 submodules, (b) VSC phase current in delta winding*.

Hence, prioritising fundamental reactive current such that 20% of overall VSC current is used for 3rd order AHF current, result into increasing the number of SMs by 3, in comparison to the situation where entire current capacity was used only for the fundamental reactive current only (basic design case in MCOP).

Now simulations were carried out assuming 40% of current capacity was available to produce 3rd order positive sequence AHF current, with its worst-case phase angle. Starting with 37 SMs, same situation happened as described in Figure 21, where DC link voltage capacity was not enough to produce the required VSC voltage. Therefore, the number of SMs was increased until all system limitations were satisfied.

The needed number of SMs to produce 0.40 p.u of AHF current was worked out to be 39, and to validate the same simulated VSC's voltage and current results are shown in Figure 23. Here, Figure 23(a) shows the values of $V_{\mathrm{VSCref_{peak}}}$ and $V_{\mathrm{DC\_max}}$ as 75.82 kV and 77.87 kV respectively and signify the remaining DC link voltage capacity of 2.05 kV. The RMS value of MV bus bar voltage was at 23.57 kV. Figure 23(b) depicts that $I_{\mathrm{vsc\_peak}}$ is much below than 2.1 kA and value of $I_{\mathrm{vsc\_rms}}$ in delta winding was at 0.9991 kA wherein RMS value of fundamental current component was at 0.9167 kA and 3rd order AHF current component was at 0.3973 kA. Thus 39 is the adequate number of SMs to produce such AHF current without violating any of the system limitations.

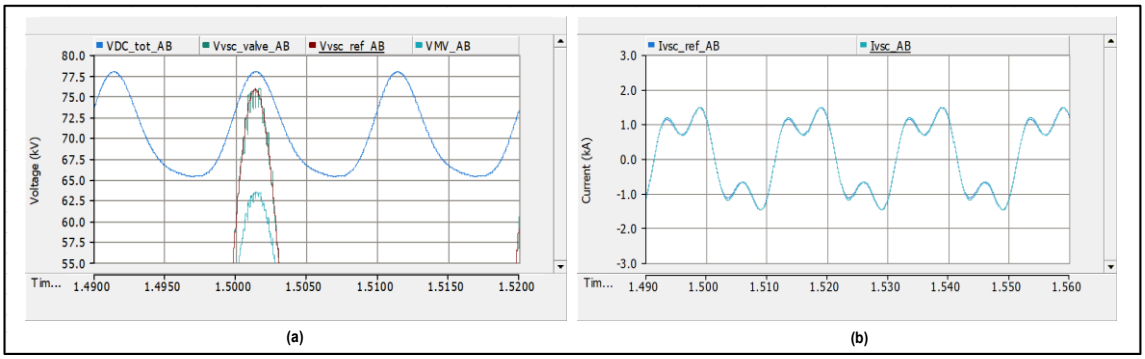

Figure 23. *Simulated (a) DC link, VSC valve and MV busbar voltages in MCOP region and 3rd order AHF current with 0.40 p.u of magnitude, worst peak phase angle (+60°) and 39 submodules, (b) VSC phase current in delta winding*.

Prioritising fundamental reactive current such that 40% of overall VSC current capacity is used for 3rd order AHF current, results into increasing the number of SMs from 34 to 39, in comparison to the basic design case in MCOP region with fundamental reactive current only.

Next simulation was carried out, assuming 60% of current capacity was available to produce 3rd order positive sequence AHF current, with its worst-case phase angle. The

needed number of SMs to produce 0.60 p.u of AHF current, with an iterative process of enough DC link capacity, sought out to be 42. Figure 24 depicts the VSC's voltage and current results when simulated with 42 SMs for 0.60 p.u of AHF current in the MCOP region.

Figure 24(a) shows that with 42 SMs there is enough DC link capacity ($\mathrm{V_{DC\_max}} - V_{\mathrm{VSCref_{peak}}} = 84.18 - 81.24 = 2.94\ \mathrm{kV}$) after producing the desired VSC voltage and so thus the current. The RMS value of MV bus bar voltage was at 23.49 kV. Figure 24(b) depicts that $I_{\mathrm{vsc\_peak}}$ is lower than 2.1 kA and value of $I_{\mathrm{vsc\_rms}}$ in delta winding was at 0.9999 kA wherein RMS value of fundamental current component was at 0.7999 kA and 3rd order AHF current component was at 0.5997 kA. Hence, prioritising fundamental reactive current such that 60% of overall VSC current capacity is used for 3rd order AHF current, result into increasing the number of SMs from 34 to 42, in comparison to the basic design case in MCOP region with fundamental reactive current only.

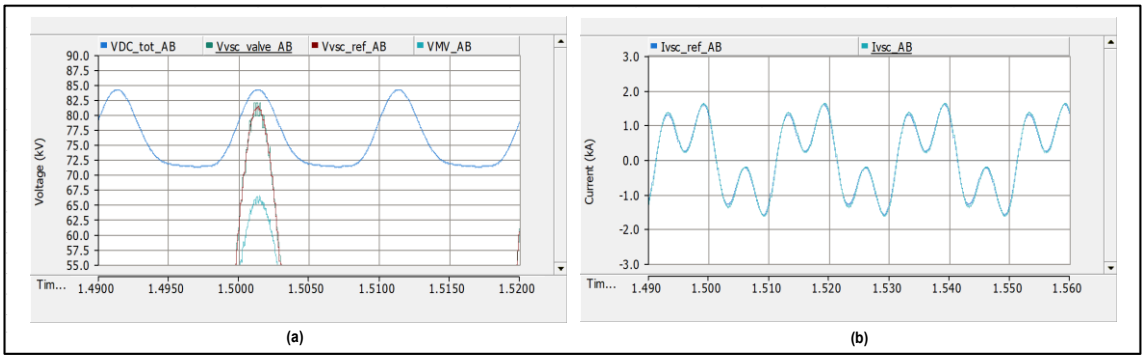

Figure 24. *Simulated (a) DC link, VSC valve and MV busbar voltages in MCOP region and 3rd order AHF current with 0.60 p.u of magnitude, worst peak phase angle (+60°) and 42 submodules, (b) VSC phase current in delta winding*.

To check how phase angle reference impacts the number of SMs with 3rd order harmonic, case of 0.40 p.u AHF current was re-simulated. But this time instead of using the worst peak phase angle references (+60° phase shift), best peak phase angle references (+240° phase shift) for AHF current were used. Figure 25(a) shows there is enough remaining DC link capacity ($V_{\mathrm{DC\_max}} - V_{\mathrm{VSCref_{peak}}} = 74.00 - 60.68 = 13.32\ \mathrm{kV}$) in phase AB and therefore the number of SMs can be reduced from 39 to an adequate value. But this DC link capacity is not equally available in all of the VSC's phases. Figure 25(b) shows the waveform of VSC voltages in phase BC with 39 SMs. Here, the remaining DC link capacity ($V_{\mathrm{DC\_max}} - V_{\mathrm{VSCref_{peak}}} = 77.82 - 74.72 = 3.01\ \mathrm{kV}$) after producing the desired valve voltage is close to the system limit defined in chapter 4.1. And decreasing SMs further would result in violation of system limitation of safety margin in DC link voltage

capacity of BC phase. So from these two results, it can be implied that choosing best peak phase angle may free some DC link capacity in one phase, but it's not necessary that same capacity will be available in other phase too.

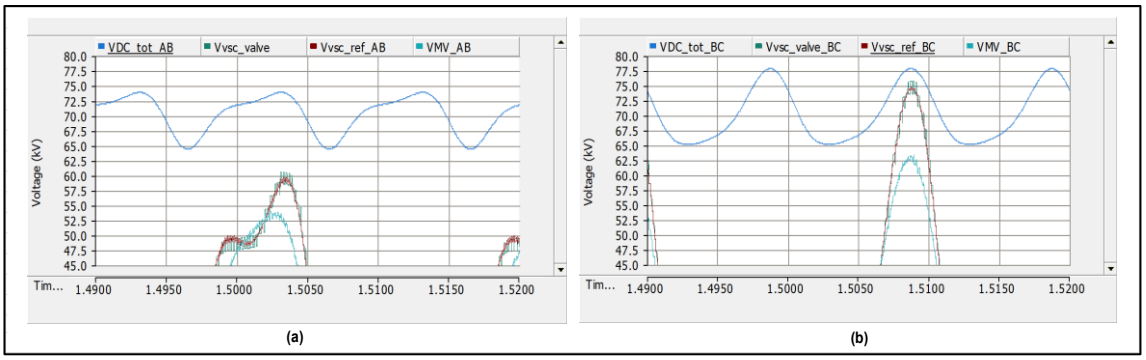

Figure 25. *Simulated DC link, VSC valve and MV busbar voltages in MCOP region and 3rd order AHF current with 0.40 p.u of magnitude, best peak phase angle (+240°) and 39 submodules (a) phase AB (b) phase BC*

So far, cases with 3rd order AHF current were simulated and its different magnitudes and phase angles impact on the needed number of SMs have been investigated. Having said that, instead of 3rd order, now all of these simulations should be repeated with 4th order, 5th order and combined order (3th, 4th and 5th) of AHF currents with the same approach of choosing 0.20, 0.40 and 0.40 p.u of magnitude references along with their respective worst phase angle references in MCOP region. However, since the method of analysing impact of these AHF currents remain the same (e.g. validating remaining DC link capacity, rms value of MV busbar voltage and VSC current limit in delta winding). Therefore, all the simulation results with these AHF currents were segregated and shown in Table 7.

Starting with 4th order AHF current, its worst and best peak conditions occured when its phase angle references are shifted by +20° and +200° w.r.t phases of MV bus bar voltage. As shown in Table 7, with worst peak angle reference in MCOP region, the needed number of SMs to produce 0.20, 0.40 and 0.60 p.u of 4th order AHF current (along with prioritised reactive current), after complying with all system limitations, sought out to be 39, 43 and 47 respectively. Thereafter, using the same approach, simulation for 5th order AHF current were carried out and its worst and best peak conditions found out to be shifted by +0° and +180° w.r.t phases of MV bus bar voltage. And, to produce the same set of magnitudes (as mentioned above) for this order of AHF current, the needed number of SMs turned out to be 40, 46 and 50 respectively.

In last, impact of combined AHF currents of different frequencies, different magnitude and phase angle references on the needed number of SMs were also investigated. The

frequency reference for these AHF currents were 150, 200 and 250 Hz (3rd, 4th and 5th order). Though each of the AHF currents was provided with its own magnitude reference but magnitude reference of net AHF current (computed through equation 4.2 mentioned in chapter 4.1) was chosen to be 20%, 40% and 60% of overall VSC's current capacity. Moreover, worst-peak phase angle references of each harmonic current were considered, such as 60° (phase shift w.r.t MV busbar voltage) for 3rd harmonic, 20° for 4th harmonic and 0° for 5th harmonic filtering current.

Thus, simulation results with combined 3rd, 4th and 5th order AHF currents are shown in Table 7. From these results it can be concluded that producing AHF current with magnitudes of 0.20, 0.40 and 0.60 p.u result into the highest number of SMs as 42, 50 and 55 respectively, in comparison to the same magnitude of AHF current comprising only single harmonic.

Table 7. *Simulation results with different magnitude and phase angle of AHF current comprising 4th, 5th and combined order of harmonics*

Available capacity for AHF current (%)	4th order AHF current with worst peak phase angle (+20°) in MCOP region				5th order AHF current with worst peak phase angle (0°) in MCOP region				Combined AHF current (3rd, 4th and 5th order) with with worst peak phase angle (60°, 20° and 0° respectively) in MCOP region			
	Needed submodules (Nos.)	Remaining DC link capacity (kV)	MV bus bar voltage (kV)	Peak of VSC delta current (kA)	Needed submodules (Nos.)	Remaining DC link capacity (kV)	MV bus bar voltage (kV)	Peak of VSC delta current (kA)	Needed submodules (Nos.)	Remaining DC link capacity (kV)	MV bus bar voltage (kV)	Peak of VSC delta current (kA)
20	39	2.73	23.35	1.56	40	2.72	23.64	1.67	42	3.14	23.45	1.43
40	43	2.68	23.10	1.76	46	2.56	23.83	1.86	50	3.61	23.29	1.56
60	47	2.39	23.68	1.90	50	2.68	23.98	2.06	55	2.72	23.06	1.97

Phase angle references of AHF current		
Order of harmonic for AHF current	Phase shift w.r.t MV busbar	
	Worst peak angle (degrees)	Best peak angle (degrees)
3rd (150 Hz)	60	240
4th (200 Hz)	20	200
5th (250 Hz)	0	180

Note*	rms value of overall VSC current in the delta winding was found to be less than 1000 A in all of the abovementioned simulated cases

4.3.4 Negative sequence AHF current impact on design

In practical application, harmonics present in the network might be of any phasor rotation. Therefore, AHF current to compensate those harmonics would also be of any phasor rotation (e.g. positive, negative or zero sequence). Since studied STATCOM is a delta arrangement of three phase MMC branches, therefore it can not be utilised to produce zero sequence AHF current. But it certainly can produce positive and negative sequence AHF current.

In the previous chapter, simulations were carried out with positive sequence AHF current of different magnitudes and frequencies. But, in this chapter, simulation results showing impact of negative sequence AHF current have been worked out. Speaking of frequency, simulations were worked out with 5th order AHF current, since 5th harmonic is negative sequence in nature if supplying network is balanced. Hence, after prioritising fundamental reactive current, the available current capacity of the AHF current was assumed to be

20% of overall VSC current. The phase angle references of AHF current were chosen to be negative sequence in worst peak condition (0° phase shift w.r.t MV busbar voltage). Figure 26 represents the simulated VSC's voltage and current waveforms with negative sequence AHF current.

The needed number of SMs to produce desired AHF current magnitude with enough remaining DC link capacity sought to be 40, through multiple iteration. As shown in Figure 26(a), the remaining DC link capacity in this case is at 2.70 kV ($V_{\mathrm{DC\_max}} - V_{\mathrm{VSCref_{peak}}} = 78.28 - 75.58$). Comparing this value with remaining DC link capacity of the same magnitude but positive sequence 5th order AHF current, shown in Table 7, it turned out that same was 2.72 kV earlier. Hence no significant difference in available DC link voltage, and therefore the number of SMs in both cases also remain the same.

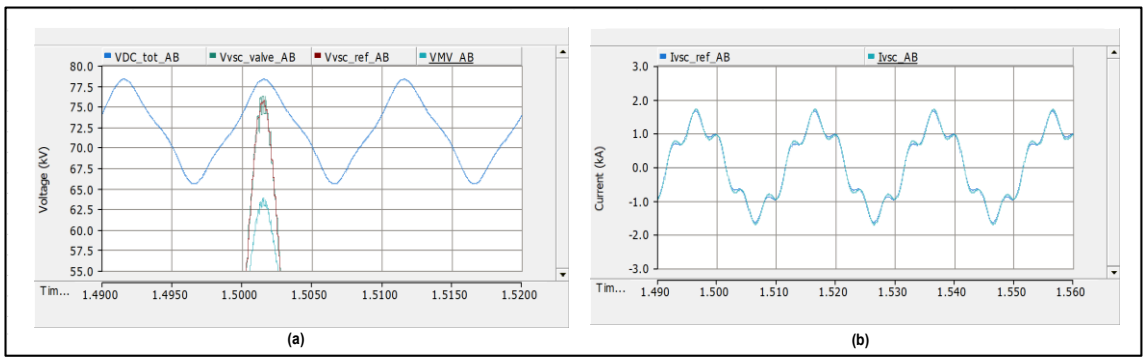

Figure 26. *Simulated (a) DC link, VSC valve and MV busbar voltages in MCOP region and 5th order AHF current with 0.20 p.u of magnitude, negative phase sequence in worst peak phase angle (0°) and 40 submodules, (b) VSC phase current in delta winding*.

Comparing VSC current results, in Figure 26(b) and Table 7 value of $I_{\mathrm{vsc\_peak}}$ remains unchanged at 1.67 kA, irrespective to the condition whether AHF current is positive or negative sequence in nature. Here, RMS value of VSC's fundamental current component in positive sequence case was 0.9686 kA and 0.9689 kA in negative sequence case. The value of zero sequence current in both of the cases was not significantly high; 3.28 and 3.14 A respectively.

Hence, the above mentioned simulation results suggest that changing phasor rotation of AHF current from positive to negative sequence doesn't affect much the overall STATCOM design. Because, the number of needed SMs to produce desired VSC voltage and other system parameters (e.g. DC link capacity, VSC current peak value) almost remain unchanged. Nevertheless, cases of 0.40 and 0.60 p.u magnitude references with negative sequence AHF current were simulated. Later these results have been compared with the results of positive sequence AHF current of the same magnitude. Table 8 represents

the data of available DC-link voltage and the needed number of SMs to produce a certain magnitude of AHF current with both positive and negative sequence in nature. Here it can be clearly seen that the value of needed SMs (e.g. 40) does not deviate whether its 0.20 p.u AHF current of positive sequence or negative sequence.

Table 8. *Comparison of Number of SMs and available DC-link voltage with 5th order positive and negative sequence AHF current*.

5th order AHF current magnitude (p.u)	Available DC-link capacity (kV)		Needed submodules (Nos.)	
	positive sequence	negative sequence	positive sequence	negative sequence
0.20	2.72	2.70	40	40
0.40	2.56	2.61	46	46
0.60	2.68	2.68	50	50

4.3.5 Coupling inductor and transformer reactance impact on design

In this chapter, the impact of coupling inductor's and transformer's reactance has been investigated. One of the main functions of the coupling inductor is to restrict the amount of harmonic current drawn from the grid due to presences of harmonics in VSC's output voltage. Moreover, VSC's net impedance seen from the grid side is the summation of coupling inductor and transformer's reactance. Higher the value of this impedance is, better the harmonic attenuation would be. But increasing the reactance value of the coupling inductor comes with two possible consequences. First, large inductor value makes the system dynamic slower. Second, as per the equation 3.7 mentioned in chapter 3.3.1, to produce a fixed amount of capacitive reactive current, more VSC voltage is needed with higher reactance value.

To produce higher VSC voltage, more SMs are needed which ultimately affects its design. Hence, to show the effect of how increasing or decreasing the reactance value affects the needed number of SMs, two cases for each coupling inductor and transformer reactance have been simulated. Thereafter, the results of these cases have been compared with the pre-defined system values.

Starting with coupling reactance, its system value of 13 mH was chosen in all of the simulations till now. But now, to check its effect on needed SMs, cases with 16 mH and 11 mH have been simulated. First simulation, with 16 mH of coupling reactance and assuming 20% of current capacity was available to produce combine 3rd, 4th and 5th

order positive sequence AHF currents, with their worst-case phase angles, was carried out. Thereafter, the same simulation was repeated with 11 mH of coupling reactance value. In last, VSC current and voltage waveform results with these two reactance values were compared with the results of 13 mH case, shown in Table 7.

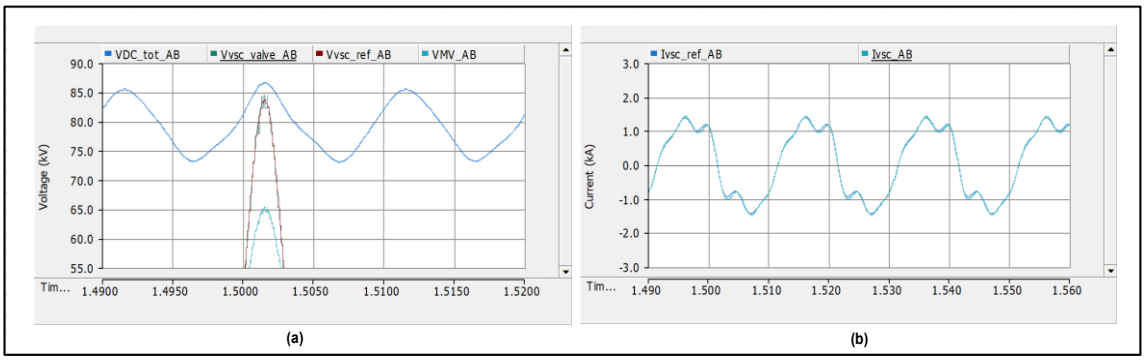

Figure 27. *Simulated (a) DC link, VSC valve and MV busbar voltages in MCOP region and com-bine 3rd, 4th and 5th order AHF currents with 0.20 p.u of overall magnitude, worst peak phase angle (60°, 20° and 0° respectively), 16mH of coupling reactance and 44 submodules, (b) VSC phase current in delta winding*.

As shown in Figure 27(a), the needed number of SMs to produce desired AHF current with 16 mH of coupling reactance sought to be 44 and the peak value of VSC reference voltage is at 83.64 kV. However, comparing these values with Table 7 where the same AHF current was produced with 13 mH of coupling reactance, then the needed number of SMs was 42 and the peak value of VSC reference voltage was 79.71 kV. Hence, it can be clearly noticed that 16 mH of coupling reactance value causes the increment in peak value of VSC reference voltage, in comparison to the case with 13 mH, and therefore result into a higher number of needed SMs as well.

Continuing further, simulation with 11 mH of coupling reactance and assuming 20% of current capacity was available to produce combine 3rd, 4th and 5th order positive sequence AHF currents, with their worst-case phase angles, was carried out. Figure 28(a) shows that the needed number of SMs to produce desired AHF current with 11 mH of coupling reactance now sought to be 41 and the peak value of VSC reference voltage is at 77.59 kV. Comparing these results with 13 mH coupling reactance case, it can be concluded that since the peak value of VSC reference voltage has decreased from 79.71 kV to 77.59 kV, therefore the needed number of SMs to produce the same AHF current has also fallen from 42 to 41.

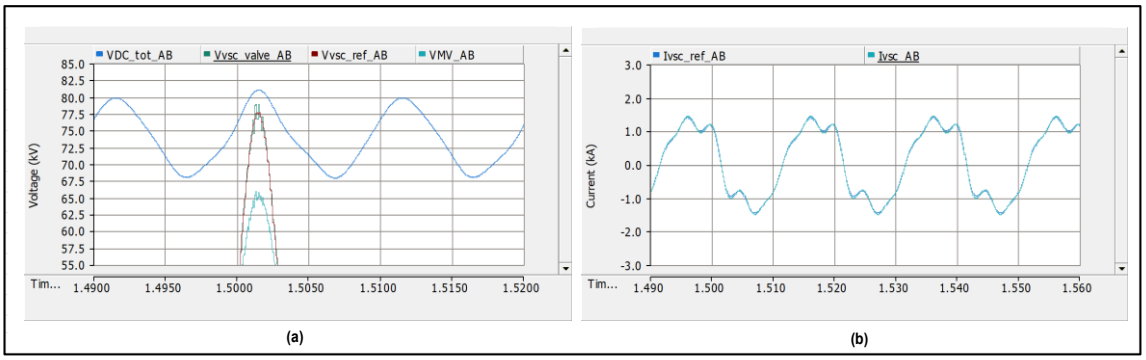

Figure 28. *Simulated (a) DC link, VSC valve and MV busbar voltages in MCOP region and com-bine 3rd, 4th and 5th order AHF currents with 0.20 p.u of overall magnitude, worst peak phase angle (60°, 20° and 0° respectively), 11mH of coupling reactance and 41 submodules, (b) VSC phase current in delta winding*.

Transformer reactance is the other crucial passive element of VSC which affects the number of needed SMs to produce the desired voltage. Its system value of 0.10 p.u was chosen in all of the simulations until now. But now to check its effect, cases with 0.15 p.u and 0.05 p.u of transformer reactance with 20% available capacity (post RPC prioritisation) for AHF current generation was carried out. Here, combined 3rd, 4th and 5th order of harmonic filtering current, positive sequence in nature and having worst-case phase angle reference, has been used. VSC current and voltage waveform results with these two reactance values were compared with the results of 0.10 p.u transformer reactance case of the same AHF current shown in Table 7.

Figure 29(a) depicts that the needed number of SMs to produce desired AHF current with 0.15 p.u of transformer reactance sought to be 45 and peak value of VSC reference voltage is at 86.31 kV. Comparing these values with Table 7 wherein the same AHF current was produced with 0.10 p.u of transformer reactance, then the needed number of SMs was 42 and the peak value of VSC reference voltage was 79.71 kV.

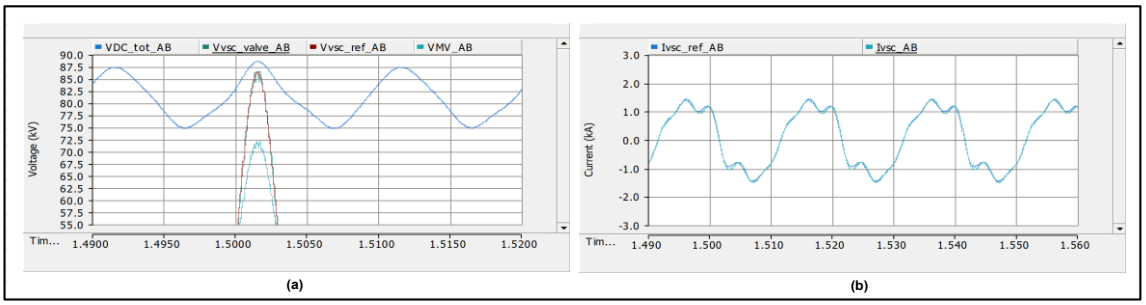

Figure 29. *Simulated (a) DC link, VSC valve and MV busbar voltages in MCOP region and com-bine 3rd, 4th and 5th order AHF currents with 0.20 p.u of overall magnitude, worst peak phase angle (60°, 20° and 0° respectively), 0.15 p.u of transformer reactance and 45 submodules, (b) VSC phase current in delta winding*.

In last, the value of transformer reactance was decreased to 0.05 p.u and simulation to produce the same AHF current (as did last case) was carried out. Here, now the needed number of SMs to produce desired AHF current sought to be 38 and the peak value of VSC reference voltage is at 73.03 kV, shown in Figure 30(a). Comparing these values with Table 7 where the same AHF current was produced with 0.10 of transformer reactance, the values of these parameters were 42 and 79.71 kV respectively.

Therefore, it can be concluded that increasing the transformer reactance value from 0.10 to 0.15 p.u result in increment in peak value of VSC voltage reference from 79.71 to 86.31 kV and consequently increment into the needed number of SMs from 42 to 45 as well. Similarly, decreasing the same reactance value from 0.10 to 0.05 p.u result into decrement in peak value of VSC voltage reference from 79.71 to 73.03 kV and consequently decrement in the needed number of SMs from 42 to 38 as well.

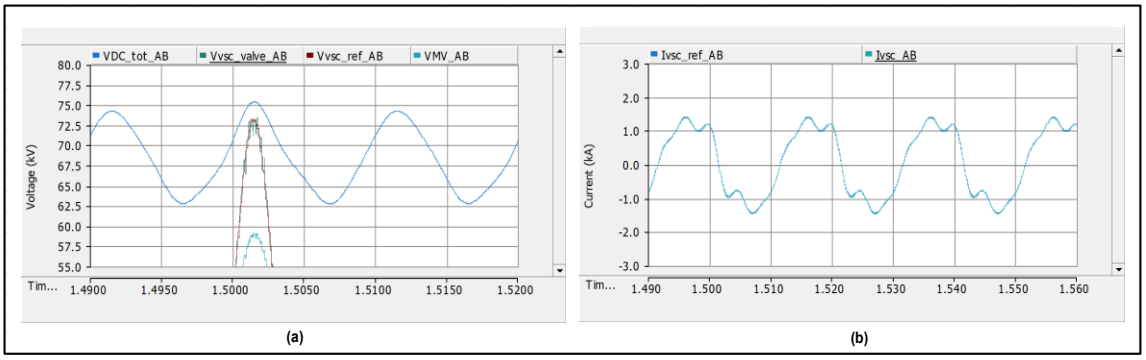

Figure 30. *Simulated (a) DC link, VSC valve and MV busbar voltages in MCOP region and com-bine 3rd, 4th and 5th order AHF currents with 0.20 p.u of overall magnitude, worst peak phase angle (60°, 20° and 0° respectively), 0.05 p.u of transformer reactance and 38 submodules, (b) VSC phase current in delta winding*.

4.3.6 Summary of case 1

In chapter 4.3, it was investigated that how combined operation of RPC and AHF of studied STATCOM affects its design. Here, combined operation was such that RPC was prioritised over the AHF operation. After reconciling all simulation results, as shown in Appendix B, Table 1, it was found out that additional AHF operation affects the STATCOM design, so thus the needed number of SMs, in three ways. First was the magnitude of AHF current. It can be clearly seen in the aforementioned table that when magnitude of an AHF current goes high (e.g. 20%, 40%), then an increment in the needed number of SMs w.r.t basic design was noticed.

Second was the phase angle references of AHF current. Here, if phase angle references of AHF current and chosen such that the peaks of produced VSC's fundamental and

harmonic voltages are aligned, then the peak of resultant VSC voltage may go even more higher, in comparison to the situation when peaks are not aligned. The higher peak of resultant VSC voltage means the requirement of higher DC link voltage and thus more SMs. But if peaks are opposite to each other, fewer SMs are required to produce the same VSC voltage. And, because AHF current angle changes according to the operating point, worst case angle should be considered in design to be able to operate in all operating points.

The third effect on STATCOM design was based on the order of AHF current produced. As shown Appendix B, Table 1, the number of needed SMs to produce an AHF current of 5th order was higher than the same magnitude AHF current of 3rd order, for instance, case of 20% of overall STATCOM current capacity. Also, when combining three harmonics, with same total RMS current magnitude, the needed number of submodules was higher than with any of the single harmonic only. This seems to be due to reason that harmonic currents cancel each other part of the cycle (reducing current RMS) but they increase the total VSC voltage peak. Further, simulations to produce the same magnitude of AHF current but with negative sequence of phasor rotation were also worked out. And, no significant impact on STATCOM design was noticed, in comparison to all positive sequence based AHF current scenarios. Additionally, the impact of transformer and coupling inductor ‘s reactance was investigated. Increasing reactance value for both of these components resulted in an increase in the needed number of SMs to produce the same amount of current.

In summary, since the number of submodules is increased significantly in some cases due to AHF, it increases costs considerably. In order to benefit from AHF without overdimensioning the STATCOM, it can also be done so that the number of submodules is kept same as in RPC mode only (e.g. 34 SMs). And, then the AHF current will be limited by control so that we will not end up into higher VSC voltage stress than in RPC mode only. This way AHF can still be utilized well in many operating points but in extreme cases its use is more limited.

4.4 Case 2: Full RPC support in parallel to AHF operation

In this chapter, the design of STATCOM when it is required to produce nominal fundamental current/power and perform active harmonic filtering at the same time has been carried out. For example, produce 100 MVAr reactive power and decrease 5^{th} and 7^{th} harmonic voltages at PCC from 2 % to 1 % simultaneously. Speaking of priority, zero sequence circulating current and active fundamental frequency current are prioritized first but then reactive current and active harmonic filtering have the same priority. Here,

it was of main interest to investigate how to design STATCOM effectively (without significant over dimensioning) so that both requirements are satisfied.

As part of the design process, first needed VSC harmonic current to filter out harmonic voltage at the PCC has been calculated. Here, while computing needed AHF current, how network impedance affects its magnitude value has also been explained. Thereafter, using the nominal value of fundamental reactive current and computed AHF current, total current at the PCC was worked out. Using this value and HV side PCC voltage, the net MVAr capacity of STATCOM was defined. MV bus bar voltage was calculated as per the system limitation of maximum phase current in delta winding and voltage insulation level defined in chapter 4.1. Next, values of coupling inductor and transformer reactance were calculated iteratively, as per the MVAr capacity. In last, the number of needed submodules to generate such a combine RPC and AHF current was investigated by the simulations.

To find out the needed number of SMs, all possible worst-case situation (highest needed VSC voltage), as worked out in chapter in 4.3, were considered. First, worst situation can be defined when network voltage is at its maximum continuous value, STATCOM producing the reactive and AHF current in MCOP region and fundamental and harmonic VSC voltage peaks occurring at the same time. Second, worst situation occurs when entire STATCOM capacity is used to produce reactive current (no AHF current) in the MIOP region during a short time overvoltage condition.

Considering above mentioned worst cases, an effective STATCOM design was carried out and, then the same was tested with unbalance supply network. The main motive to test STATCOM design with an unbalance supply was to see the effect of zero sequence current on the needed number of SMs and effect on needed MV busbar voltages to produce the required reactive and AHF currents. Further, it was also of interest to check whether any worst-case situation with voltage unbalance also exists.

Parameters of simulation model almost remain the same, except STATCOM MVAr rating, secondary side nominal L-L RMS voltage and inductance of coupling coil. These parameters have been recalculated in chapter 4.4.2, hence mentioned accordingly. Information on the number of submodules used per branch was retrieved after simulating the worst-case scenarios as mentioned in chapter 4.4.2. Finally, detailed information on the network and STATCOM parameter have been enclosed in Appendix A, Table 2.

4.4.1 Calculating needed harmonic current for AHF

Characteristics of frequency-dependent system impedance at PCC affects the STATCOM design and its rating. Changing impedance of transmission line, passive components (e.g. capacitors, inductors) and voltage control devices available in the vicinity and changing dynamics of loads are among those affecting factors. Further, information on harmonic emission caused by STATCOM, phase angles, magnitude and level of background harmonics, any other harmonic source in the vicinity and permissible harmonic distortion limit at the PCC are other aspects for a STATCOM design. [57]

Hence, considering the objectives of this thesis, the harmonic compensation performance of studied STATCOM has not been evaluated in this work. Because, the main goal of this thesis is to check whether studied STATCOM can produce a certain harmonic filtering current of a different order and phase sequences, combined with the fundamental reactive current. Therefore, background harmonic source, other harmonic filtering devices, any capacitor, inductor, other voltage control devices and system loads have not been considered in the simulation except the transmission line impedance.

Since transmission line impedance is a frequency-dependent function, therefore its value changes with different harmonic orders. To compensate certain voltage distortion, information on needed harmonic filtering current is needed. This harmonic filtering current then further depends on system harmonic impendence and can be computed with the following equation.

$$I_{\mathrm{h}} = \frac{V_h}{Z_{\mathrm{h}}} \tag{4.6}$$

Where, V_{h} is the RMS value of harmonic voltage, Z_{h} is transmission line harmonic impedance in ohm and I_{h} is the RMS value of filtering current produced by STATCOM to mitigate the harmonic voltage, same is shown in Figure 31(a). Equation 4.6 shows that the amount of needed filtering current is inversely proportional to the system impedance. It means the higher filtering current is needed to compensate the same amount of voltage distortion when system impedance is at its lowest, comparison to the situation when it is high.

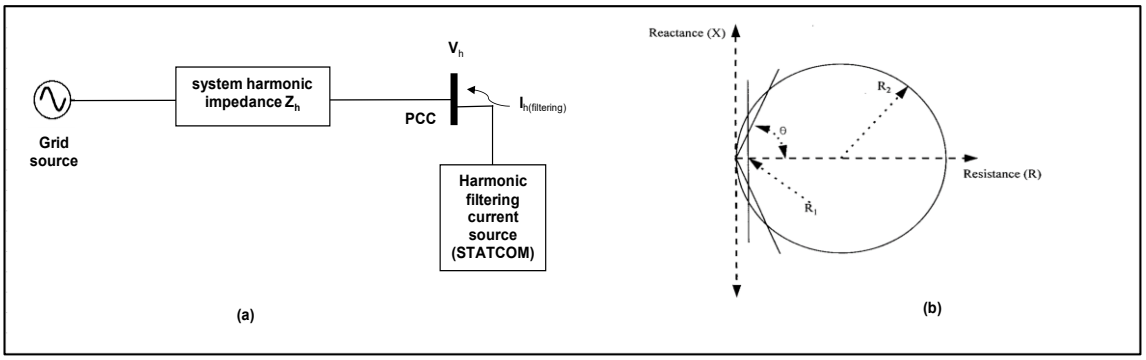

Figure 31. *(a) Harmonic filtering and system impedance, (b) Impedance characteristics at PCC* [57].

Hence, transmission line impedance data considering different network conditions (e.g. other available filtering devices) should be measured. But if impedance measurements are not available, then its value can be assumed to be any magnitude within the circle shown, as shown in Figure 31(b). This circle represents the information on impedance data where the y-axis denotes the reactance and the x-axis denotes the resistance of a transmission line. Typically value of maximum possible impedance magnitude (shown by R_2) varies from 100-200 ohms with impedance angle in the range of 75-80 degrees respectively. In last, R_1 represents the minimum network impedance can be of any minimum value possible. [57]

Subsequently, since no transmission line impedance data was available for this work, therefore, STATCOM design has been carried out while assuming the minimum value of system impedance, as suggested in Figure 31(b). Because, choosing lower system impedance would result in higher harmonic filtering current requirement, and thus one of the worst conditions a network can offer.

Therefore, using network data mentioned in Appendix A, Table 2, a case of 2% voltage distortion at PCC (primary side voltage of 220 kV) was assumed. Here, voltage distortion was decided to be mitigated to 1% with minimum transmission line harmonic impedance of 22 ohms (an arbitrary value), at 150 Hz of frequency or in other words, 3rd harmonic. Consequently, the maximum needed filtering current from the STATCOM to perform such compensation will be as followed.

$$I_{\mathrm{h}} = \frac{V_{\mathrm{h(max)}}}{Z_{\mathrm{h(min)}}} = \frac{(2\% * 220\ \mathrm{kV} - 1\% * 220\ \mathrm{kV})}{22\ \mathrm{ohms}} = \frac{2.2}{22} = 100\ \mathrm{A}$$

Hence, 100 A of needed primary side AHF current has been worked out to dimension a STATCOM for mitigating voltage harmonic distortion from 2% to 1% at PCC, with 22 ohms of minimum harmonic impedance.

4.4.2 Dimensioning STATCOM parameters

Earlier 100 MVAr rated STATCOM was producing 1000 A of current in MCOP region with its maximum current capacity. This current was prioritised in a way that entire current capacity was used for reactive power when needed and when all was not needed the remaining capacity was used to produce the AHF current. However, now, a STATCOM has been designed which should produce 100 MVAr of reactive power and thereafter some more capacity should be added in a way that it can produce the 100 A of AHF current too, as computed in chapter 4.4.1. Hence, it was of interest to rate the STATCOM's MVAr with such parallel RPC and AHF operation.

The primary side fundamental reactive current (RMS) of a 100 MVAr STATCOM, connected to PCC through a 220/34.1 kV step down transformer (in YNd11 connection), can be calculated as follows.

$$I_{\text{fund\_reactive}} = \frac{Q_{\text{STATCOM}}}{(\sqrt{3} * V_{\text{LL\_primary}})} \tag{4.7}$$

$$I_{\text{fund\_reactive}} = \frac{100\ \text{MVAr}}{\left(\sqrt{3} * 220\ \text{kV}\right)} = 262.43\ \text{A}$$

The above-mentioned current is the maximum amount of reactive current present on the primary side of PCC to regulate its voltage. However, to compensate voltage distortion at PCC from 2% to 1%, the needed value of maximum filtering current (due to minimum harmonic impedance) on the primary side is 100 A. Hence, on the primary side of PCC now there will be two current components as fundamental reactive current and active harmonic filtering current.

From equation 4.2, total RMS value of fundamental and AHF current to be produced by a STATCOM can be calculated as mentioned below.

$$I_{\text{PCC\_primary}} = \sqrt{I_{\text{fund\_reactive}}^2 + I_{\text{h,max}}^2} = \sqrt{262.43^2 + 100^2} = 280.83\ \text{A} \tag{4.8}$$

The earlier STATCOM was only rated to produce 262.43 A of reactive current on the primary side of its transformer. Hence, in order to produce a combine AHF and reactive current of 280.83 A of magnitude, the MVAr capacity of STATCOM should be revised as mentioned below.

$$Q_{\text{STATCOM,revised}} = I_{\text{PCC\_primary}} * \sqrt{3} * V_{\text{LL\_primary}} \tag{4.9}$$

$$Q_{\text{STATCOM,revised}} = 280.83\ \text{A} * \sqrt{3} * 220\ \text{kV} = \ 107\ \text{Mvar}$$

After calculating the needed MVAr of STATCOM and primary side PCC current, next was to check whether secondary side current remain below the maximum RMS current

limit of STATCOM. In delta winding maximum RMS current limit of studied STATCOM (VSC) was 1000 A or 1732.05 ($\sqrt{3}$*1000) in wye-winding (secondary side of PCC).

Since transformer was rated with 220/34.1 kV, its secondary side current would be as follows.

$$I_{\text{PCC\_secondary}} = \frac{Q_{\text{STATCOM,revised}}}{(\sqrt{3} * \text{V}_{\text{LL\_secondary}})} \tag{4.10}$$

$$I_{\text{PCC\_secondary}} = \frac{107 \text{ MVAr}}{\left(\sqrt{3} * 34.1 \text{ kV}\right)} = 1811.62 \text{ A} = \text{I}_{\text{VSC\_wye}}$$

The value of secondary side current calculated through equation 4.10 certainly exceeds the limit of wye-winding current of VSC ($I_{\text{VSC\_wye}}$). To restrict this value, there were two options either to decrease the MVAr of STATCOM or increase the line to line secondary side voltage of the transformer. MVAr can not be decreased, since it has been calculated according to the needed fundamental reactive and AHF current. Therefore, increasing the value of secondary side voltage was decided. The value of 1730.43 A secondary current or wye-winding VSC current (close to the defined limit) was chosen and accordingly, adequate secondary side voltage was worked out to be 35.7 kV.

$$I_{\text{PCC\_secondary(revised)}} = \frac{107 \text{ MVAr}}{(\sqrt{3} * 35.7 \text{ kV})} = 1730.43 \text{ A or } 1.730 \text{ kA} = \text{I}_{\text{VSC\_wye}} \tag{4.11}$$

Since MVAr of STATCOM and value of secondary side voltage have been revised, therefore the earlier value of coupling reactor (e.g. 13 mH) and the needed number of SMs (e.g. 34) were also no longer valid and needed to be re-calculated using the equation mentioned below (4.12) and simulator.

A fault happening on the secondary busbar results into the flow of a fault current from VSC to the secondary busbar. This current is then limited by the coupling inductor and if capacity has been increased and so thus the DC link voltage, then reactance value of coupling inductor should also be increased directly proportional to the increase of number of submodules. Hence, it was decided that to compute the adequate reactance of coupling inductor, an iterative approach should be adopted while linking information coming from both platforms (equation 4.12 and simulator). As a part of the iteration, first 13 mH of reactance value was used and the needed number of SMs was retrieved through simulation. Thereafter, new reactance was computed after rationalising the value of needed SMs coming from the simulator, initial reactance of 13 mH and needed SMs suggested by the equation 4.12, example given below.

$$\frac{\text{Inductance in the original 100 MVAr design}}{\text{SMs in the original 100 MVAr design}} = \frac{\text{X mH}}{\text{SMs computed with simulation}} \tag{4.12}$$

$$\frac{13\ \text{mH}}{38} = \frac{\text{X mH}}{46}$$

Now, newly computed reactance value was supplied to the simulator to validate whether the recommended number of SMs from the last iteration comply with the new reactance value or there was a change in it. Because, if there was an increment in the number of needed SMs for the simulator, then again new value of reactance was computed through equation 4.12 and this iterative process was continued until there was no increment in the number of SMs.

Hence, simulation to produce desired positive sequence AHF current of 3rd order (or 150 Hz of frequency) along with fundamental reactive current were carried out. And, after three iterations, final reactance value of coupling inductor and the needed number of SMs worked out to be were 15.73 mH and 41 SMs respectively, in accordance with both equation 4.12 and simulation-based limitations. The value of transformer reactance has been kept the same as 0.10 p.u. Hence, all STATCOM related parameters to produce 280.83 A of combined fundamental reactive current and AHF current have been dimensioned. Now next was to simulate a sample case with these values to check whether system limitations mentioned in chapter 4.1 have been fulfilled or not.

Figure 32 represents the simulation results carried out to produce 280.83 A of VSC (STATCOM) current on the primary side of PCC. This current should comprise of 262.43 A (RMS) of fundamental reactive current and 100 A of AHF current on the primary side of PCC. The phase angle references of AHF current was chosen to be 60° phase shifted w.r.t MV busbar voltage (worst peak angle reference). Here, secondary side PCC current or VSC current in wye-winding should not exceed more than 1730.43 A (RMS), as calculated through equation 4.1, and accordingly VSC current in delta winding should not exceed 1000 A (RMS).

The needed number of SMs to produce the desired current at the primary side of PCC with enough remaining DC link capacity sought to be 41. As shown in Figure 32(a), the remaining DC link capacity in this case was at 3.02 kV ($V_{\text{DC\_max}} - V_{\text{VSCref}_{\text{peak}}} = 81.60 - 78.58$). Moreover, MV busbar voltage was found to be 24.71 kV. Hence, all voltage-based system limitations were satisfied.

However, there were some violations based on the defined current limits. Starting with Figure 32(b), RMS value of primary side PCC current (I_{PCC}) in all phases was close to 280 A, depicted in Figure 32(d). Using FFT block function of PSCAD, values of fundamental current ($I_{\text{PCC\_fund}}$) and AHF ($I_{\text{PCC\_filtering}}$) current at the PCC were also validated and turned out to be 262.84 and 99.79 A respectively. But, VSC current RMS value in

some of the phases of delta winding was founded to be more than 1000 A, shown in Figure 32(b). Also, the maximum RMS value of VSC current in wye-winding (I_{VSC_Y}), as shown in Figure 32(c) was found to be 1737.51 A (A-phase) which is more than the defined limit of 1730.43 A as computed in equation 4.11.

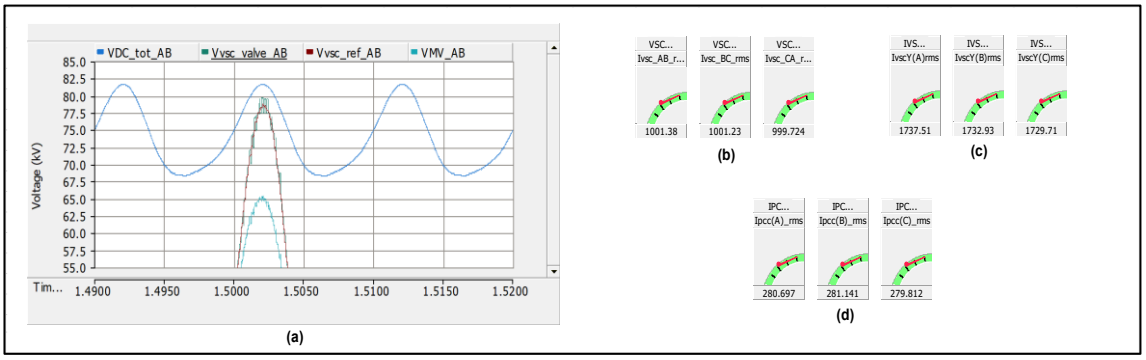

Figure 32. *Simulated (a) DC link, VSC valve and MV busbar voltages in MCOP region (with worst peak angle) to produce maximum AHF and fundamental reactive current at PCC, simultaneously, (b) VSC phase current RMS values in delta-winding (c) VSC phase current RMS values in wye-winding (d) Phase current RMS values at primary side of PCC.*

The simulation results shown in Figure 32 signify the violation of defined VSC current limit in wye/delta winding. Here, one of the possible reasons behind such violation was expected to be caused by the worst peak angle references of AHF current. Therefore, it was of interest to check whether other phase angle reference of AHF current can help in achieving the desired 280 A of combined current without violating wye or delta winding VSC current limit. Hence, simulation with different phase angle references was carried out and phase shift of 240° w.r.t busbar voltage (best peak angle case) turned out to be the phase angle reference of the AHF current where combined current of 277.18 A at the PCC was achieved, which was very close to the desired combined current of 280 A, without violating any current or voltage limit.

Figure 33 shows the simulation result with the best peak angle reference (240° w.r.t busbar voltage) of AHF current. Here, 41 SMs were needed to produce the desired current with enough remaining DC link capacity as shown in Figure 33(a) ($V_{\mathrm{DC\_max}} - V_{\mathrm{VSCref_{peak}}} = 81.51 - 78.47 = 3.04\ \mathrm{kV}$) and MV busbar voltage was at 24.68 kV. VSC current RMS values in both wye and delta winding remained below their defined limits and can be validated from Figure 33(b) and Figure 33(c). RMS value of primary side PCC current (I_{PCC}) in all phases was slightly less than 280 A, depicted in Figure 33(d). Further, RMS values of fundamental current and AHF current at the PCC were also validated and turned out to be 260.01 and 99.72 A respectively.

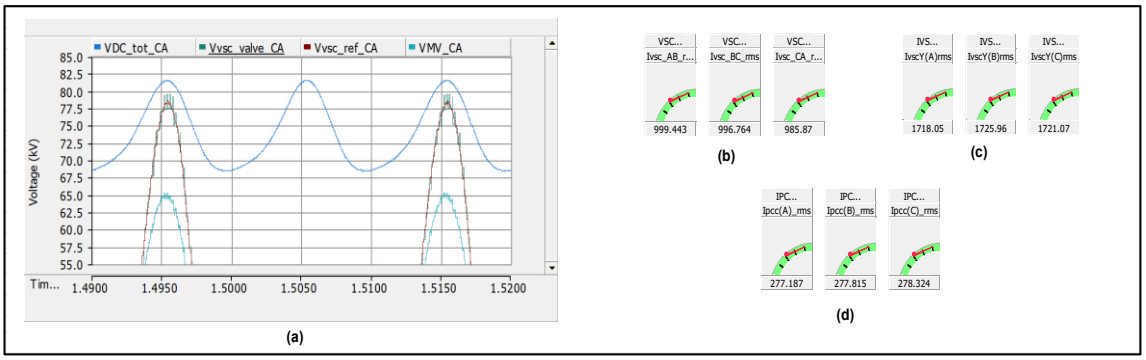

Figure 33. *Simulated (a) DC link, VSC valve and MV busbar voltages in MCOP region (with best peak angle) to produce maximum AHF and fundamental reactive current at PCC, simultaneously, (b) VSC phase current RMS values in delta-winding (c) VSC phase current RMS values in wye-winding (d) Phase current RMS values at primary side of PCC.*

Results shown in Figure 32 suggest that even after choosing an adequate secondary side voltage of 35.7 kV and required MVAr of STATCOM, RMS value of $I_{\mathrm{VSC\_wye}}$ exceeded its defined limit due to certain phase angle of AHF current. Further, it explains that the summation principle given in literature (equation 4.8) seems not to be enough to quite satisfy the both maximum of fundamental reactive current and maximum of AHF current requirements even though we are close to the requirements. Also, many worst-case assumptions occurring at the same time (maximum needed harmonic voltage filtering, minimum network impedance present, maximum reactive current needed) were also considered.

Hence, it would be pertinent to say that, to see the design capability with this summation principle, any of these currents' magnitude should be decreased and this kind of small deviation might be acceptable. But if not acceptable, then another option to avoid current limitation violation is through higher MV busbar voltage (to restrict increasing PCC current) which further results in requiring larger number of submodules and therefore increased overall costs. Having said that, first an economical design utilising this geometrical summation principle but slightly decreased value of AHF current to fulfil the system limitation has been carried out. Thereafter, a conservative design in chapter 4.4.5, based on an arithmetical summation principal and where both current requirements are easily achieved, has been discussed.

Speaking of economical design, since reactive power compensation was assumed to be a critical system requirement, the value of AHF current was decided to be decreased from the target value of 100 A to a certain value until $I_{\mathrm{VSC\_Y}}$ limit was achieved. Hence, simulations with multiple harmonic filtering current references were carried out. And, In

the end, it was found that choosing 90 A of PCC side harmonic filtering current (with worst peak angle reference) result in restricting the value of wye-winding VSC current well below 1730.0 A.

Thus, STATCOM of 107 MVAr capacity with 41 SMs has been dimensioned to produce 262.43 A of maximum fundamental reactive current and 90.0 A of AHF current to mitigate the voltage distortion at PCC. Now In upcoming chapters impact of worst-case situations on the designed STATCOM, in a balanced and unbalanced network, has been investigated.

4.4.3 Design in balanced network

In this chapter, designed STATCOM with 41 SMs has been investigated with other possible worst situations a network and added harmonic filtering function could offer. Speaking of worst situations, first can be referred to the same scenario of balanced network, as shown in Figure 42, but here simulation was carried out with decreased AHF current (from 100 A to 90 A). Second worst situation can happen when entire STATCOM capacity is used to produce the fundamental reactive current (no AHF current) in the MIOP region during a short time overvoltage condition. In last, a worst situation due to unbalance voltage in the network may cause the circulation of zero sequence current inside the delta branch of STATCOM and can further affect its ability to produce rated RPC and AHF currents. But keeping the length of this chapter into mind, Impact of zero sequence current on worst case design has been investigated separately in chapter 4.4.4

In this chapter, to carry out the simulations, magnitude references for fundamental reactive and AHF current have been chosen such that their values on the primary side of PCC should be close to 262.43 and 90.0 A respectively. Network parameters for MCOP and MIOP region remain the same as defined in the simulations of chapter 4.3. Further, in MIOP region, AHF functionality has been assumed to be disabled and STATCOM only producing the fundamental reactive current to alleviate the short time overvoltage condition (harmonic performance is usually measured in longer intervals). The number of needed SMs used for producing the desired PCC side current was 41. The frequency of produced AHF current was chosen to be 150 Hz or in other words, 3rd order harmonic. Phasor rotation of AHF current has been chosen to be positive sequence in nature. The phase angle references of 3rd order AHF current for worst peak situation, as explained in chapter 4.3.2, were sought to be shifted by +60° w.r.t phases of MV bus bar voltage, thus same has been used here as well.

Figure 34 represents the simulation results carried out when network voltage was at its maximum continuous value and STATCOM producing the reactive and AHF current in the MCOP region with worst-peak angle. Here, Figure 34(a) validates that there was enough remaining DC link capacity ($V_{\mathrm{DC\_max}} - V_{\mathrm{VSCref_{peak}}} = 81.44 - 78.17 = 3.27\ \mathrm{kV}$) with 41 SMs, after producing the desired current. The RMS value of MV busbar voltage was 24.70 kV. Figure 34(b) shows that VSC phase current remained under the defined limit of 2.1 kA of peak value. The RMS value of $I_{\mathrm{VSC\_Y}}$ was at 1724.78 A. Fundamental reactive current and AHF current RMS values at the PCC were 262.46 and 90.98 A respectively. Hence, all system limitations were satisfied and desired current values on the PCC side were also achieved. Conclusively, 41 SMs were enough to produce the desired current while maintaining the adequate DC link safety margin, in this worst case.

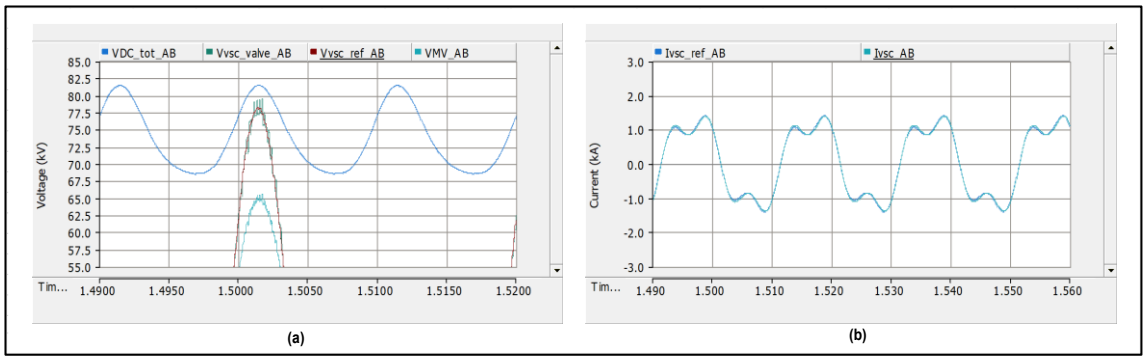

Figure 34. *Simulated (a) DC link, VSC valve and MV busbar voltages with 41 SMs in MCOP region to produce 90 A of AHF and maximum rated fundamental reactive current at PCC, simultaneously, in worst peak situation (b) VSC phase current in delta winding*.

Figure 35 represents the simulation results carried out when entire STATCOM current capacity is used to produce only reactive current in the MIOP region during a short time overvoltage condition. Here, Figure 35(a) validates that there was enough remaining DC link capacity ($V_{\mathrm{DC_{min}}} - V_{\mathrm{VSCref_{peak}}} = 68.71 - 56.05 = 12.66\ \mathrm{kV}$) with 41 SMs, after producing the desired current. The RMS value of MV busbar voltage was 25.76 kV. Figure 35(b) shows that VSC phase current remained under the defined limit of 2.1 kA of the peak value. The RMS value of $I_{\mathrm{VSC\_Y}}$ was at 1730.1 A. Fundamental reactive current RMS value at the PCC was 281.20 A because now the entire current capacity was used to produce just the inductive current.

Simulation results shown in Figure 34 and Figure 35 proves that STATCOM dimensioned in chapter 4.4.2 can produce the desired current even in worst peak angle and overvoltage situations, without over dimensioning it in term of the needed number of SMs.

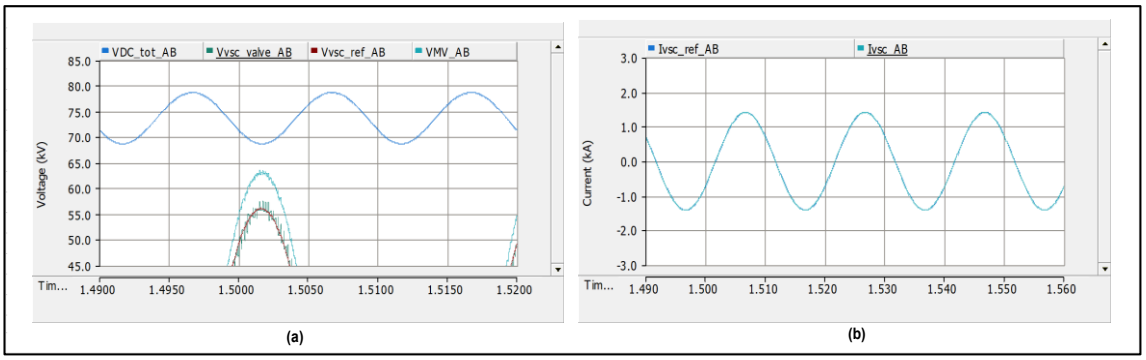

Figure 35. *Simulated (a) DC link, VSC valve and MV busbar voltages with 41 SMs in MIOP region to produce maximum rated fundamental reactive current at PCC (b) VSC phase current in delta winding*.

4.4.4 Zero-sequence current and design in unbalanced network

In this chapter, the impact of unbalanced grid voltage on STATCOM design, an extension to the worst situations explained in the last chapter, has been investigated. During unbalance conditions, though the net three phase power exchange of STATCOM is kept at zero but its phasor powers may deviate w.r.t each other. In this condition, DC link voltage started drifting and required a mean to keep it constant at a certain level. Circulating a zero-sequence current inside the delta winding of STATCOM branches can help to prevent drifting of DC link voltage. This current enables the power exchange among the phases of delta windings, without affecting grid operation. To compute the required amount of zero sequence current in delta winding during unbalanced network conditions, the following equation can be utilised. [58]

$$I_{\text{zero}} = \frac{V_{\text{pos}}^{*} V_{\text{neg}} I_{\text{neg}} - V_{\text{pos}}^{2} I_{\text{neg}}^{*} + V_{\text{neg}}^{2} I_{\text{pos}}^{*} - V_{\text{pos}} V_{\text{neg}}^{*} I_{\text{pos}}}{|V_{\text{pos}}|^{2} - |V_{\text{neg}}|^{2}} \tag{4.13}$$

Here, V_{pos} and V_{neg} are positive and negative sequence network connection point voltages and I_{pos} and I_{neg} are positive and negative sequence arm/branch currents of the STATCOM.

It would be pertinent to mention that zero sequence current computed through equation 4.13 is valid only when STATCOM is producing the fundamental current component. Adding AHF current in STATCOM output and then computing I_{zero} value with some unbalanced network cases doesn't give the exact results, but rather close in comparison to its recorded value in the simulation model. However, since the objective of this thesis is to show how zero sequence current affects the rating of STATCOM and thus its design. Therefore, mathematical derivation for zero sequence calculation in combined RPC and AHF operation of STATCOM has not been carried out in this thesis work.

Speaking of zero sequence current, increasing in its magnitude has direct consequences on the fundamental reactive current. Because, as per the equation 4.5 mentioned in chapter 4.1, the maximum allowed limit of overall VSC current is 1000 A for the studied STATCOM. And, since first priority in terms of utilising VSC's current capacity has been given to the zero-sequence current. Therefore, any increment in zero sequence current would decrease the available current capacity for fundamental reactive and AHF current magnitudes. To prove the aforementioned fact, the designed STATCOM case from the last chapter was re-simulated with 2% of unbalanced supply and results are shown in Figure 36.

Figure 36(a) shows that adequate DC link capacity ($V_{\mathrm{DC_{max}}} - V_{\mathrm{VSCref_{peak}}} = 81.37 - 77.66 = 3.71\ \mathrm{kV}$) remained after producing the desired current and RMS value of MV busbar voltage was also at 24.88 kV. But RMS value of fundamental reactive current at the PCC has been decreased to 261.56 A as depicted in Figure 36(b), in comparison to the case shown in Figure 35 where the same was 262.46 A. The main reason behind such decrement is due to the higher value of circulating zero sequence current of 9.09 A, which was 6.15 A in balanced case shown in Figure 35. This 2.94 A of increment in zero sequence current occupied the available capacity for fundamental current in delta winding and thus, less reactive current was produced.

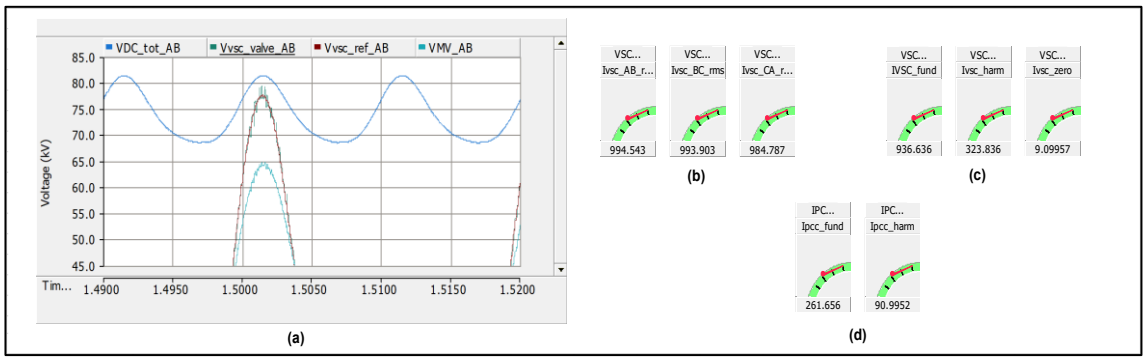

Figure 36. *Simulated (a) DC link, VSC valve and MV busbar voltages in MCOP region to produce 90 A of AHF and maximum fundamental reactive current at PCC, simultaneously, (b) VSC phase current RMS values in delta-winding (c) Fundamental, AHF and zero sequent current components in delta-winding of a certain phase (d) Fundamental and AHF current RMS values at primary side of PCC.*

Moreover, it would be relevant to highlight that the overall RMS value of VSC phase current in the delta winding doesn't provide the complete information on the presence of zero sequence. For instance, Figure 36(a) shows that even after the presence of fundamental, AHF and zero sequence component, in AB phase of delta winding, the value of VSC current is at 994.54 A instead of 1000 A. But doing the FFT analysis of the same

phase current provide the information on the presence of 936.63 A, 323.86 A and 9.09 A of fundamental, AHF and zero sequence current component respectively. Therefore, using equation 4.5 these currents correctly summed to 1000.17 A of overall VSC current. Having said that, it can be implied that due to the phasor difference among fundamental, AHF and zero sequence current, the overall RMS value of VSC's phase current varies at every instant (e.g. higher when their peaks are aligned or lower when opposite).

Behrouzian et al. [59] suggested that the demand of zero sequence current depends on two factors. First, the degree of unbalance ($\frac{V_{\mathrm{neg}}}{V_{\mathrm{pos}}}$) where if unbalance in a network is such that V_{neg} equals to V_{pos} then using equation 4.13 infinite zero sequence current is required to balance the DC link voltage. Second is the phase shift between positive and negative sequence voltage where maximum zero sequence demand occurs when positive and negative sequence voltages/currents are aligned (e.g. phase shift of 0°,120° and 240°). [59]

Hence, earlier designed STATCOM can only produce the desired fundamental reactive current of 262.43 A, along with 90 A of AHF current, if the margin for needed zero sequence current is also added into the design. Therefore, an approximate value of needed zero sequence current in case of a 2% unbalance network using equation 4.13 was computed and worked out to be 20.0 A in the delta winding. Thereafter, deducting this value from the overall VSC current capacity, now available current capacity in delta winding for the combined fundamental and AHF current is 980.0 A. And, referring this 20.0 A to the secondary side ($\sqrt{3}$*20 = 34.46 and rounding to 40.0), the maximum VSC current in wye-winding should be close to 1692.0 A (1732.0 – 40.0 = 1692). Thereby, to restrict the VSC current in wye-winding to 1692.0 A and to achieve 262.43 A of fundamental reactive and 90.0 A of AHF current simultaneously at the PCC, new value of required secondary side line to line voltage was computed using equation 4.11 and turned out to be 36.5 kV.

Changing the value of the secondary side line to line voltage increases the needed number of submodules and thus also coupling reactor inductance value needs to be increased, as explained in chapter 4.4.2. Consequently, following the same iterative process mentioned in equation 4.12, the value of reactance for the coupling conductor and the needed number of SMs in such conditions were recalculated and worked out to be 16.07 mH and 42 SMs (or 47 with 10% redundancy; in case of SM failure) respectively. Thus, new STATCOM design with 42 SMs has been rated such that it can produce the combined 262.43 A of fundamental reactive current and 90 A of AHF current at the PCC while maintaining 1692 A of current in its wye-winding with enough margin of zero sequence current for 2% unbalance network.

To continue validating with worst situations initially results for the designed STATCOM with worst peak angle reference of AHF current in 2% unbalance supply (without phase shift between positive and negative sequence grid voltage) have been simulated out.

Figure 37 represents the simulation results carried out when network voltage was 2% unbalance and STATCOM producing the reactive and AHF current in the MCOP region along with the worst-peak angle. Here, Figure 37(a) confirms the enough remaining DC link capacity ($V_{\mathrm{DC\_max}} - V_{\mathrm{VSCref_{peak}}} = 83.20 - 78.95 = 4.25\ \mathrm{kV}$) with 42 SMs, after producing the desired current. Figure 37(b) shows that VSC phase current remained under the defined limit of and 2.1 kA of the peak value. The RMS value of needed zero sequence current in this case was 10.57 A, wherein without unbalance the same value was 6.15 A for the case shown in Figure 34. The RMS value of $I_{\mathrm{VSC\_Y}}$ was at 1687.28 A. Fundamental reactive current and AHF current RMS values at the PCC were 262.50 and 90.07 A respectively. Hence, all system limitations were fulfilled with 42 SMs. And, due to the unbalance network, the increased value of zero sequence current and the needed number of SMs were noticed in comparison to the balanced case shown in Figure 34.

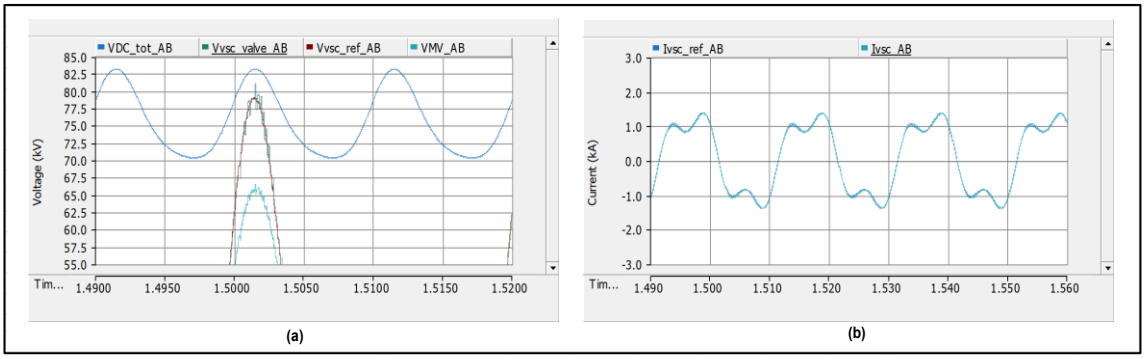

Figure 37. *Simulated (a) DC link, VSC valve and MV busbar voltages with 42 SMs in MCOP region to produce 90 A of AHF and maximum rated fundamental reactive current at PCC, simultaneously, in worst peak situation and 2% unbalance (without phase shift between PS and NS voltages) (b) VSC phase current in delta winding*.

Figure 38 shows the simulation results when the entire STATCOM current capacity is used to produce only reactive current in the MIOP region with a 2% unbalance supply. Here, Figure 38(a) validates that there was enough remaining DC link capacity ($V_{\mathrm{DC_{min}}} - V_{\mathrm{VSCref_{peak}}} = 70.48 - 56.88 = 13.60\ \mathrm{kV}$) with 42 SMs, after producing the desired current. Figure 38(b) shows that VSC phase current values remained under the defined limit of 2.1 kA of the peak value. The RMS value of $I_{\mathrm{VSC\_Y}}$ was at 1704.42 A. Fundamental reactive current RMS value at the PCC was 284.64 A. Here, value of VSC current in wye-winding and fundamental reactive current at PCC is more than required values of 1692.0 A and 280.0 A respectively. Because zero sequence current in delta winding didn't fully

utilise its allotted limit and therefore, remaining part has been utilised by the fundamental reactive current component. The RMS value of needed zero sequence current in this case was 15.93 A, wherein without unbalance same value was 0.07 A for the case shown in Figure 35. Thus, all system limitations were fulfilled in this case with the same design of 42 SMs.

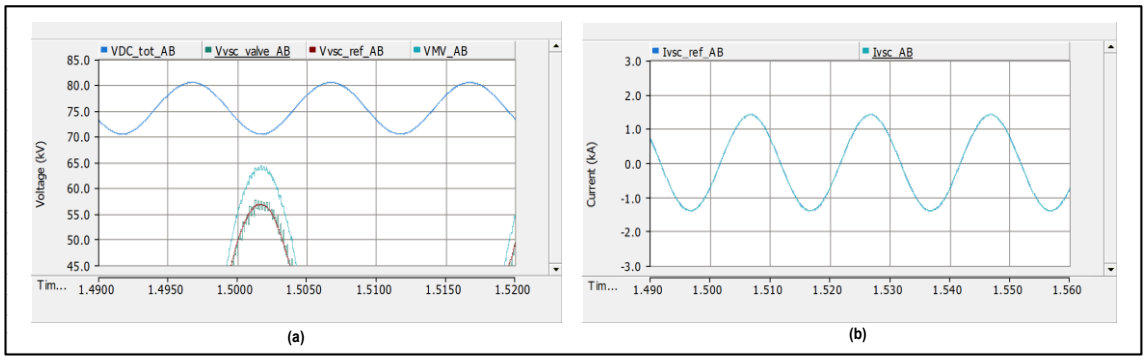

Figure 38. *Simulated (a) DC link, VSC valve and MV busbar voltages with 42 SMs in MIOP region to produce maximum rated fundamental reactive current at PCC with 2% unbalance (without phase shift between PS and NS voltages) (b) VSC phase current in delta winding*.

Thereafter, simulation results for the same design with an added phase shift between positive sequence and negative sequence voltage of unbalanced supply were carried out to check the assertation made by Behrouzian et al. [58] for maximum demand of zero sequence current. In last, designed STATCOM for “the worst case” has been tested. Here, “the worst case” has been referred to as the combination of all worst situations such as, maximum continuous voltage in MCOP region, worst peak angle of AHF current, negative sequence nature of AHF current and phase shifted (between PS and NS) unbalanced supply.

As Behrouzian et al. [59] argued that maximum demand of zero sequence current occurs when values of phase shift between PS and NS voltage are 0°, 120° or 240°. Therefore, expanding the worst-case design criteria now simulations were carried out when network voltage was 2% unbalanced with phase shift between PS and NS voltage mentioned above. And, STATCOM producing the reactive and AHF current in MCOP region along with worst-peak angle. Hence, maximum demand of zero sequence current was recorded when phase shift between positive and negative sequence voltages was at 120° along with other worst conditions explained above.

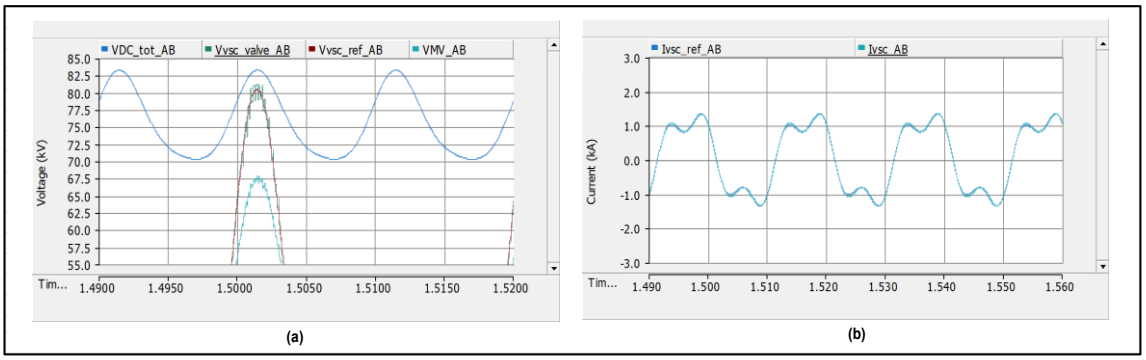

Figure 39. *Simulated (a) DC link, VSC valve and MV busbar voltages with 42 SMs in MCOP region to produce 90 A of AHF and maximum rated fundamental reactive current at PCC, simultaneously, in worst peak situation and 2% unbalance (with 120° phase shift between PS and NS voltages)) (b) VSC phase current in delta winding*.

Figure 39(a) confirms the enough remaining DC link capacity ($V_{\mathrm{DC\_max}} - V_{\mathrm{VSCref_{peak}}} = 81.18 - 78.29 = 2.89\,\mathrm{kV}$) with 42 SMs, after producing the desire current. Figure 39(b) shows that VSC phase current remained under the defined limit of 2.1 kA of peak value. The RMS value of needed zero sequence current in this case was 20.01 A wherein without phase shift same value was 10.57 A for the case shown in Figure 37. The RMS value of $I_{\mathrm{VSC\_Y}}$ was at 1686.99 A and values of fundamental reactive and AHF current at PCC side was 262.60 A and 90.70 A respectively. Hence, all system limitations were fulfilled with same design of 42 SMs. And, due to the unbalance network along with phase shift of 120° between PS and NS grid voltages, increased value of zero sequence were noticed.

Next simulations were carried out when network voltage was 2% unbalanced, entire STATCOM current capacity is used to produce only reactive current in MIOP region along with different phase shift values (e.g. 0°, 120° or 240°) of positive and negative sequence voltage. Here, the maximum demand of zero sequence current was recorded, when phase shift between positive and negative sequence voltages was at 240° along with other worst conditions explained above.

Figure 40(a) validates that there was enough remaining DC link capacity ($V_{\mathrm{DC_{min}}} - V_{\mathrm{VSCref_{peak}}} = 70.49 - 56.79 = 13.70\,\mathrm{kV}$) with 42 SMs, after producing the desired current. Figure 40(b) shows that VSC phase current value remained under the defined limit of 2.1 kA of the peak value. The RMS value of needed zero sequence current in this case was 16.06 A wherein without phase shift same value was 15.93 A for the case shown in Figure 38. The RMS value of $I_{\mathrm{VSC\_Y}}$ was at 1704.30 A and combined value of fundamental reactive and AHF currents at PCC side was 284.61 A. Thus, all system limitations were fulfilled in this case with same design of 42 SMs.

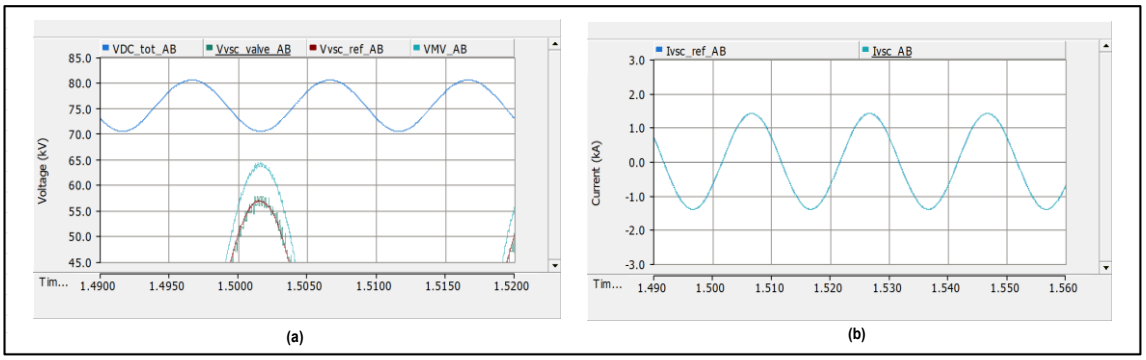

Figure 40. *Simulated (a) DC link, VSC valve and MV busbar voltages with 42 SMs in MIOP region to produce maximum rated fundamental reactive current at PCC and 2% unbalance (with 240° phase shift between PS and NS voltages) (b) VSC phase current in delta winding*.

In last, simulations for “the worst case” were worked out where STATCOM was producing the combined fundamental reactive and negative sequence AHF current in the MCOP region with the worst peak angle of AHF current. And, a 2% unbalanced supply with certain phase shift between PS and NS grid voltages. Here, maximum demand of zero sequence was recorded when phase angle references of negative sequence AHF current was 60° phase shifted wr.t. MV busbar voltage and phase shift between PS and NS grid voltages was at 240°.

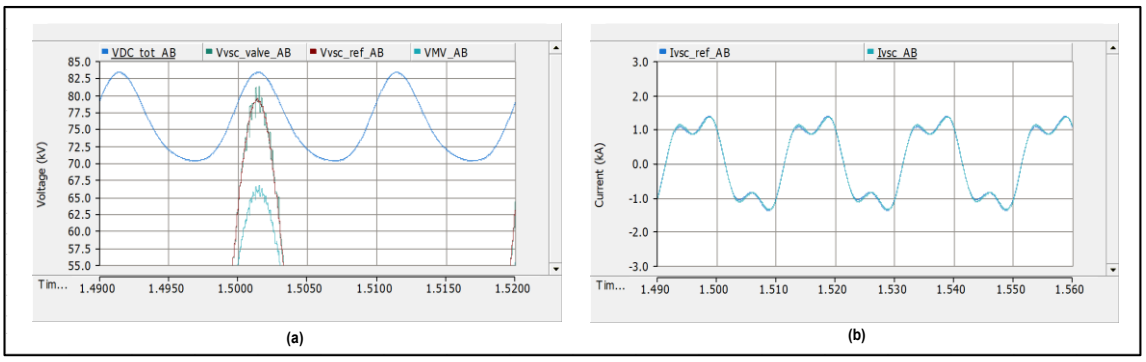

Figure 41. *Simulated (a) DC link, VSC valve and MV busbar voltages with 42 SMs in MCOP region to produce 90 A of negative sequence AHF and maximum rated fundamental reactive current at PCC, simultaneously, in worst peak situation and 2% unbalance (with 240° phase shift between PS and NS voltages) (b) VSC phase current in delta winding*.

Figure 41 shows that there was enough remaining DC link capacity ($V_{\mathrm{DC\_max}} - V_{\mathrm{VSCref_{peak}}} = 83.29 - 79.35 = 3.94\ \mathrm{kV}$) with 42 SMs, after producing the desired current. Figure 41(b) shows that VSC phase current remained under the defined limit 2.1 kA of the peak value. The RMS value of needed zero sequence current in this case was 23.52

A wherein with positive sequence AHF current same value was 20.01 A for the case shown in Figure 39. Here, value of zero sequence current which is higher than the calculated value with the equation in the beginning of this subchapter (20 A) but due to the safety margin (rounding wye current up to 40 A) it is still within the limit. Further, the RMS value of $I_{\mathrm{VSC\_Y}}$ was at 1684.32 A and the value of fundamental reactive and negative sequence AHF current at the PCC was as desired.

Finally, STATCOM design with 42 SMs has been able to produce the desired current at PCC in all possible worst conditions. The capacity for zero sequence current to be reserved in delta winding turned out to be approximately equals to the percent of unbalance in the network (2% unbalanced network requires 2% capacity reservation of 1000 A). But this applies only for the tested combination of reactive current and 3rd harmonic only. Because with different order of harmonics, the results might be different.

4.4.5 Conservative design for case 2

In chapter 4.4.2 of case 2, it was realised that due to the geometric sum principle of fundamental reactive current and AHF current($\sqrt{I^2_{\mathrm{I_{fund\_reactive}}} + I^2_{\mathrm{filtering}}}$), the maximum of these currents can not be achieved always at the same time. Figure 32 shows that if the phase angle reference of AHF current are such that they cause the worst peak angle situation of VSC voltages, then corresponding value (of desired PCC side max. reactive and AHF current) in terms of VSC current in wye-winding exceeds its limit of 1730 A. Moreover, Figure 33 shows that if the phase angle references of AHF current are such that they cause the best peak angle situation of VSC voltages then corresponding value of wye-winding VSC current remains lower than 1730 A with almost 100 A of AHF current at the PCC but slightly less value (260.01 A) of desired (262.43 A) fundamental reactive current. Hence, still maximum of both these currents couldn't be achieved simultaneously.

Having said that, it was of interest to design a case where both maximum of fundamental current (e.g. 262.43 A) and maximum of AHF current (e.g. 100 A) can be achieved simultaneously without compromising any of the system limitations. Hence, it was assumed that instead of rating the VSC's current with the geometric sum, an arithmetical sum of fundamental reactive and AHF currents should be utilised. Because, an arithmetical sum of RMS values of fundamental and AHF current might result in taking all current phase angles (e.g. worst peak angle) related worst situations into the account.

According to chapter 4.4.2, RMS value of maximum fundamental and maximum AHF current to be achieved at the PCC were 262.43 A and 100 A respectively. Hence, considering the conservative design, and thus their arithmetic sum, the overall primary side PCC current would be as follows

$$I_{\text{PCC\_primary}} = I_{\text{fund\_reactive}} + I_{\text{h,max}} = 262.43 + 100 = 363.43\ \text{A} \quad (4.14)$$

In order to produce a combine AHF and reactive current of 363.43 A of magnitude, the MVAr capacity of STATCOM should be revised as mentioned below.

$$Q_{\text{STATCOM}} = I_{\text{PCC\_primary}} * \sqrt{3} * V_{\text{LL\_primary}}$$

$$Q_{\text{STATCOM}} = 363.43 * \sqrt{3} * 220 * 1000 = \ 138.10\ \text{Mvar} \quad (4.15)$$

Thereafter, to keep the maximum RMS value of VSC current in delta winding below 1000 A and also to consider situation of 2% unbalance supply, the maximum RMS value of secondary side PCC current or VSC current in wye winding should be as follow

$$I_{\text{PCC\_secondary}} \text{ or } \text{I}_{\text{VSC\_wye}} = 1000 * \sqrt{3} - 40 = 1692.0\ \text{A} \quad (4.16)$$

To get this value of current, secondary side line to line PCC voltage of the transformer should be calculated as mentioned below.

$$V_{\text{LL\_secondary}} = \frac{Q_{\text{STATCOM}}}{\left(\sqrt{3} * I_{\text{PCC\_secondary}}\right)}$$

$$V_{\text{LL\_secondary}} = \frac{138.10\ \text{MVAr}}{\left(\sqrt{3} * 1692\ \text{A}\right)} = 47.12\ \text{kV} \quad (4.17)$$

In last, following the same procedure as mentioned in chapter 4.4.2, the reactance of coupling inductor and the needed number of SMs to produce the desired current, as calculated through equation 4.14, were carried out and worked out to be 19.49 mH and 51 SMs respectively. Thereafter, this designed STATCOM with a pessimistic or conservative approach was tested in “the worst” network condition, as explained in the end of last subchapter, and respective simulation results are shown in Figure 51.

Figure 42(a) confirms the enough remaining DC link capacity ($V_{\text{DC\_max}} - V_{\text{VSCref}_{\text{peak}}} = 99.63 - 96.14 = 3.49\ \text{kV}$) with 51 SMs, after producing the desired current at PCC. Figure 42(d) shows that with conservative design (arithmetic summation of currents), the maximum RMS value of fundamental reactive current as 262.43 A and 100 A of AHF current can be achieved simultaneously at the PCC without exceeding VSC current limit in wye or delta winding. Here, VSC current in delta and wye winding remains well below than 1000 A and 1730 A respectively and can be validated from Figure 42(b)&(c). However, achieving the maximum of both fundamental reactive and AHF current simultaneously

was not possible with an economical design (geometric summation of currents) as per the results shown in Figure 32.

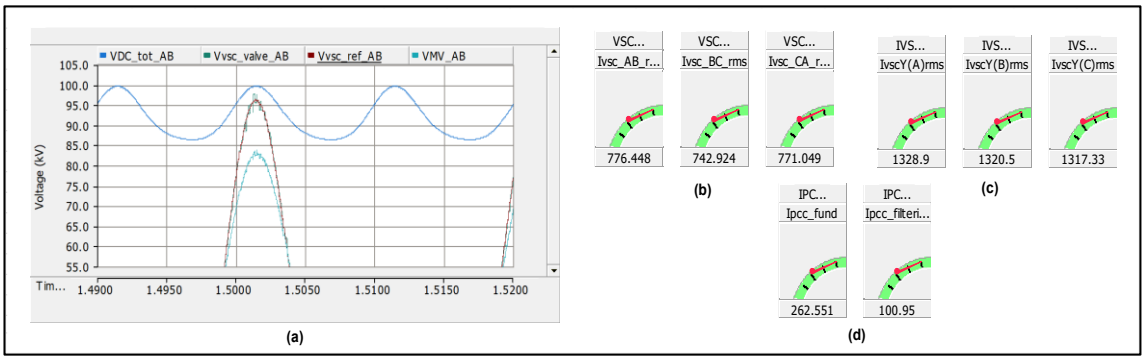

Figure 42. *Simulated (a) DC link, VSC valve and MV busbar voltages with 51 SMs in MCOP region to produce maximum rated fundamental reactive and negative sequence AHF current at PCC simultaneously, in worst peak situation and 2% unbalance (with 240° phase shift between PS and NS voltages) (b) VSC phase current in delta winding.*

Moreover, it was interesting to note that with a conservative design number of needed SMs to produce combined 262.43 A of fundamental reactive and 100 A of AHF current at the PCC was 51. But, with an economical design though there was slightly less current (262.43 A fundamental and 90 A AHF) at the PCC but the number of needed SMs was only 42. Further, in conservative design, even after producing the desired current at the PCC, only the maximum of 772 A of overall VSC current in delta winding out of 1000 A was utilised. And, it clearly signifies that though, a conservative design of STATCOM with high MVAr rating and number of SMs help in achieving the maximum current objectives, but it does not fully utilise its rated capacity, therefore not an optimum design.

Conclusively, an optimum design exists between economical and conservative design which fulfills all the requirements but does not have an easy current summation principle (arithmetical or geometrical). Since the requirements were almost achieved with geometric summation and there was a lot extra current capacity with arithmetical summation, optimal design current summation principle is closer to the geometrical summation.

4.4.6 Summary of case 2

In chapter 4.4, a STATCOM capable of producing nominal reactive power and to perform active harmonic filtering at the same time was designed. While designing, worst conditions sought in chapter 4.3 along with the influence of minimum system impedance characteristics were also considered.

The designed STATCOM was tested with unbalanced supply, in MCOP and MIOP region, to see its effect on the required zero sequence current for the arm balancing. All simulation results were reconciled and shown in Appendix B, Table 2. Here, it was noticed that the demand of zero sequence current increases when first 2% of unbalance along with worst peak angle reference of AHF current was introduced. Thereafter, introducing phase shift between positive and negative sequence voltages such that their peaks are aligned resulted in further increasing the demand of zero sequence current. In last, maximum zero sequence current was needed when simulation in MCOP region of STATCOM with phase shifted (PS and NS peak aligned) unbalanced supply, worst peak angle reference and negative sequence type of AHF current was worked out.

In designing process, amount of zero sequence to be reserved can be computed through the equation mentioned chapter 4.4.4. However, it is only valid when STATCOM is operating in RPC mode. After adding AHF operation, value of zero sequence current depends upon the degree of unbalance, phase shift between PS and NS network voltage, magnitude of AHF current, its phase angle and order of harmonic. Further, results of case 2 suggested that amount of required zero sequence current was approximately equal to the percent of unbalance (2% network unbalanced = 2%*1000 A= 20 A of zero sequence current in delta winding). But it applies only to the AHF current magnitude, order and phase angle used in chapter 4.4.4, and therefore value of zero sequence current may vary with different AHF current. Moreover, demand of zero sequence current result in decreasing the fundamental reactive current from its nominal value, due to summation principle and VSC current limitation shown in equation 4.5. Hence, to achieve the nominal fundamental reactive current and to fulfil the zero-sequence current demand as well, MV busbar voltage needs to be increased which further affects the reactance value of coupling inductor, needed number of SMs and thus the overall STATCOM design.

In last, it was noticed that with an economical design (geometric reactive and harmonic current summation) condition for maximum fundamental reactive current and maximum filtering current can not be fulfilled at the same time, without violating VSC current limitation in delta winding. However, same was possible with conservative design (arithmetical reactive and harmonic current summation) at the cost of higher MVAr rating, a higher number of needed SMs and less utilisation of overall capacity. Hence, there is an optimal current summation principle (or optimal design) exists; something in between the aforementioned geometrical and arithmetical principles, but closer to the geometric one.

5. FUTURE WORK

Keeping the length of this thesis in mind, there are so many other aspects and ideas which were decided not to include in this work. To get high magnitude harmonic current, needed to investigate the worst impact on a STATCOM design, a short-circuited network impedance based easier approached was used in this thesis work. However, more complex and rather realistic condition would be to inject the current harmonics using the grid side voltage source in presence of a certain network impedance and then verify the STATCOM design and its performance for active harmonic filtering and reactive current production simultaneously.

Second, the effect of zero sequence AHF current on STATCOM design was not carried out in this thesis because of the topology-based restrictions. Since SDBC based MMC STATCOM was studied in this thesis where VSC branches were placed in a delta arrangement. Therefore, using this topology, a zero sequence AHF current cannot be produced. Hence, SSBC based MMC STATCOM model can be used in future work to carry out such studies.

The effect on STATCOM design when active harmonic filtering is prioritized over fundamental reactive current has not been investigated. Hence recommended for the future work. Additionally, optimum summation principle for AHF and reactive current was not found/investigated in greater details which might be needed to fulfill all requirements without significant over dimensioning.

6. CONCLUSION

The main objective of this thesis was to design a STATCOM when its fundamental reactive current is prioritized over active harmonic filtering and when it is required to produce nominal fundamental reactive current/power and perform active harmonic filtering at the same time. For such a combined RPC and AHF operation of the studied STATCOM, it was of interest to investigate how adding AHF functionality affects its design in terms of the needed number of SMs, DC link voltage capacity, MV busbar voltage, transformer and coupling inductor reactance. Additionally, how to sum the fundamental and AHF current and Impact on zero sequence current demand due to such a combined operation in unbalance grid operation were also among those interests

Starting with the design case where RPC operation was prioritised over AHF, it was found that producing AHF current affects the STATCOM design in three ways. First was the magnitude of AHF current where the number of needed SMs to produce the required voltage increases with increasing AHF current magnitude. The second was the phase angle references of AHF current. If they are chosen such that the peaks of produced VSC's fundamental and harmonic voltages are aligned, then the situation of worst peak angle occurs. In this situation, the needed number of SMs to produce the same magnitude of AHF current increases in comparison to the situation where VSC voltage peaks are either not aligned or in opposite directions. The third effect on STATCOM design was based on the order of AHF current to be produced. Here, simulation results suggested that the number of needed SMs to produce the same magnitude of AHF current increases as the order of harmonic of filtering current increases. The highest SM number was needed when same current capacity (RMS) was used for a current of three combined harmonics. Alongside, it was also found that increasing the reactance of transformer and coupling inductor results into increase in the needed number of SMs to produce the same amount of voltage, as with lower reactance values.

Another option for aforesaid prioritisation case (extra AHF when RPC is not needed) is not to utilize the whole current capacity and limit the operation based on the number of submodules needed in RPC mode only, instead not to produce so high AHF current that number of sub-modules should be increased). This brings benefit to a network operator most of the time without over dimensioning the STATCOM and saving significantly in term of additional hardware costs.

In case of designing STATCOM capable to produce nominal reactive power and performing active harmonic filtering at the same time, simulation results suggested that operating with the maximum current in both operations creates a bottleneck with the overall current limit of studied STATCOM in delta winding. Here, the maximum fundamental reactive current and maximum filtering current can not be achieved at the same time with an economical design (geometrical summation of currents). However, achieving maximum RMS values for both of these currents is possible in a conservative design (arithmetical summation of currents); with a trade-off between significant safety margin of VSC current in delta winding due to high MVAr rating (and higher cost) or optimum utilisation of current capacity (even closer to the limit) with less MVAr rating. Hence, an optimum design current summation principle exists between these two designs which fulfils all the requirements and seems to be quite close to the geometrical summation principle of economical design.

Further, testing the designed STATCOM with unbalanced supply, it was noticed that the maximum demand of zero sequence current occurs when STATCOM was producing fundamental reactive current and negative sequence AHF current in the MCOP region simultaneously. And, here peaks of positive and negative sequence network voltage were aligned along with the worst peak angle reference of AHF current. Furthermore, when STATCOM was producing only reactive power in MIOP region, then the highest demand of zero sequence was recorded when peaks of positive and negative sequence network voltage were aligned.

REFERENCES

[1] S. R. Durdhavale and D. D. Ahire, “A Review of Harmonics Detection and Measurement in Power System,” *International Journal of Computer Applications*, vol. 143, no. 10, pp. 42–45, 2016.

[2] H. Akagi, “Active Harmonic Filters,” *Proceedings of the IEEE*, vol. 93, no. 12, pp. 2128–2141, 2005.

[3] N. G. Hingorani and L. Gyugyi, *Understanding FACTS: Concepts and Technology of Flexible AC Transmission Systems*. New York: Wiley-IEEE Press, 1999.

[4] F. C. De La Rosa, *Harmonics and power systems*. Boca Raton: Taylor & Francis, 2006.

[5] E. Fuchs and M. A. S. Masoum, *Power Quality in Power Systems and Electrical Machines*. San Diego: Elsevier Science, 2008.

[6] W. M. Grady and S. Santoso, “Understanding power system harmonics,” *IEEE Power Engineering Review*, vol. 21, no. 11, pp. 8–11, 2001.

[7] V. E. Wagner *et al.*, “Effects of harmonics on equipment,” *IEEE Transactions on Power Delivery*, vol. 8, no. 2, pp. 672–680, 1993.

[8] A. Elmoudi, M. Lehtonen, and H. Nordman, “Effect of harmonics on transformers loss of life,” in *Conference Record of the 2006 IEEE International Symposium on Electrical Insulation*, 2006, pp. 408–411.

[9] G. J. Wakileh, “Harmonics in rotating machines,” *Electric Power Systems Research*, vol. 66, no. 1, pp. 31–37, 2003.

[10] N. Eghtedarpour, M. Karimi, and M. Tavakoli, “Harmonic resonance in power systems - a documented case,” *2014 16th International Conference on Harmonics and Quality of Power (ICHQP)*, pp. 857–861, 2014.

[11] N. D. Rao, S. I. Sporea, and A. Sawma, “Analysis of resonance problems and harmonic filter design in power factor correction capacitor applications,” in *Conference Proceedings. IEEE Canadian Conference on Electrical and Computer Engineering (Cat. No.98TH8341)*, 1998, vol. 1, pp. 293–296.

[12] M. Nasiri, M. Rostami, and Seyed Hamid Fathi, “Parallel and series harmonic resonance prevention by anti-resonance hybrid capacitor system for power factor correction,” in *2010 5th IEEE Conference on Industrial Electronics and Applications*, 2010, pp. 1023–1027.

[13] S. Vlahinic, D. Brnobic, and N. Stojkovic, “Indices for Harmonic Distortion Monitoring of Power Distribution Systems,” in *2008 IEEE Instrumentation and Measurement Technology Conference*, 2008, pp. 421–425.

[14] S. M. Halpin, “Comparison of IEEE and IEC harmonic standards,” in *IEEE Power Engineering Society General Meeting, 2005*, 2005, vol. 3, pp. 2214–2216.

[15] “IEEE Recommended Practice and Requirements for Harmonic Control in Electric Power Systems,” *IEEE Std 519-2014 (Revision of IEEE Std 519-1992)*, pp. 1–29, 2014.

[16] McGranaghan and Beaulieu, “Update on IEC 61000-3-6: Harmonic Emission Limits for Customers Connected to MV, HV, and EHV,” in *2005/2006 IEEE/PES Transmission and Distribution Conference and Exhibition*, 2006, pp. 1158–1161.

[17] “IEC TR 61000-3-6, Limits - Assessment of emission limits for the connection of fluctuating installations to MV, HV and EHV power systems,” IEC, 2008.

[18] J. Persson, “Comparing Harmonics Mitigation Techniques,” *In Comsys AB, Lund*, p. 6, 2014.

[19] H. A. Kazem, “Harmonic Mitigation Techniques Applied to Power Distribution Networks,” in *Advances in Power Electronics*, 2013, p. 11.

[20] D. Schwanz, M. Bollen, and A. Larsson, “A review of solutions for harmonic mitigation,” in *2016 17th International Conference on Harmonics and Quality of Power (ICHQP)*, 2016, pp. 30–35.

[21] B. Singh, A. Chandra, and K. Al-Haddad, *Power Quality: Problems and Mitigation Techniques*. John Wiley & Sons, 2014.

[22] J. C. Das, “Passive filters - potentialities and limitations,” *IEEE Transactions on Industry Applications*, vol. 40, no. 1, pp. 232–241, 2004.

[23] B. Singh, K. Al-Haddad, and A. Chandra, “A review of active filters for power quality improvement,” *IEEE Transactions on Industrial Electronics*, vol. 46, no. 5, pp. 960–971, 1999.

[24] K. HAYAFUNE, T. UESHIBA, E. MASADA, and Y. OGIWARA, “Microcomputer Controlled Active Power Filters,” *Proc. of the IEEE-IECON*, pp. 1221–1226, 1984.

[25] J. H. Choi, G. W. Park, and S. B. Dewan, “Standby power supply with active power filter ability using digital controller,” in *Proceedings of 1995 IEEE Applied Power Electronics Conference and Exposition - APEC’95*, 1995, vol. 2, pp. 783–789.

[26] Chingchi Chen and D. M. Divan, “Simple topologies for single phase AC line conditioning,” *IEEE Transactions on Industry Applications*, vol. 30, no. 2, pp. 406–412, 1994.

[27] D. A. Torrey and A. M. A. M. Al-Zamel, “Single-phase active power filters for multiple nonlinear loads,” *IEEE Transactions on Power Electronics*, vol. 10, no. 3, pp. 263–272, 1995.

[28] S. D. Round and N. Mohan, “Comparison of frequency and time domain neural network controllers for an active power filter,” in *Proceedings of IECON ’93 - 19th Annual Conference of IEEE Industrial Electronics*, 1993, vol. 2, pp. 1099–1104.

[29] Mrs. M. A. Chaudhari and Chandraprakash, “Three-phase Series Active Power Filter as Power Quality Conditioner,” in *2012 IEEE International Conference on Power Electronics, Drives and Energy Systems (PEDES)*, 2012, pp. 1–6.

[30] G. W. Chang, S. K. Chen, Y. C. Chin, and W. C. Chen, “An a-b-c Reference Frame-Based Compensation Strategy for Series Active Power Filter Control,” in *2006 1ST IEEE Conference on Industrial Electronics and Applications*, 2006, pp. 1–4.

[31] J. Dixon, L. Moran, J. Rodriguez, and R. Domke, “Reactive Power Compensation Technologies: State-of-the-Art Review,” *Proceedings of the IEEE*, vol. 93, no. 12, pp. 2144–2164, 2005.

[32] Hong Chen, “Practices of reactive power management and compensation,” in *2008 IEEE Power and Energy Society General Meeting - Conversion and Delivery of Electrical Energy in the 21st Century*, 2008, pp. 1–4.

[33] O. Akwukwaegbul and O. G. Ibe, “Concepts of Reactive Power Control and Voltage Stability Methods in Power System Network,” in *IOSR Journal of Computer Engineering*, 2013, vol. 11, pp. 15–25.

[34] X. Zhou, K. Wei, Y. Ma, and Z. Gao, “A Review of Reactive Power Compensation Devices,” in *2018 IEEE International Conference on Mechatronics and Automation (ICMA)*, 2018, pp. 2020–2024.

[35] A. K. Pathak, M. P. Sharma, and M. Gupta, “Static Var Compensator rating finalization and review of high wind penetration effect in Western Rajasthan,” in *2016 IEEE 1st International Conference on Power Electronics, Intelligent Control and Energy Systems (ICPEICES)*, 2016, pp. 1–6.

[36] R. M. Mathur and R. K. Varma, *Thyristor-Based FACTS Controllers for Electrical Transmission Systems*. IEEE, 2002.

[37] N. Sabai, H. N. Maung, and T. Win, “Voltage Control and Dynamic Performance of Power Transmission System Using Static Var Compensator,” in *World Academy of Science, Engineering and Technology*, 2008, pp. 425–429.

[38] L. L. Grigsby, *Power system stability and control*. Boca Raton: Taylor & Francis, 2012.

[39] GE Grid Solutions, “Static Synchronous Compensator (STATCOM) Solutions,” *Broucher GEA31986*, 2016. [Online]. Available: https://www.gegridsolutions.com/products/brochures/powerd_vtf/STATCOM_GEA31986_LR.pdf. [Accessed: 17-Jul-2019].

[40] C. Schauder, “Vector analysis and control of advanced static VAr compensators,” in *International Conference on AC and DC Power Transmission*, 1991, pp. 266–272.

[41] C. Schauder *et al.*, “Development of a /spl plusmn/100 MVAr static condenser for voltage control of transmission systems,” *IEEE Transactions on Power Delivery*, vol. 10, no. 3, pp. 1486–1496, 1995.

[42] F. Shahnia, S. Rajakaruna, and A. Ghosh, Eds., *Static Compensators (STATCOMs) in Power Systems*. New York, NY: Springer, 2014.

[43] B. Singh, R. Saha, A. Chandra, and K. Al-Haddad, “Static synchronous compensators (STATCOM): a review,” *IET Power Electronics*, vol. 2, no. 4, pp. 297–324, 2009.

[44] O. K. Shinde and V. R. S. V. B. Pulavarthi, “STATCOM converters and control: A review,” in *2017 International Conference on Data Management, Analytics and Innovation (ICDMAI)*, 2017, pp. 145–151.

[45] H. Akagi, “Classification, terminology, and application of the modular multilevel cascade converter (MMCC),” in *The 2010 International Power Electronics Conference - ECCE ASIA -*, 2010, pp. 508–515.

[46] Fang Zheng Peng, Jih-Sheng Lai, J. McKeever, and J. VanCoevering, “A multilevel voltage-source inverter with separate DC sources for static VAr generation,” in *IAS ’95. Conference Record of the 1995 IEEE Industry Applications Conference Thirtieth IAS Annual Meeting*, 1995, vol. 3, pp. 2541–2548.

[47] J. Park, S. Yeo, and J. Choi, “Development of ±400Mvar World Largest MMC STATCOM,” in *2018 21st International Conference on Electrical Machines and Systems (ICEMS)*, 2018, pp. 2060–2063.

[48] E. Behrouzian, “Operation and control of cascaded H-bridge converter for STATCOM application,” PhD Thesis, Chalmers University of Technology, 2016.

[49] J. Mei, Y. Ji, X. Du, T. Ma, C. Huang, and Q. Hu, “Quasi-Fixed-Frequency Hysteresis Current Tracking Control Strategy for Modular Multilevel Converters,” *Journal of Power Electronics*, vol. 14, no. 6, pp. 1147–1156, 2014.

[50] N. D. Marks, T. J. Summers, and R. E. Betz, “Challenges for capacitor voltage balancing in a cascaded h-bridge StatCom utilising finite control set Model Predictive Control,” in *2013 Australasian Universities Power Engineering Conference (AUPEC)*, 2013, pp. 1–6.

[51] J. Honkanen, “Harmonic Performance Improvement of STATCOM,” Master Thesis, Tampere University of Technology, 2018.

[52] J. S. Pridaaa, P. Tamizharasi, and J. Baskaran, “Implementation of synchronous reference frame strategy based Shunt active filter,” in *2011 3rd International Conference on Electronics Computer Technology*, 2011, vol. 2, pp. 240–244.

[53] J. Venkatesan and S. Natesan, “A SRF-PLL Control Scheme for DVR to Achieve Grid Synchronization and PQ Issues Mitigation in PV Fed Grid Connected System,” *Circuits and Systems*, vol. 7, no. 10, pp. 720–726, 2016.

[54] J. Pérez-Ramírez, V. Cárdenas, and H. Miranda, “DC-bus voltage regulation scheme for asymmetric cascade H-bridge converter working as STATCOM and active filter,” in *12th IEEE International Power Electronics Congress*, 2010, pp. 21–26.

[55] R. Simpson, A. Plumpton, M. Varley, C. Tonner, P. Taylor, and X. Dai, “Press-pack IGBTs for HVDC and FACTs,” *CSEE Journal of Power and Energy Systems*, vol. 3, no. 3, pp. 302–310, 2017.

[56] “IEC 60071-1, Insulation co-ordination - Part 1: Definitions, principles and rules,” IEC, 2011.

[57] CIGRE Working Group 14.19, “Static synchronous compensator (STATCOM),” 1999.

[58] D. Basic, M. Geske, and S. Schroeder, “Limitations of the H-bridge multilevel STATCOMs in compensation of current imbalance,” in *2015 17th European Conference on Power Electronics and Applications (EPE’15 ECCE-Europe)*, 2015, pp. 1–10.

[59] E. Behrouzian and M. Bongiorno, “Investigation of Negative-Sequence Injection Capability of Cascaded H-Bridge Converters in Star and Delta Configuration,” *IEEE Transactions on Power Electronics*, vol. 32, no. 2, pp. 1675–1683, 2017.

APPENDIX A: PARAMETERS OF SIMULATIONS

Appendix A, Table 1. Simulation parameters for case 1

Parameter	Value
Network	
Network frequency (Hz)	50
Nominal line to line source voltage (p.u)	1.0
Network impedance	short circuited
Transformer	
Rated power (MVA)	100
Connection type	YNd11
Primary line to line nominal voltage (kV, rms)	220
Secondary line to line nominal voltage (kV, rms)	34.10
Leakage reactance (p.u)	0.10
STATCOM	
Rated power (MVAr)	100
Needed submodules per branch with RPC mode only (Nos)	34
Capacitance of one submodule (μF)	7000
Reactance of MMC branch coupling inductor (mH)	13
Resistance of MMC branch coupling inductor (mΩ)	27.20
Maximum VSC current in delta branch (Amps)	1000
Network voltage for maximum capacitive operating point (p.u)	1.10
Network voltage for maximum inductive operating point (p.u)	1.35

Appendix A, Table 2. Simulation parameters for case 2

Parameter	Value
Network	
Network frequency (Hz)	50
Nominal line to line source voltage (p.u)	1.0
Degree of unbalance (%)	2
Network impedance	short circuited
Transformer	
Rated power (MVA)	107
Connection type	YNd11
Primary line to line nominal voltage (kV, rms)	220
Secondary line to line nominal voltage (kV, rms)	35.7 & 36.5
Leakage reactance (p.u)	0.10
STATCOM	
Rated power (MVAr)	107
Needed submodules per branch as per new design (Nos)	41 & 42
Capacitance of one submodule (μF)	7000
Reactance of MMC branch coupling inductor (mH)	15.73 & 16.07
Resistance of MMC branch coupling inductor (mΩ)	27.20
Maximum VSC current in delta branch (Amps)	1000
Network voltage for maximum capacitive operating point (p.u)	1.10
Network voltage for maximum inductive operating point (p.u)	1.35

APPENDIX B: SIMULATION RESULT SUMMARY

Appendix B, Table 1. Summary of simulation results from case 1 (RPC operation prioritized over AHF)

Available capacity for AHF current (%)	3rd order AHF current with worst peak (+ seq.)		4th order AHF current with worst peak (+ seq.)		5th order AHF current with worst peak (+ seq.)		5th order AHF current with worst peak (- seq.)		Combined AHF current (3rd, 4th and 5th order) with worst peaks (+ seq.)	
	Needed submodules (Nos.)	Increment w.r.t basic design (Nos.)	Needed submodules (Nos.)	Increment w.r.t basic design (Nos.)	Needed submodules (Nos.)	Increment w.r.t basic design (Nos.)	Needed submodules (Nos.)	Increment w.r.t basic design (Nos.)	Needed submodules (Nos.)	Increment w.r.t basic design (Nos.)
20	37	3	39	5	40	6	40	6	42	8
40	39	5	43	9	46	12	46	12	50	16
60	42	8	47	13	50	16	50	16	55	21

Basic design (without AHF current)	
Maximum operating point	Needed submodules (Nos.)
Capacitive	34
Inductive	34

Phase angle references of AHF current		
Order of harmonic for AHF current	Phase shift w.r.t MV busbar voltage	
	Worst peak angle (degrees)	Best peak angle (degrees)
3rd (150 Hz)	60	240
4th (200 Hz)	20	200
5th (250 Hz)	0	180

Appendix B, Table 2. Summary of simulation results from case 2 (Full RPC support in parallel to AHF operation)

Particulars	Without unbalance grid		With 2% unbalance grid		With 2% unbalance grid and phase shifted PS and NS voltage		With 2% unbalance grid, phase shifted PS and NS voltage and negative sequence AHF current	
	MCOP	MIOP	MCOP	MIOP	MCOP	MIOP	MCOP	MIOP
Needed submodules (Nos.)	41	41	42	42	42	42	42	N/A
Zero sequence current (Amps)	6.15	0.07	10.57	15.93	20.01	16.06	23.52	N/A
Order of harmonic for AHF current	3rd	N/A	3rd	N/A	3rd	N/A	3rd	N/A
Phase shift between PS and NS voltage (degrees)	N/A	N/A	N/A	N/A	120	240	240	N/A

Note*
MCOP — Maximum capacitive operating point
MIOP — Maximum inductive operating point
PS — Positive sequence
NS — Negative sequence
AHF current with worst peak angle of 60 degree was used in all cases
PS and NS voltages refer to the network (PCC) PS and NS voltages